DASA-1199

WATERWAYS EXPERIMENT STATION
CORPS OF ENGINEERS, UNITED STATES ARMY
CONTRACT DA-22-079-eng-224
R & D SUBPROJECT 8-12-95-420
and the DEFENSE ATOMIC SUPPORT AGENCY

THE RESPONSE OF SOILS
TO DYNAMIC LOADS
REPORT 4

ONE-DIMENSIONAL COMPRESSION AND WAVE VELOCITY TESTS

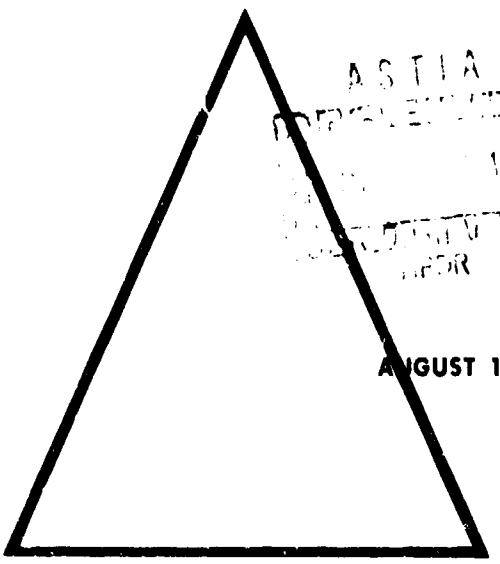

MASSACHUSETTS INSTITUTE
OF TECHNOLOGY

DEPARTMENT OF CIVIL
AND SANITARY ENGINEERING
SOIL ENGINEERING DIVISION

PUBLICATION 106

AUGUST 1960

DASA-1199

THE RESPONSE OF SOILS TO DYNAMIC LOADINGS

Report 4: One-dimensional compression and wave velocity tests

Robert V. Whitman
James E. Roberts
Shieh-Wen Mao

August, 1960

Soil Engineering Division
Massachusetts Institute of Technology
for
U.S. Army Engineers, Waterways Experiment Station
Department of the Army
R and D Subproject 8-12-95-420
Contract No. DA-22-079-eng-224
and for the
Defense Atomic Support Agency

ERRATA SHEET

In the course of reproducing this report, the words dilatation and dilatational were misspelled. Please excuse the mistake.

ABSTRACT

This interim report describes one portion of the Soil Dynamics Research effort during the past year. Included in the report are:

(a). A general discussion of the stress-strain relationship for particulate masses

(b). Specifications for the preparation of fat, backswamp clay samples by static compaction

(c). Data concerning creep, using a load rise-time of 30 milliseconds

(d). Description of a preliminary attempt to measure pore pressures during compression creep

(e). Data concerning the sonic dilitational wave velocity in a core of soft clay

(f). Description of a preliminary attempt to measure the sonic dilitational wave velocity in a soft clay sample during consolidation

LIST OF CHAPTERS

TABLE OF CONTENTS

LIST OF TABLES

LIST OF FIGURES

Distribution List for DASA-1199

Addressee	No. of Cys
Bureau of Mines, Washington, D.C., Attn: J. E. Crawford	1
Chief, Defense Atomic Support Agency, Washington 25, D.C., Attn: Document Library	12
Chief, Bureau of Yards and Docks, ND, Washington 25, D.C., Attn: D-440	1
Chief of Naval Operations, ND, Washington 25, D.C., Attn: Op-75	1
Chief of Research and Development, DA, Washington 25, D.C., Attn: Atomic Division	1
Commander, Air Force Ballistic Missile Division, Air Research and Development Command, Attn: WDFN, P.O. Box 262, Inglewood 49, California	1
Commander, ASTIA, Arlington Hall Station, Arlington 12, Va.	20
Commander, Air Force Special Weapons Center, Kirtland Air Force Base, Albuquerque, New Mexico	1
Commander, Wright Air Development Center, Wright-Patterson AFB, Ohio, Attn: WCOSI	1
Commanding Officer and Director, U.S. Naval Civil Engineering Laboratory, Port Heuneme, California	1
Director, Weapons Systems Evaluation Group, OSD, Room 1E880, The Pentagon, Washington 25, D.C	1
Director, U.S. Army Engineer Waterways Experiment Station, P.O. Box 631, Vicksburg, Miss.	20
Director of Civil Engineering, Hq, USAF, Washington 25, D.C., Attn: AFOCE	1
Director of Defense Research and Engineering, Washington 25, D.C., Attn: Tech Library	1
Hq, USAF (AFTAC - C. F. Romney), Washington 25, D.C.	2

Addressee	No. of Cys.
U.S. Coast and Geodetic Survey, Washington, D.C., Attn: D.S. Carder	1
U.S. Coast and Geodetic Survey, San Francisco, California Attn: W.K. Cloud	1
U.S. Geological Survey, Washington, D.C., Attn: J.R. Balsley	1
Dr. Harold Brode, RAND Corporation, 100 Main Street, Santa Monica, California	1
California Institute of Technology, Pasadena, California Attn: F. Press H. Benioff	1
Columbia University, New York, Attn: J.E. Oliver	1
Edgerton, Germeshausen, and Grier, Inc., Las Vegas, Attn: H.E. Grier	1
Holmes and Narver, Los Angeles, Attn: S.B. Smith	1
Mr. Kenneth Kaplan, Broadview Research Corporation, 1811 Trousdale Drive, Burlingame, California	1
Professor Robert L. Konder, The Technological Institute Northwestern University, Evanston, Illinois	1
Dr. N.M. Newmark, Civil Engineering Hall, University of Illinois, Urbana, Illinois	1
Mr. W.R. Perret, 5112, Sandia Corporation, Sandia Base, Albuquerque, New Mexico	1
Professor F.E. Richart, Jr., Dept. of Civil Engineering, University of Florida, Gainesville, Florida	1
Mr. Fred Sauer, Physics Department, Stanford Research Institute, Menlo Park, California	
Dr. T.H. Schiffman, Armour Research Foundation, Illinois Institute of Technology, Technology Center, Chicago 16, Illinois	1
Professor H. Bolton Seed, Dept. of Civil Engineering, University of California, Berkeley, California	1

Addressee	No. of Cys
Space Technology Laboratory, Inglewood, California, Attn: B. Sussholz	1
Stanford Research Institute, Physical Sciences Division, Menlo Park, California, Attn: Dr. R.B. Vaile, Jr.	2
Mr. A.A. Thompson Terminal Ballistic Laboratory, Aberdeen Proving Ground, Maryland	1
Professor J. Neils Thompson, Civil Engineering Department University of Texas, Austin 12, Texas	1
Mr. Eric Wang, Air Force Special Weapons Center, Kirtland AFB, Albuquerque, New Mexico	3
Chief of Engineers, Department of the Army, Washington 25, D.C. ATTN: ENGRD-S	3
Chief of Engineers, Department of the Army, Washington 25, D.C. ATTN: ENGMC-EB	2

Chapter 1
INTRODUCTION

1.1 Scope of report

This report brings together the results of research into two different but distinctly related subjects.

(a). Additional study of compression creep in compacted fat clay during one-dimensional compression tests, in continuation with work previously started: see MIT(1959b).

(b). The development of techniques for the measurement in the laboratory of sonic wave velocity in soils.

The test program has been summarized in Table 1.1. Also included in this report is a general discussion (see Chapter 2) of stress-strain relations to serve as background information for the experimental work.

The earlier one-dimensional compression tests upon the fat clay involved samples prepared by dynamic compaction on the wet side of the optimum water content and employed a loading apparatus which gave a rise-time of approximately 100 milliseconds. In the present effort, this work has been extended by preparing samples for a wide range of molding water contents using static compaction, and through the development of a loading technique which provided a rise-time of approximately 30 milliseconds. Greater dry densities were developed in the samples used in the current tests, and, in accordance with principles developed during the previous work, these denser samples showed more important creep effects. It has also been found that the creep effects which developed with very short rise-times were much more pronounced than would have been expected on the basis of the earlier tests with longer rise-times. Preliminary efforts were made towards the development of techniques for measuring pore pressures during

Table 1.1

SCOPE OF ONE-DIMENSIONAL COMPRESSION AND WAVE PROPAGATION STUDIES

Series	Soil	Scope	Chapter
A	Fat clay	Development of specifications for static compaction, using different mold sizes	3
B	Fat clay		3
C	Fat clay		3
D	Fat clay		3
E	Fat clay	Rapid rise-time; 6 molding water contents	4
F	Fat clay	Long term tests, with pore pressure measured	5
G	Fat clay	Rapid rise-time, with pore pressure measured	5
H	Deep sea core	Several hundred tests with acoustic probe	6
I	Deep sea core	Preliminary development of velocity measuring system	6

one-dimensional compression tests, as a means for studying the mechanism through which the creep behavior is developed.

The objective of the second part of the program has been the development of techniques for measuring the sonic wave velocity of soils in the laboratory. An accoustic probe technique was adapted to permit measurement of wave velocity in undisturbed samples of a soft clay, and many such measurements were made. To study the variation in wave velocity with changes in water content and in other properties of soil, the development of techniques for measurement of wave velocity in lightly consolidated soils contained within an oedometer was undertaken.

1.2. The MIT soils dynamic research program

The work described in this report was performed under Contract No. DA-22-079-eng-224 between the Waterways Experiment Station, a research facility of the Corps of Engineers, United States Army, and the Massachusetts Institute of Technology. The work has been sponsored by: (1) the Army Research and Development Program for Nuclear Weapons' Effects on Structures, Terrains, and Waterways, Subproject 8-12-95-420; and (2) the Defense Atomic Support Agency, a joint agency of the three armed services.

The long-range objective of the research under this contract is the determination and explanation by laboratory tests and theoretical analyses of the behavior of cohesive and noncohesive soils when subjected to transient loadings, and the effect of basic soil properties on this behavior. The results of this research should lead to a better understanding of soil behavior as related to trafficability studies, blast loadings, stress and strain distribution for aircraft wheel loads, and other problems involving transient loads.

The contract commenced in November, 1957, was renewed in November, 1958, and again renewed in November 1959. This is the fourth report issued under

contract. The first report (MIT, 1957)* was prepared to provide basic information for MIT personnel and subcontractors participating in the design of testing equipment. This first preliminary report was largely superseded by the first annual report, Report No. 2 (MIT, 1959a), which described the design, construction, and performance of apparatus for carrying out triaxial compression tests under rapid loading conditions and for measuring the stresses and strains during such tests. As this description suggests, the first year of the contract was devoted to the development of test equipment and procedures. The third report (MIT, 1959b) which was the second annual report, described the work performed during the second year of the contract. This work consisted of triaxial compression and one-dimensional compression tests, and included tests upon five soils ranging from a fat clay to a clean sand.

The current report is not an annual report, but rather deals with only a limited portion of the total research effort for the third year of the contract. The total effort has also included continuation of the triaxial compression test research and extensive efforts in the development of pore pressure measuring techniques for use during rapid loading tests. The other portions of the total effort are to be covered in separate reports.

In a research effort as large as this one, the attempt to develop an identification code so that each test is designated in accordance with its proper position in the overall program soon leads to a hopelessly complex coding system. Hence, for the purposes of this report, the several series of tests which are involved have been designated simply by letters A, B, C, etc. While this same designation system has been used in the previous report and will be used in subsequent reports, it is felt that no major confusion will result.

The research reported herein has been performed by the Soil Engineering Division of the Civil Engineering Department. Professor T.W. Lambe, as head

*See Appendix A for the listing of references

of the Soil Engineering Division, has overall responsibility for the work. Professor Robert V. Whitman has immediate responsibility for all phases of the work. Shieh-Wen Mao, Research Assistant, carried out the static compaction studies discussed in Chapter 3 and the one-dimensional compression tests reported in Chapters 4 and 5. Lynn R. Sykes, a graduate student, carried out the wave propagation experiments described in Chapter 6. Professor James E. Roberts supervised directly all of the experimental work described in this report and participated directly in the efforts to develop suitable techniques for measuring wave velocities in the laboratory. Mr. Charles C. Ladd, Instructor, and the following Research Assistants all contributed to this work: Richard M. Harkness, Kent A. Healy, Nasim M. Nasim and Archie M. Richardson, Jr.

Chapter 2
GENERAL DISCUSSION OF STRESS-STRAIN RELATIONS

2.1 Objectives of this review

There are a number of viewpoints which might be taken on the subject of deformations and wave propagation, and with each viewpoint, different aspects of the subject will be emphasized. The thoughts presented in this review were developed as the problem was viewed: (1) from the standpoint of how stress is transmitted through soil; and (2) from the standpoint of what information concerning soil behavior has been important in recent protective construction efforts. From these thoughts have come the ideas for the laboratory tests described in the latter chapters of this report. The aim of this chapter is thus to provide background for the present and future research efforts into the nature of the stress-strain relations of soils. The reader's attention is called to earlier efforts along these same lines in MIT (1954), Chapters 6 and 7, and in SAUER et al. (1958), Chapter 6.

While this report is hardly the place for a treatise on elastic theory, it does seem pertinent to review certain ideas which are basic to a discussion of soil behavior. This material has been included in the next section.

2.2 Deformations and wave propagation in linear elastic media

Many different "elastic constants" appear in the theory of elasticity. Many of these constants are in the form of a ratio of stress to strain and each of these is called a modulus. Another important constant is Poisson's ratio μ, which expresses the ratio of strains which exist and is one particular condition of deformation. At the first acquaintance with elastic theory, this multiplicity of moduli often presents a somewhat confusing picture.

The main reason why there are so many moduli is that each modulus is the ratio of stress to strain for some particular set of boundary conditions.

Bulk modulus B, Young's modulus E, and shear modulus G are familiar quantities with clear physical meanings. Another common form, which here will be called dilitational modulus M, is the ratio of axial stress to axial strain in the case where the strains are zero in directions at right angles to the axis. There are other forms which are encountered frequently, such as the modulus D, found in plate theory, which applies to problems in plain strain. The moduli which have been enumerated here are in common usage because the boundary conditions to which they correspond are simple and, therefore, are easily used. Each such moduli has usefulness and clear physical meaning for an important class of problems, regardless of whether the material is isotropic or anisotropic. Many other forms of moduli appear occasionally, each corresponding to still another pattern of boundary conditions.

If a material is isotropic, only two elastic constants are necessary in order to describe completely the state of strain for a general case of very complex stress patterns. Correspondingly, each of the many elastic constants can be expressed in terms of any other two of the constants. For example, the dilitational modulus can be expressed as:

$$M = \frac{E(1-\mu)}{(1+\mu)(1-2\mu)} \tag{2.1}$$

The question often arises: which two of the elastic constants are the most basic of the various stress-strain relations? There is no one answer to this question, and the response depends upon the viewpoint of the investigator. From one standpoint, E and μ are the most important constants, for the expressions for all other elastic constants in terms of E and μ are particularly simple. E also occupies a prevalent place in the literature because so many problems which the engineer has met in the past have involved stress change in one direction only. To the person interested in material behavior, B and G may appear to be the most basic forms because these moduli correspond to the two simplest patterns of deformation. The person who wishes to visualize the deformation patterns within an elastic body may find it easiest to work with M and G. Thus, for an axially symmetrical load over a portion of the surface of

a semi-infinite mass, one can first envision the pattern of axial strains which would develop if there are no movements perpendicular to the axis, and then the additional strains which would occur if the mass is allowed to distort in shear with no further volume change. It is interesting that the condition of one-dimensional compression with zero lateral strain, a condition which actually involves shear strain, is more useful for the synthesis of complex deformation patterns than is the condition of volume change without shear. Finally, the Lame constant λ together with the shear modulus G appear most important to the mathematician, because the differential equations of the theory of elasticity take on their most elegant form when expressed in terms of these constants.

The main thoughts of the foregoing paragraphs can be expressed by the following statements: (1) there is no such thing as THE modulus of a material, and one must always be careful to specify which modulus is being used; (2) the modulus which is most useful for the description of a deformation pattern will vary with the nature of the boundary conditions which apply to the problem; and (3) the dilitational and shear moduli M and G are particularly useful, since they correspond to simple strain states which are useful in synthesizing more general states of strain.

There is a similar group of thoughts which pertain to the propagation of waves through an elastic body. For the case of the propagation of waves originating at a point within the body well removed from any boundary, it is frequently said that two different waves exist: a dilitational wave and a shear wave. These two waves would travel at velocities given by the following formulae, where ρ is the mass density:

$$v_D = \sqrt{\frac{M}{\rho}} \quad ; \quad v_S = \sqrt{\frac{G}{\rho}} \tag{2.2}$$

Actually it is an oversimplification to speak of only one compression type wave velocity for an infinite medium. The very front of a compression wave will travel at a velocity, v_D, for as the very first disturbance reaches a point of an infinite elastic medium and imparts particle velocity to this point, the material at the point is in a state of one-dimensional compression. However,

as soon as this point moves, there will be (provided the wave front is curved) strains in directions transverse to the direction of propagation, and the material at the point is no longer in one-dimensional compression. Thus the peak of a compression wave in an infinite medium may travel at a velocity less than v_D. In the case of spherical waves, for example, the phase velocity (velocity of the wave peak) will depend upon the relative magnitudes of the radial and circumferential strains, and hence upon the wave length of the disturbance. Thus a compression wave is said to be "dispersed". Particular emphasis is placed upon v_D in the literature only because the dispersion effect is small for the short wave lengths which make up most common of compression waves, i.e., seismic disturbances in the earth.

As soon as boundary conditions enter into a wave propagation problem, other types of waves appear, called surface of boundary waves. The appearance of many such waves corresponds in a rough way to the existence of many different moduli, each existing because of interest in a particular set of boundary conditions. The Rayleigh wave is but one of the most important surface waves for a semi-infinite medium.

It is of particular interest to examine the propagation of a compression disturbance along a circular rod. It will be assumed that no stresses develop upon the cylindrical surface of the rod, which is thus free to expand in the lateral direction. Suppose this rod is impacted by a large mass moving a constant velocity $\dot{s}_o$. During a short interval after the impact, there will not have been time for the rod to expand laterally. Hence the rod will behave as though it were in one-dimensional compression, and the energy imparted during this short time interval after impact will propagate at a velocity v_D. Thus, as far as the point A is concerned, the arriving wave appears as a pure dilitational wave, as is indicated in Figure 2.1. However, lateral strains appear immediately at the surface of the rod, and at this surface a certain amount of energy of compression is converted into energy of shear. The shear waves thus originated, move down along the surface and also spread out through the interior of the rod. When shear waves originating at one

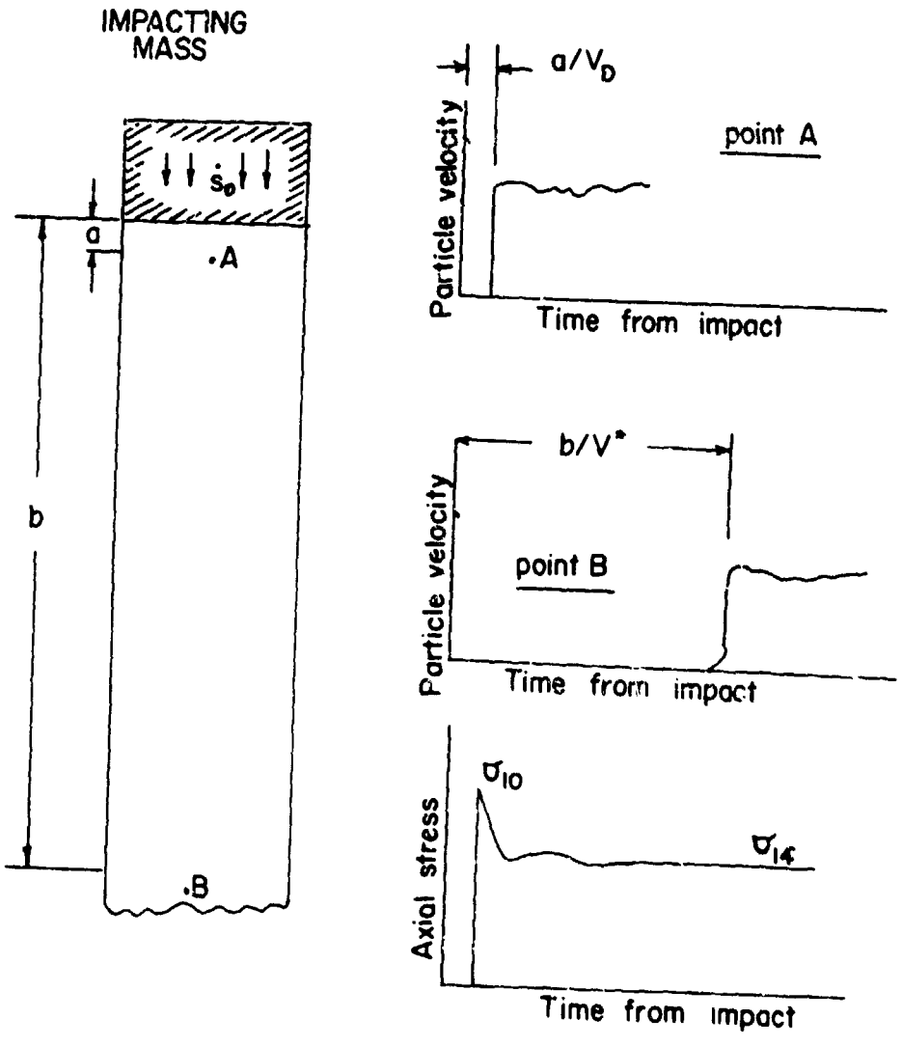

FIGURE 2.1 WAVE PROPAGATION IN UNCONFINED ROD

point of the surface arrive at another point of the surface, they reflect and refract, and new shear and compression waves are created. Thus there is a gradual conversion of the energy in the original dilitation wave into energy in the form of a new wave which is consistent with the surface boundary conditions of the rod. Thus, the pattern of energy arrival at point B indicates the arrival of a wave which is something other than a dilitational wave.* The pattern of deformation which an unconfined rod desires to take is that for which Young's modulus applies and hence it is not surprising that the compression wave velocity in long, thin rods has been found from measurements to be:

$$v^* = \sqrt{\frac{E}{\rho}} \tag{2.3}$$

This example of wave propagation in a rod has illustrated the interrelationship between the boundary conditions and the wave velocities which exist in any particular problem. The example also points out the complex conditions which exist even in the simplest of problems. To further illustrate the complexity of this problem, consider the stresses which are generated at point A. When the dilitational wave first arrives, the axial stress is given by the following formula from wave propagation theory:

$$\sigma_{10} = \frac{\dot{\varepsilon}_o M}{v_D} = \dot{\varepsilon}_o \sqrt{\rho M} \tag{2.4}$$

This axial stress causes a lateral stress within the material, and since there is no stress on the surface of the rod, the material between point A and the exterior of the rod is accelerated outward. As lateral strains develop, σ_{10} must decrease and following a period of adjustment come to equilibrium at a new value:

$$\sigma_{1f} = \frac{\dot{\varepsilon}_o E}{v^*} = \dot{\varepsilon}_o \sqrt{\rho E} \tag{2.5}$$

---

*An observer at point B who had extremely sensitive instruments would be able to see a very small amount of energy arriving at the velocity v_D.

In an elastic material with $\mu = 0.4$, σ_{10} will be approximately 45% higher than the final axial stress σ_{1f}. As μ approaches 0.5, the difference rapidly becomes much larger. Thus the stress at the impact end of a rod will appear to be time-dependent even though the rod is composed of ideal elastic material.

These ideas concerning wave propagation can be summarized by the following statements which follow the outline of the earlier summary paragraph: (1) there is no such thing as THE wave velocity for a material, not even THE compressional wave velocity; (2) the wave velocity of interest in any problem is the one for the wave which transmits the major fraction of the energy, and the form and velocity of this wave depends upon the boundary conditions for the problem at hand; and (3) the dilitational wave is a very important wave form, especially near the origin of the disturbance, and the very first portion of a compression wave always travels at the velocity v_D.

2.3 Deformation and wave propagation in soils

In order to emphasize the differences between wave propagation in soil and wave propagation in an ideal elastic medium, it seems appropriate to emphasize the two major ways in which soil differs from a nearly ideal material such as steel: (1) soil is an assemblage of discrete particles; and (2) when a soil is saturated or nearly so, the interactions between the pore fluid and mineral skeleton must be considered.

2.3.1 Consequences of particulate nature of soils

The mineral skeleton of a soil is a disorganized assemblage of discrete mineral particles of varying size, shape, and smoothness. Any one particle will be in contact with one or more of its neighbors (contact meaning approach of portions of two crystals to within 10 Angstroms or so), and it is through these points of contact that the forces carried by the mineral skeleton are transmitted. The deformation and wave propagation

characteristics of a soil are in turn determined by the events at the many points of contact within the mass of soil.

It would be an understatement to say that behavior at these points of contact is poorly understood. Any one point of contact is likely to be very small, perhaps involving (as a pure guess) an area of 1,000 to 10,000 square Angstroms on the surface of each of the two crystals. Certainly the force transmission between the two crystals is through the same type of electrical field which holds together the various atoms within the crystal, but the force fields are much more disorganized and the intracrystalline forces are much weaker than the intracrystalline forces. The mechanism of contact may well involve one or more layers of water interspersed between the mineral crystals, but still the general mechanism of force transmission is the same. In order to distort the structure of a well-formed crystal, a considerable energy density (energy per unit volume) must be introduced into the crystal. In order to distort the weak atomic formations which are set up at the points of contact, must less energy density is required. Furthermore, for a given volume of soil mass, the total volume of material involved in the contact zones will be much less than the total volume involved in the mineral particles themselves. Hence two statements follow: (1) the deformations of a soil mass are brought about largely by distortions of the atomic formations at the points of contact (by which one means significant relative motions between atoms); and (2) the resistance of a soil mass to deformation is determined largely by the distortion resistance at the points of contact. As the resistance to distortion in the contact zones becomes greater and greater, the soil mass begins to behave more and more as a coherent material such as rock, and the demarcation line between soil and rock is inevitably an arbitrary one.

Consider first the compression of a particulate mass within a one-dimensional compression test. At some time, the particles are considered to be in equilibrium under the existing load, meaning that a constant pattern of interparticle forces has been established. The force which exists at any one contact point undoubtedly will not be merely normal to the contact sur-

face, but rather will have tangential components as well. (The reader is asked to use his imagination as to the meaning of "normal to the contact surface" when matter is being viewed on a scale only slightly larger than atomic sizes). Now the axial load is increased at a very slow rate. The result will be a complex pattern of change in the interparticle forces: the normal forces increasing at some contact points, but decreasing at others; the resultant shear forces changing in magnitude and direction at various contact points. The patterns of distortion at the various contact points will correspondingly be complex.

The very first increments of force change will, at almost all contact points, be accompanied by elastic type distortions of the atomic formations at the points of contact. If the external load were to be removed at this stage, these local distortions would prove to be largely reversible. As the load is increased further, however, the limit of elastic load transmission is reached at numerous points of contact, and large movement of atoms (large on the atomic scale) begins. The possibilities at this stage are numerous, but each possible type of action must somehow lead to greater load carrying ability. If the force at a contact area is mainly normal to the contact surface, the atoms of one or both crystals may dislocate enough so that the two crystals come closer together with a greater contact area. If there is a large shear force at the contact point, some atoms may dislocate enough to allow the surfaces to slip past one another and hence allow the particles to rearrange themselves so that additional contact points are formed - perhaps additional contact points between the same particles, perhaps contacts with other particles. Or, when there are large shear forces at contact points, some atoms may be sheared off from one particle and either form a new, tiny particle or attach themselves to the other particle; now as before the particles can slip into new arrangements and form additional contact points. This matter of forming new contact points is a statistical one, for it is not hard to imagine that the number of contacts upon any one particle may actually decrease at some point of the rearrangement process.

The amount of load increase which can be accepted before irreversible deformations occur is determined by the strength of the elastic forces at the contact points. Any particulate system certainly has some range of stress change for which its response is essentially elastic. Past compression, which has eliminated the weaker contact points, or formation of interparticle bonds through gradual growth of amorphous or weak crystalline atomic formations, may raise the elastic range to measurable magnitudes. Once this initial elastic range is exceeded, the rate of deformation will suddenly increase as a large number of local contact zone deformations occur. But now a work hardening phenomenon occurs, for each of the happenings described in the previous paragraph will increase the resistance to further compression. Eventually stable particle arrangements are formed wherein the tendency to shear across any contact surface becomes small. At this stage, the energy required to distort the contact zones approaches that of the crystals themselves. With still further load increase, there is the possibility that the particles themselves will crack along planes of weakness. This particle-breaking action leads to a sudden increase in the deformation rate as particle rearrangements occur, followed by a decreasing deformation rate as even more compact particle arrangements develop.

The sequence of events described in this last paragraph is depicted in Figure 2.2 and has been well documented by tests upon many soils. Least is known about the initial elastic portion, which, in many soils, is so short as to be undetectable for many test conditions.

Most of what has been said in this sub-section applies to the deformations which occur during triaxial compression tests. An initial elastic range is to be expected: almost non-existent for some test conditions but significant for others. As this elastic range is exceeded, particle rearrangements occur, leading to greater numbers of more stable contacts. However, a point reached where further deformation leads merely to the rolling of some particles up, over, and around other particles rather than to more stable arrangements of particles. Thus a yield point has been reached, as indicated

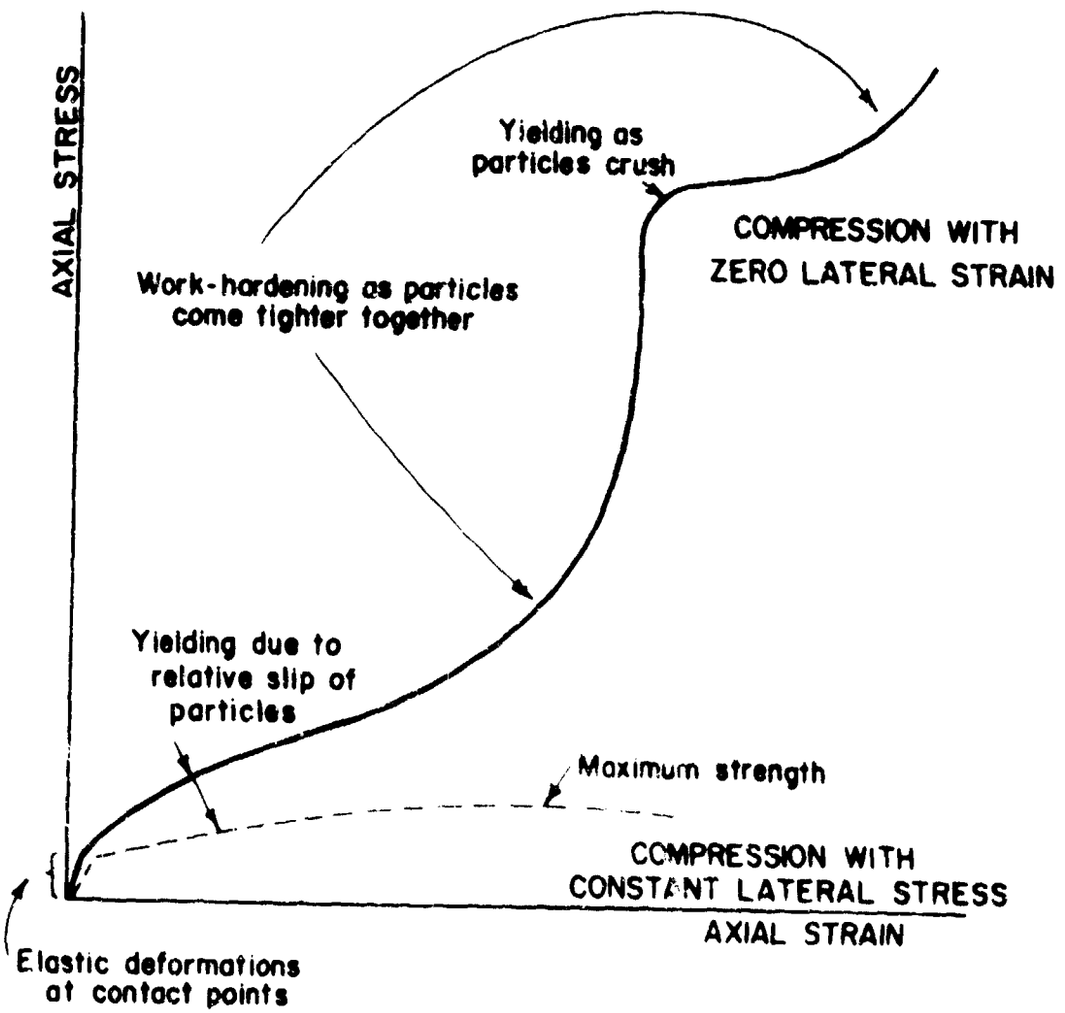

FIGURE 2.2 STRESS VS. STRAIN FOR PARTICULATE MASS

by curve B of Figure 2.2.

From the general picture of soil behavior presented in this sub-section, four items of behavior can be listed as requiring special consideration in studies of wave propagation through soil. Any material will exhibit these properties to some degree, but these properties seem especially important in particulate masses.

(a). Non-linear in confined compression: That such non-linearity is present is shown for many soils by the value of M calculated from field seismic wave velocities and the M measured in laboratory tests upon undisturbed samples. Little is known about the range of initial elastic behavior for natural soils.

(b). Extremely sensitive to stress system: For corresponding and quite moderate stress levels, the values of M and E can differ greatly. Data on this subject was presented in MIT(1954). This situation results simply from the much greater resistance of an assemblage of particles to compression rather than to shear. Because of this behavior, it is very difficult to evaluate the resistance of a soil to compression from a test which involves a large degree of shearing action; i.e., a triaxial compression test will provide information on the resistance of soil to shear, but will not tell much about the dilitational modulus. A general theory which relates the stress-strain relations of soil for varying boundary conditions is still not available.

(c). Dissipative: As relative particle motions occur, external work done upon the soil is converted irreversibly into heat energy.

(d). Time dependent: Creep under constant load is shown by data presented in Chapter 4 of this report. In a particulate mass, all deformation after a very short initial range occurs through gross relocations of atoms in the contact zone. Since all atoms have thermal movements, it is to be expected that an element of time will enter the relocations at the various

contact points.*

Rheological models which consider these effects have been described by SAUER et al (1958).

2.3.2 Consequences of two-phase nature of soils

The bulk modulus K of water is much larger than the bulk modulus of the mineral skeleton of soil, except perhaps during the initial elastic range for the mineral skeleton. Thus, if a saturated soil is compressed slowly, water will be squeezed out. On the other hand, if a saturated soil is compressed rapidly so that loss of water is prevented by the hydrodynamic time-lag, then the compressibility of the soil is largely that of water. It is obvious that, putting aside the non-linearity problems discussed in the previous sub-section, the dilitational velocity v_D cannot be estimated from the modulus M measured in a test where water is squeezed from the sample. Since water has no resistance to shear, the shear modulus G of soil will be that of its mineral skeleton.

Because the M of water is generally several orders of magnitude higher than the G of unconsolidated soils, the difference between the dilitational and shear wave velocities of soft saturated soils will be very large. Just such behavior has been recorded by WILSON and DIETRICH (1960). With soft saturated soil, the apparent value of Poisson's ratio approaches very close to one-half. Under such a condition, it is not possible to determine v_D from a laboratory measurement of v^*, since a very slight uncertainty in Poisson's ratio can lead to a huge discrepancy in the ratio of v_D/v^*.

---

*One must be careful to distinguish time-dependent effects arising from soil behavior from those arising from inertial effects. PARKIN (1959) has interpreted results presented in MIT(1954) as indicating a large strain-rate effect in soil behavior. The senior author clings to his original view that the large variation in impact stress with time resulted from the lateral inertia effect described in section 2.2.

Other problems involved in wave propagation through saturated soils are mentioned in Chapter 6. With partly saturated soils, the pore phase is as compressible as the mineral skeleton, and all of the discussion in the previous sub-section applies. That portion of the water phase which occurs right at the points of contact between particles certainly does influence the stresses and deformations at these points, but this influence has already been taken into consideration in the previous discussion.

2.4 Perspective on current protective construction problems

The task of designing underground shelters for the nation's system of defense and counterattack has helped clarify the types of necessary knowledge concerning the deformation resistance of soils. In these cases, concern has been with damage produced by air blast waves sweeping over the surface of the ground and having wave lengths quite large compared to the dimensions of the shelters. The evolution of criteria for design earth pressures and ground motions has been described by PECK and WHITMAN (1959). There were four key assumptions involved in the derivation of these design criteria:

(a). The energy adsorbing characteristics of soil prevents development of true sharp-fronted shock wave in soil, for pressure rises up to several hundred pounds per square inch; i.e. the rise time of the air-blast induced pressure wave lengthens considerably as the wave travels through the top feet of the earth's surface. The fact that there is not a very sharp rise time of less than 5 or 10 milliseconds influences the design criteria as applied to underground structures.

(b). Low frequency ground motions in the vertical direction, which influence greatly the design of shock isolation systems for heavy equipment within the shelters, could be estimated by assuming that the design air blast overpressure is applied to the end of an infinitely long column of soil and rock having the same vertical profile as does the actual earth, and that the soil in this column is confined against strains in the

horizontal directions. The pattern of wave propagation and vertical motion within this soil column is controlled by the modulus M and its variation with depth. M was estimated from in situ measurements of dilitational seismic velocity, with a judgement applied to take care of the possibility that the M for high pressure levels is not the same as the M which exists for the pressure levels within seismic waves.

(c). High frequency vertical ground motions, which influence the design of shock isolation systems for the lighter contents of the shelters, were estimated from a blend of field experience, analysis of one-dimensional wave patterns as in item (b), and judgement as to changes in the rise-time of pressure waves as they travel through earth and are reflected from various layers within the earth.

(d). Horizontal ground motions were taken to be some fraction of the vertical motions, based upon the judgement that the effects of surface waves were negligible compared to the effects of the dilitational wave propagated downward from the air blast wave traversing the ground surface.

Viewing these four assumptions, several areas can be delineated in which much further knowledge of soil behavior is essential: (1) the influence of the energy adsorbing characteristics of soil upon the high frequency content of a pressure wave; (2) the magnitude of the modulus M of in situ soils as a function of pressure magnitude and duration; and (3) the influence of soil properties upon the existence and likely magnitude of surface waves.

2.5 Role of laboratory tests

Laboratory tests will certainly not by themselves clear up all of the uncertainties in our knowledge of ground motions as they affect protective construction. Field tests, in so far as they are possible, are the ultimate proving ground for theories aimed at clarifying these uncertainties.

There would seem to be three general roles which might be assigned to laboratory tests upon soil systems from the standpoint of improving our knowledge of ground motions. Other aspects of the protective construction problem, such as soil-structure interaction, are not considered in this review.

(a). Determination of patterns of wave propagation: The motion and deformations which will be experienced by the soil at any point in the vicinity of a large explosion are determined far more by the geological structuring of the soil mass than by the properties of the soil at that particular point. Hence it is hopeless to expect that wave propagation patterns can be reproduced in their entirety in the laboratory so as to provide ground motion data of direct use in design. The role of laboratory wave propagation tests must be to clarify certain aspects of the wave propagation problem so that data from existing and future field tests can be understood and applied in an intelligent manner. Laboratory tests which are to provide clarity must create very simple patterns of wave propagation which can be measured adequately in such a way that the effects of the several parameters present can be isolated. The soil column tests under development at the Stanford Research Institute, which will make it possible to study the specific questions of energy dissipation and attenuation of high frequency components of waves, are a good example of the type of laboratory tests which are worthwhile.

(b). Evaluation of properties of natural soils: There are several misgivings as to the extent to which laboratory tests can be used to evaluate in a precise, quantitative way the in situ deformation resistance of actual soils, because of the problems of sample disturbance. The slight loosening of the soil at the two ends of a sample, as these ends are trimmed so that the sample may be placed in a testing device, may give the soil an apparent compressibility many times its natural in situ compressibility. Hence relatively inexpensive field tests which might be used to measure the in situ dilitational modulus of many different

natural soils at pressure levels of several hundred pounds per square inch would be of great value. Techniques under development at the Poulter Laboratories of the Stanford Research Institute appear to have great value in this regard. Efforts to develop laboratory test procedures, such as those underway at the engineering firm of Shannon and Wilson, should be encouraged, even though there is an element of doubt as to their eventual success. Laboratory tests, of course, always have value as an aid to the judgement of the designing engineer even though they fail to provide precise, quantitative results.

(c). Basic research into deformation resistance: The most important role of laboratory testing appears to lie in this area of basic research into the effects of time, stress level, and other factors upon the deformation resistance of soil systems. Much of this research must, of necessity, be carried out using reconstituted soils, and the direct application of the data to natural soils will always be in doubt. However, tests upon reconstituted soils will be of great eventual assistance to design efforts if these tests: (1) establish clearly the manner in which deformation resistance of several typical soil types varies as the important parameters are changed; and (2) indicate precisely the relationships between these behavior patterns and the basic physical properties of the soils.

The work at MIT which is described in subsequent chapters of this report falls into this final category of basic research. The current work is aimed at such questions as: (1) the effect of load duration upon the dilitational modulus; (2) the effect of pore phase behavior upon the relation between dilitational modulus and duration of stress application; (3) the relation between sonic dilitational velocity and dilitational modulus measured at relatively high stress levels; and (4) the mechanisms of wave propagation through soil-water systems.

Although these current efforts at MIT are aimed largely at the study of dilitational deformation and waves, there is need for similar re-

search into shear deformation resistance, especially in so far as it influences possible surface waves in soil masses. The problem in its entirety is large enough to merit the efforts of many research groups. Studies now underway at the Broadview Research Corporation will supplement, from a different viewpoint, those at MIT and will certainly form a valuable contribution.

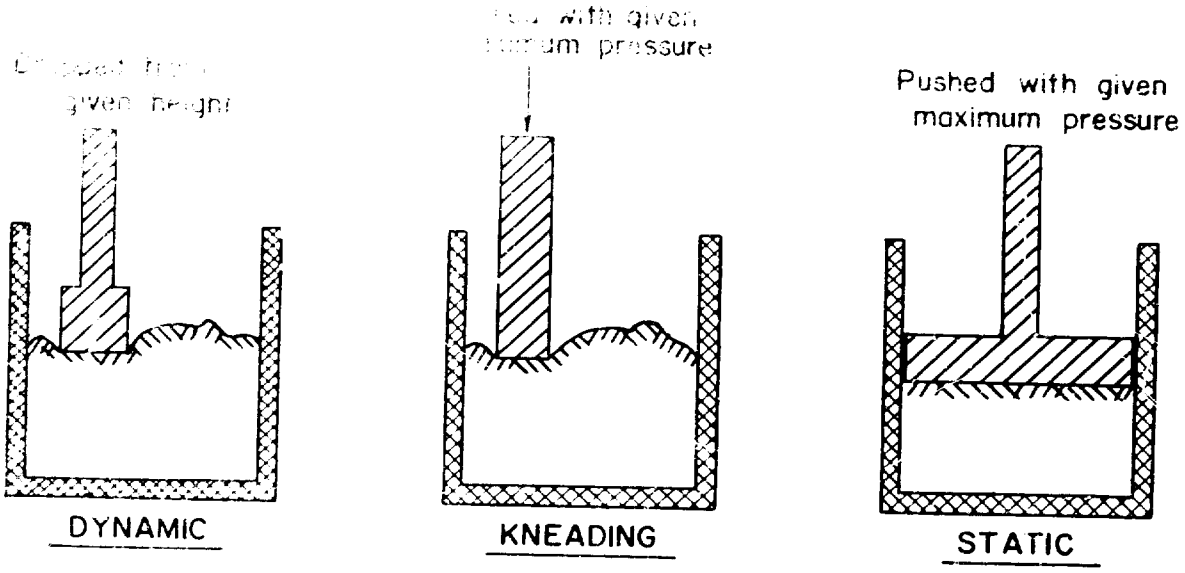

FIGURE 3.1 LABORATORY COMPACTION PROCEDURES

Chapter 3

PREPARATION OF ONE-DIMENSIONAL COMPRESSION TEST SPECIMENS BY STATIC COMPACTION

3.1 Objectives of static compaction study

There are essentially three different procedures used to compact clay containing soils in the laboratory: dynamic compaction, kneading compaction, and static compaction. These procedures are illustrated schematically in Figure 3.1. There are, of course, many versions of each scheme. For each version, there generally exists a set of specifications developed on the basis that laboratory compaction should produce a sample with the same maximum dry density as can be obtained in the field with normal compaction procedures. There have been many discussions of the relative merits of these procedures involving consideration of the simplicity of the methods, the degree of simulation of field compaction, and the relation to previous compaction studies. For a recent discussion of one aspect of this problem, see SEED, MITCHELL, and CHAN (1960).

In the dynamic compaction procedures, such as the Proctor and AASHO method, a given amout of energy is applied to the soil by dropping a given weight from a given height for a given number of blows. The specifications vary with each version of the dynamic compaction procedure. There are also specifications upon the mold size and the number of layers in which the soil is to be placed. Dynamic compaction was the first of the standard laboratory procedures, and hence has a long heritage of use.

In kneading compaction, a plunger is pushed into the soil with a specified maximum pressure. An example is the Harvard Miniature compaction method. Large, hydraulic kneading compactors are also available for laboratory use. Again the pressure, mold size, number of blows and number of soil layers depend upon the version of the method which is selected. Kneading compaction is a post-war development, but is gaining favor be-

cause it is a simpler procedure. There is also some evidence to the effect that kneading compaction best simulates compaction produced in the field.

In static compaction, the soil is squeezed to its final volume by one stroke of a piston which covers the entire end surface area of the sample. In some procedures, the sample may be compressed simultaneously from both ends. Usually, compaction control is accomplished through a specification upon the maximum pressure. When there is a desire to produce several samples with exactly the same density, the motion of the piston can be specified. Static compaction procedures are extremely simple but do the the poorest job of simulating field compaction conditions. Static compaction has its greatest use in research wherein reproduction of field compaction work is not essential.

At the present stage of research into one-dimensional compression under dynamic loads, close simulation of field compaction conditions - either as to dry density or as to the structure of the soil - is not an important criteria. Simplicity, uniformity of soil samples, and reproducibility of soil properties are rather the essential problems. For these reasons, it was decided that the feasibility of using static compaction should be explored. The desire to use specimens with very large diameters and the need for great uniformity - particularly over the thickness of the sample - presented problems which required research effort. Of special interest was the question: how thick a layer of soil can be used before the portion of the layer away from the piston is compacted to a significantly smaller degree than the portion of the layer adjacent to the piston? The Stanford Research Institute has expressed interest in using static compaction to prepare the soil for soil column wave propagation experiments which they are developing under contract to the Air Force Special Weapons Center, and the results of the present study should be of considerable interest to that and other similar efforts.

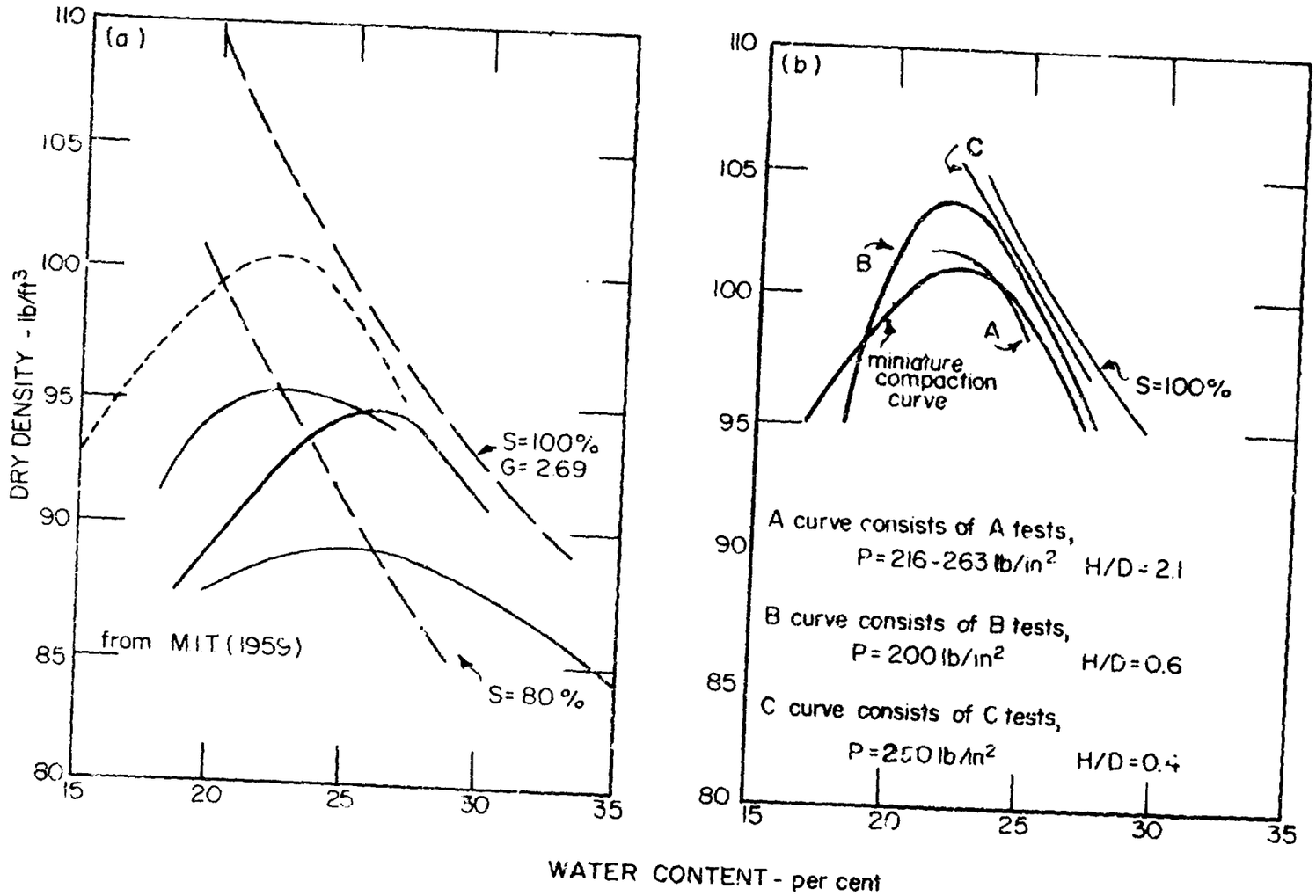

FIGURE 3.2 DRY DENSITY VS. MOLDING WATER CONTENT

3.2 Test procedure and results

3.2.1 Soil, apparatus and procedure

Backswamp clay from the vicinity of Vicksburg, Mississippi was used in this study. The clay and its properties were treated extensively in a previous report: MIT (1959b). The material from the current work came from Barrel 3, and the following classification data were obtained on the fraction passing a No. 20 sieve.

Specific gravity = 2.69	Plastic limit = 25 percent
Liquid limit = 65 percent	Shrinkage limit = 13.5 percent

Several preliminary tests revealed that this material had somewhat different compaction characteristics than those presented in the previous reports. Hence complete dry density vs. molding water content curves were obtained by the standard Proctor and Harvard Miniature methods. The results are presented in Figure 3.2(a) along with those from the previous report. For the Harvard Miniature work, the soil was compacted in 3 layers with 25 tamps per layer using a 40 pound tamping force.

The exact reasons for the difference in compaction characteristics are not known, although the differences are typical of those which occur when different operations and different batches of material are involved. It should be noted that the clay shipped in Barrel 3 had been dried and ground prior to shipment, whereas the earlier material had apparently received little processing.

The experimental work involved four different series of tests, as indicated by the following table:

Series	Mold No.	Mold Size	
		Diameter	Height
A	A	1.312"	2.816"
B	B	2.500"	2.816"
C	C	6.000"	6.000"
D	C'	6.000"	6.000"

All of the molds were constructed with steel. Mold C had a coating of Teflon on its interior surfaces. The samples in test series A and B were compacted using a small hand-operated loading frame with a capacity of 4000 lbs. The piston force was measured with a proving ring. The samples in test series C and D were compacted using a 100,000 lb. material testing machine, available in another laboratory in the Institute. This machine had a built-in load measuring cell. By appropriate observations, it was possible to evaluate the applied pressures as a function of dry density continuously throughout each test. The rate of compression was about 0.1 - 0.2 inches per minute, although a controlled stress rate of 20 lb/in^2 per minute was used in some tests and was deemed a more desirable procedure.

In all tests, the soil was first prepared at the desired water content and then allowed to equilibrate for from 18 hours to 3 days in a humid room. A known weight of wet soil was placed in the mold, and then was compacted either to a predetermined volume (volume control test) or to a desired pressure (pressure control test). After compaction the sample was extruded from the mold and was weighed and dried in order to determine the moisture content. In many of the tests, the sample after extrusion from the mold was divided into several parts, and the volume of each part determined by a mercury displacement technique. Thus, once the water content of each part was determined upon drying, the dry densities of the several parts could be calculated.

3.2.2 Special tests with marker layers

The non-uniform strains produced when a thick sample is com-

pressed by static compaction were clearly shown in a few special tests in which a marker layer was inserted within the sample. For these tests, one half of the soil sample was first placed in the mold without any compaction. Dry powdered kaolinite was sprinkled upon the surface of this portion of the sample. The remainder of the soil was then placed in the mold and the whole of the sample was compacted. When these samples were extruded from the mold, they broke in two at the location of the kaolinite. The nature of this kaolinite surface is shown in Figure 3.3.

3.2.3 Summary of test program

The tests performed as part of this static compaction study have been summarized in Table 3.1. This table lists the compaction pressure used in each test, together with the average dry density and average water content of the resulting soil specimens. The final heights of the specimens after compaction were used to calculate the height of the diameter ratios tabulated in the second column of the table. Variation of the height to diameter ratio for a given mold size simply means that the full height of the mold was not utilized. The symbols in the final column of this table indicate those specimens which were cut into smaller pieces to study the distribution of dry density, and other special test conditions. In the case of series A and B, the force required to extrude the sample from the mold was measured. With series A, the extrusion force ranged from about 70 lbs for the wetter samples up to 140 lbs for the dryer samples. With series B, the extrusion force ranged from about 100 lbs for the wetter samples to approximately [illegible] lbs for the dryer specimens.

Curves of dry density as a function of compaction pressure, obtained from constant observations during each compaction test, have been plotted in Figure 3.4. Figure 3.5 through 3.9 present data on the variation of dry density and degree of saturation throughout the several samples which were cut into smaller pieces. Data regarding the range of variation of dry density have been summarized in Table 3.2. Table 3.3 presents data regarding the effect of repeated application of the compaction pressure upon the dry density.

Table 3.1

STATIC COMPACTION TEST PROGRAM

Test	Ratio height to diameter	Compaction pressure lb/in^2	Average dry density lb/ft^3	Average water content percent	Note
A-1	2.14	237	101.8	21.8	b
A-2	2.14	189	100.5	22.1	b
A-3	2.14	112	96.4	24.7	b
A-4	2.14	216	100.0	24.0	bcd
A-5	2.14	218	98.0	25.0	bcd
A-6	2.14	226	101.0	21.5	ac
A-7	2.14	233	101.5	21.3	ac
A-8	1.09	1090	100.0	25.2	ae
A-9	1.18	263	101.5	23.2	ae
A-10	1.10	1755	110.8	19.1	ae
B-1	1.12	169	101.5	23.1	a
B-2	1.12	168	100.5	22.0	ac
B-3	1.12	167	100.5	22.2	ac
B-4	1.12	179	99.0	19.8	ac
B-5	0.56	291	99.5	25.1	a
B-6	0.62	306	108.0	20.5	a
B-7	0.69	200	99.2	19.0	a
B-8	0.19	200	99.0	25.8	af
B-9	0.75	200	99.5	25.0	acf
B-10	0.93	117	97.5	25.8	af
C-1	0.45	227	99.7	24.8	ac
C-2	0.79	271	101.3	24.2	ac
C-3	0.81	370	96.0	27.5	ac
C-4	1.00	274	96.8	26.6	ac
D-1	0.80	264	97.8	25.8	ac
D-2	0.77	271	99.4	25.3	ac
D-3	0.41	271	105.0	21.8	ac

Table 3.1

STATIC COMPACTION TEST PROGRAM

Notes

a Compaction from top end only

b Compaction from both ends

c Samples cut into parts for density and water content determinations

d Density based upon water content established during preparation

e Soil squeezed out around piston during last stages of compaction

f Compaction pressure repeated several times

Kaolinite layer at approximately mid-height

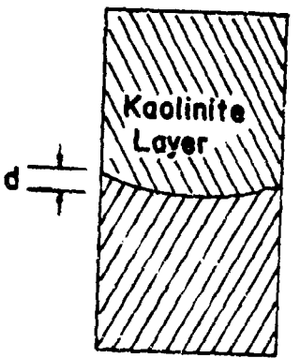

Cross section through sample after extrusion.

Mold	Water Content per cent	Dry Density lb/ft³	d in
A	23.2	98.2	0.02
A	21.5	86.5	0.04
B	23.0	97.4	0.02

FIGURE 3.3 EFFECT OF SIDE FRICTION

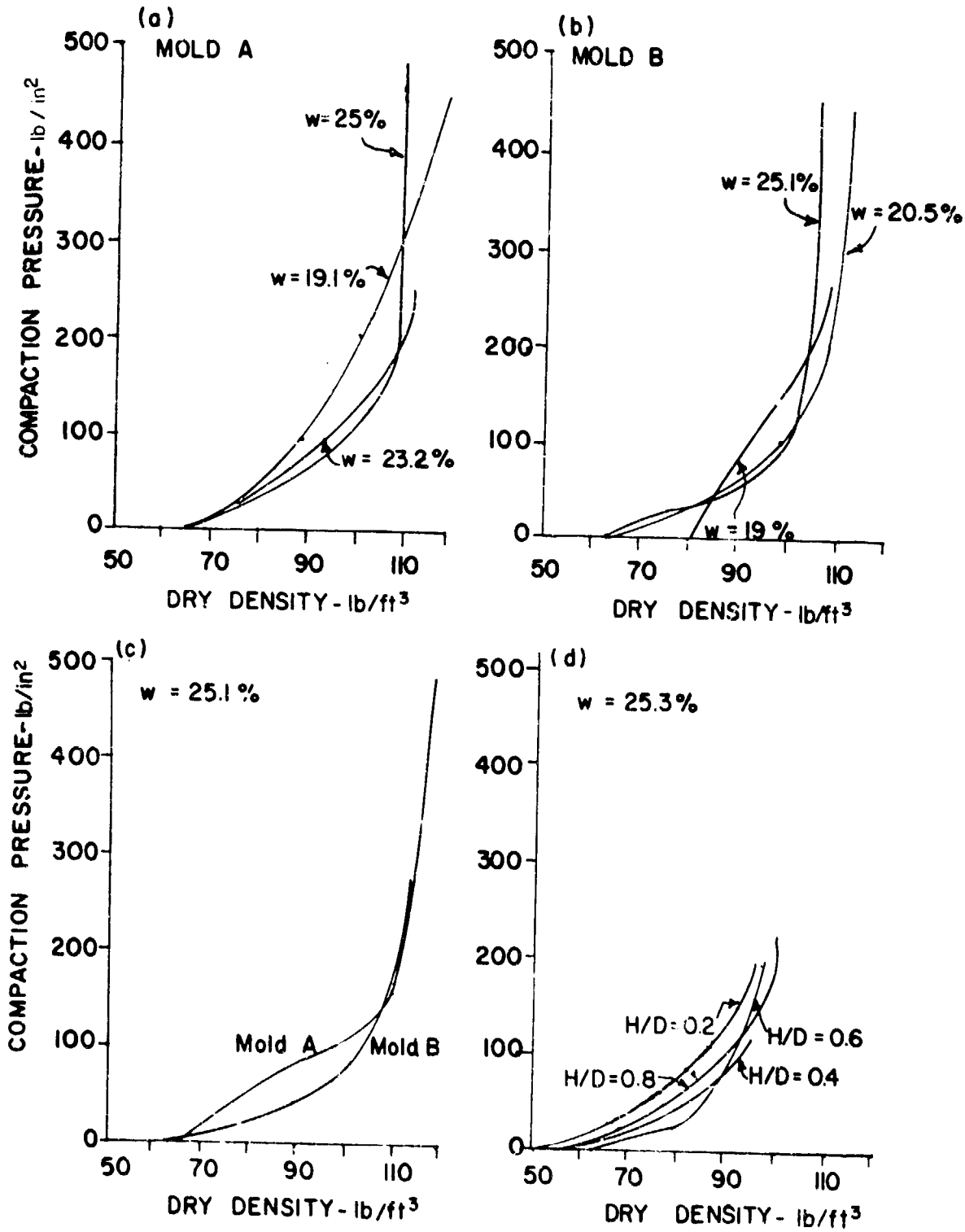

FIGURE 3.4 DRY DENSITY VS. COMPACTION PRESSURE

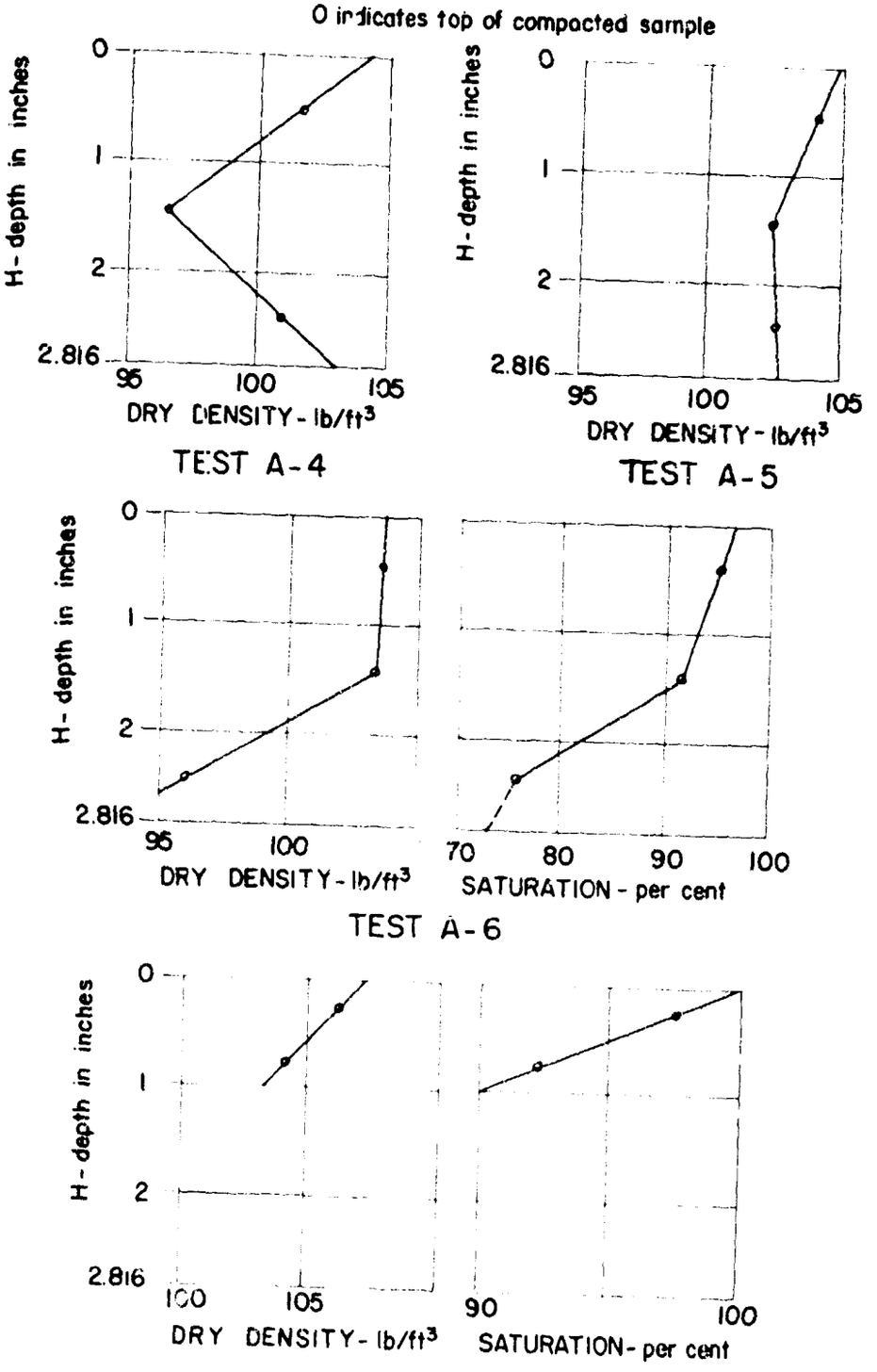

FIGURE 3.5 VARIATION OF DENSITY IN TEST SERIES A

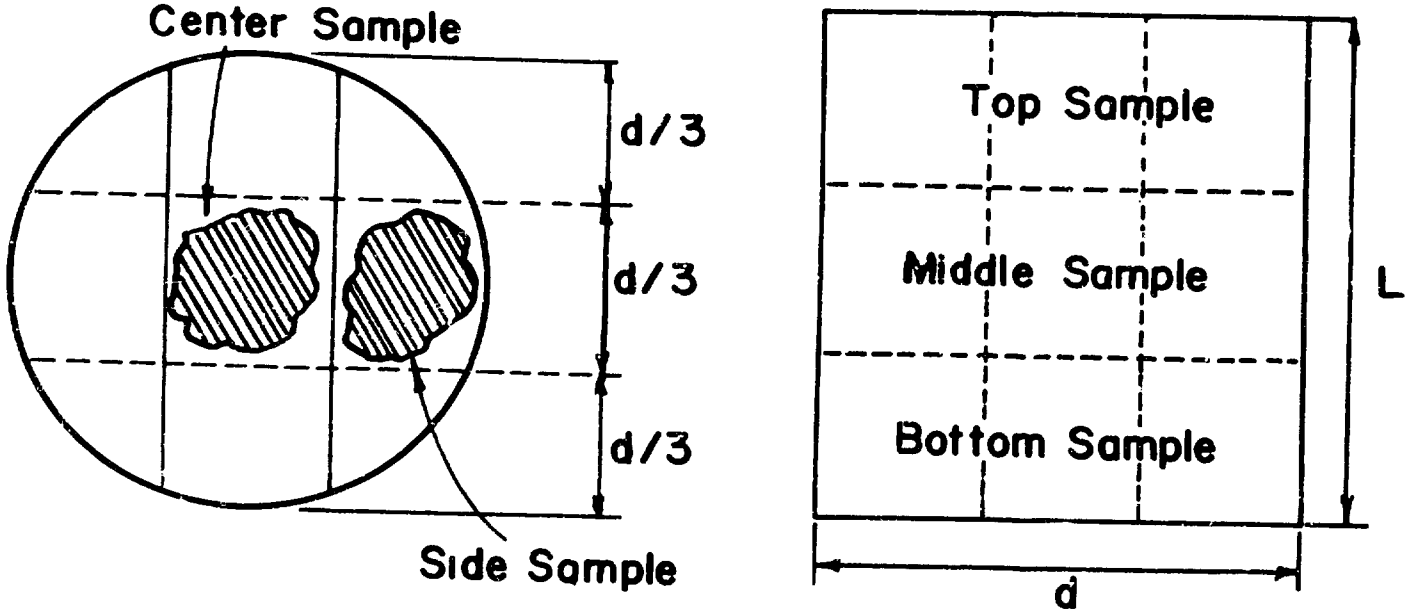

SERIES - B d = 2.5"; L = 2.816"
SERIES - C d = 6.0"; L varies

FIGURE 3.6 METHOD OF SLICING LARGER SPECIMENS

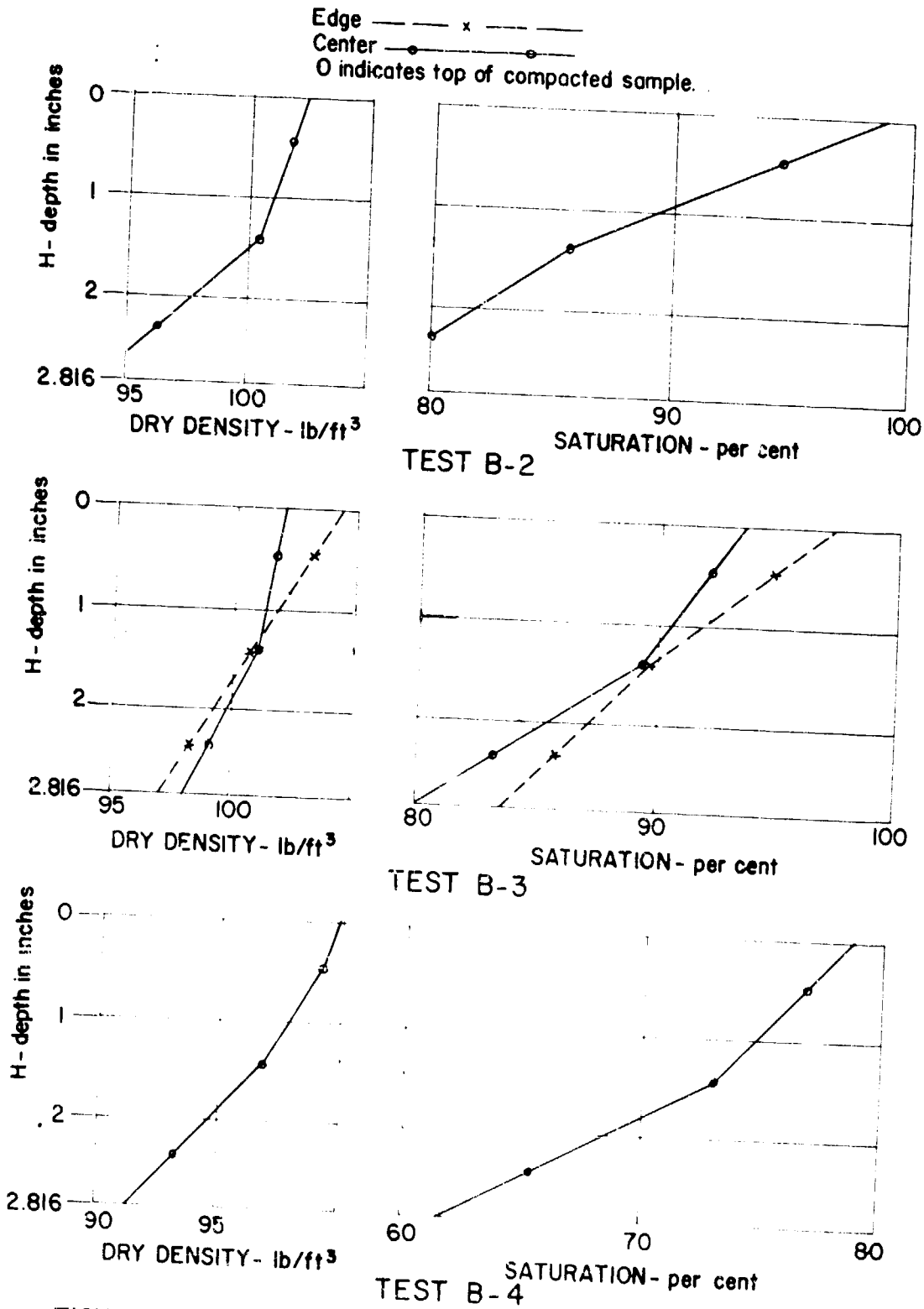

FIGURE 3.7 VARIATION OF DENSITY IN TEST SERIES B

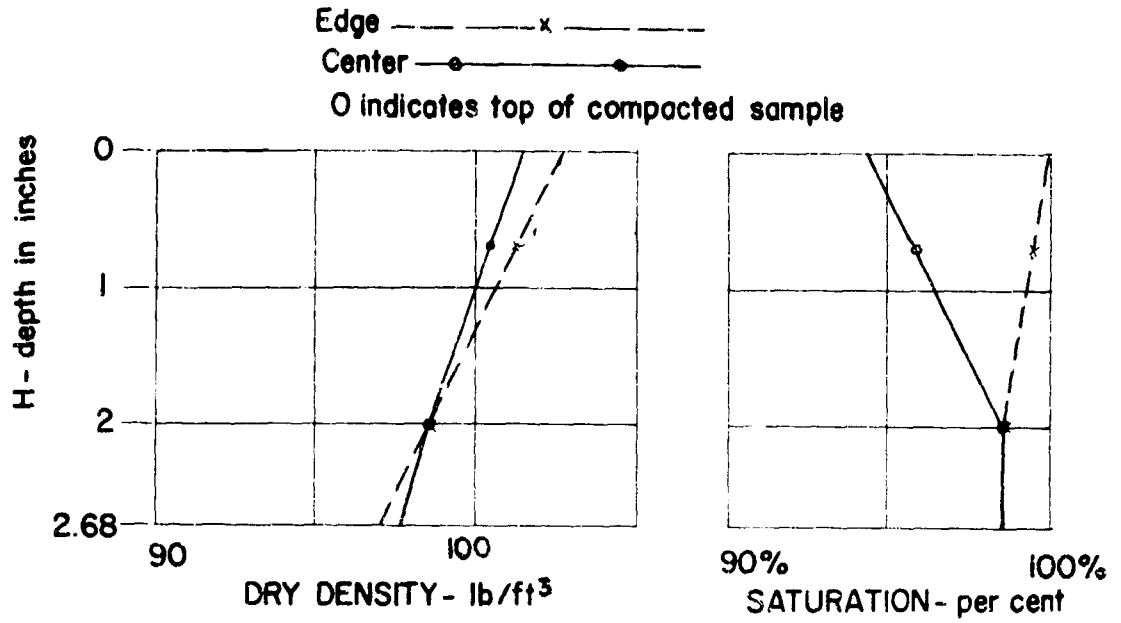

TEST C-1

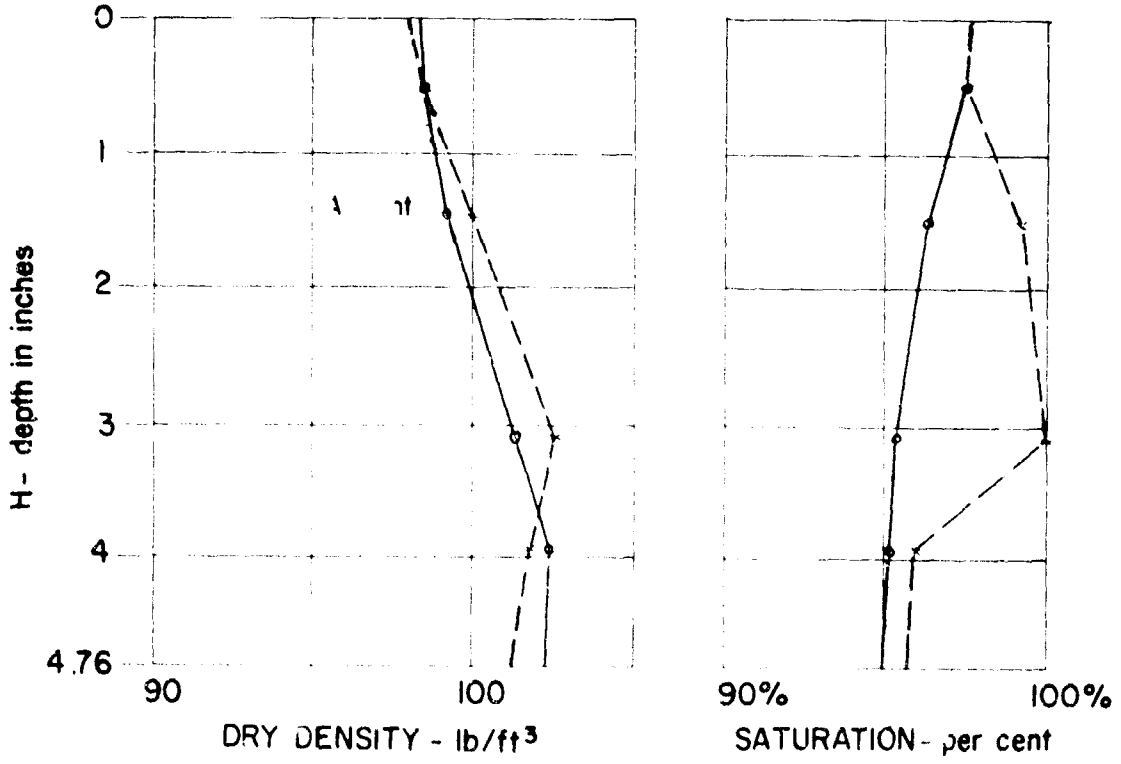

TEST C-2

FIGURE 3.8 VARIATION OF DENSITY IN TEST SERIES C

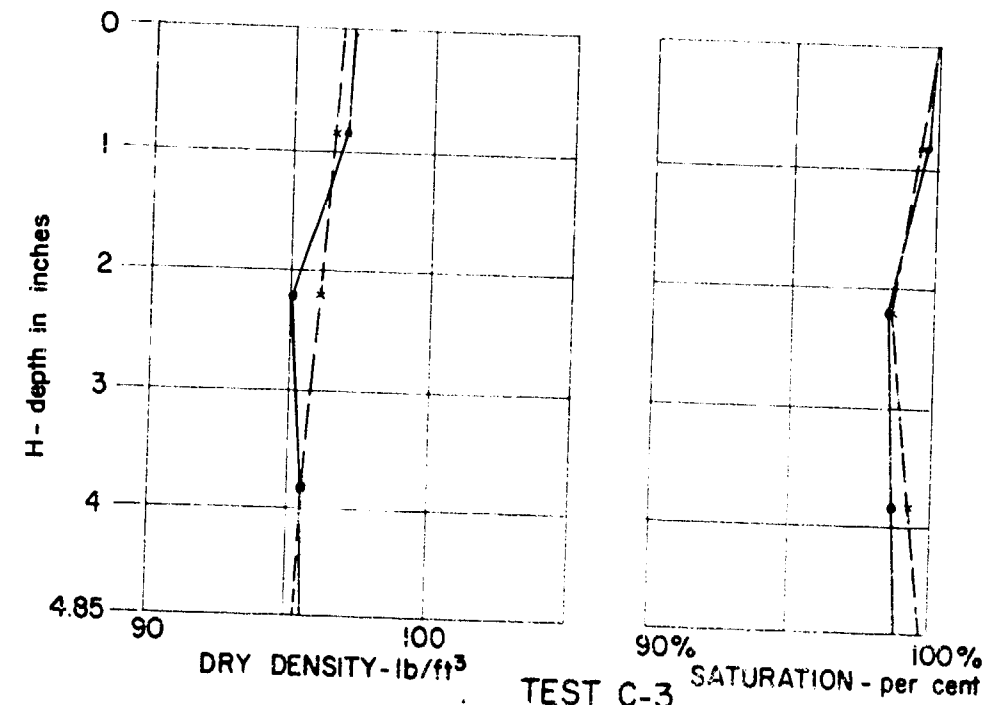

TEST C-3

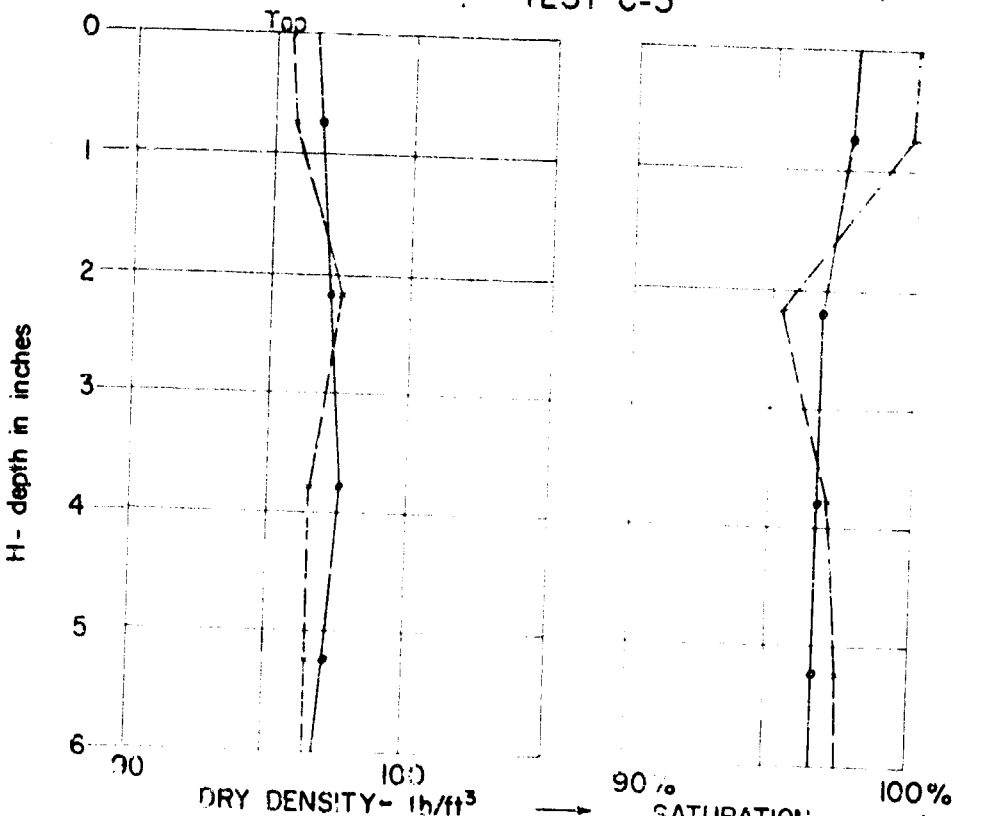

TEST C-4

FIGURE 3.8 cont.

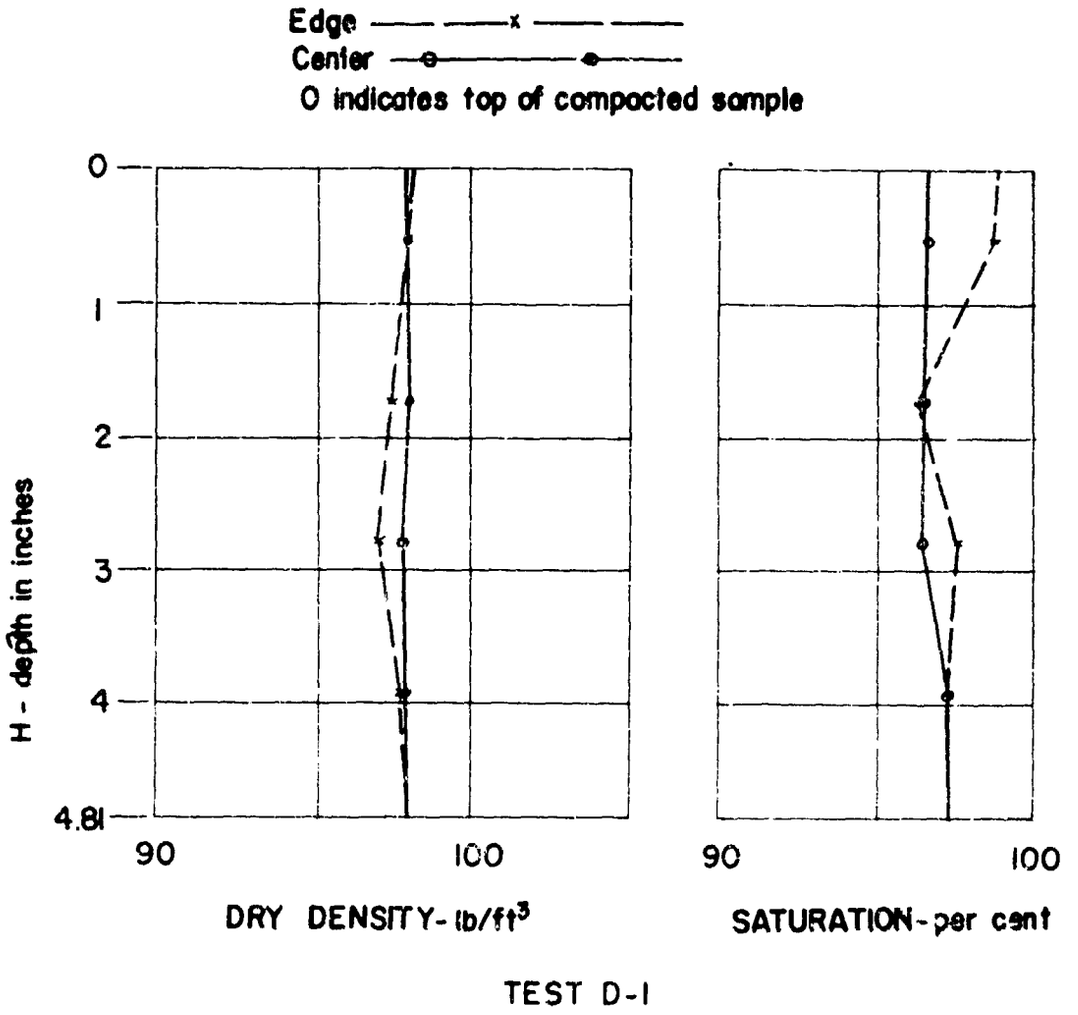

FIGURE 3.9 VARIATION OF DENSITY IN TEST SERIES D

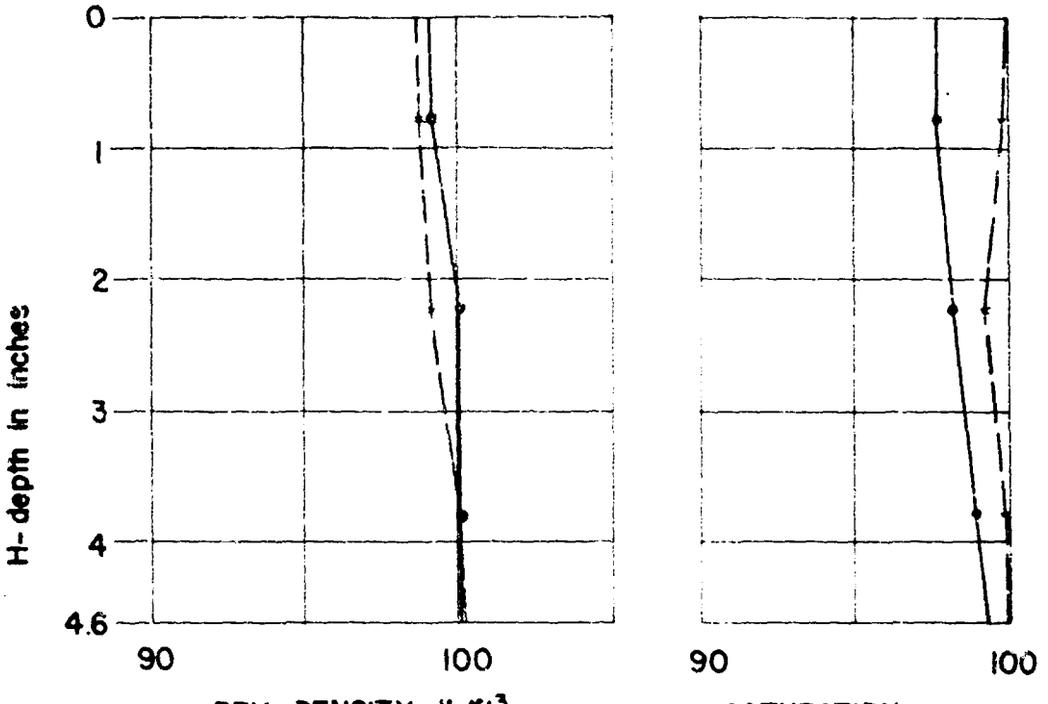

TEST D-2

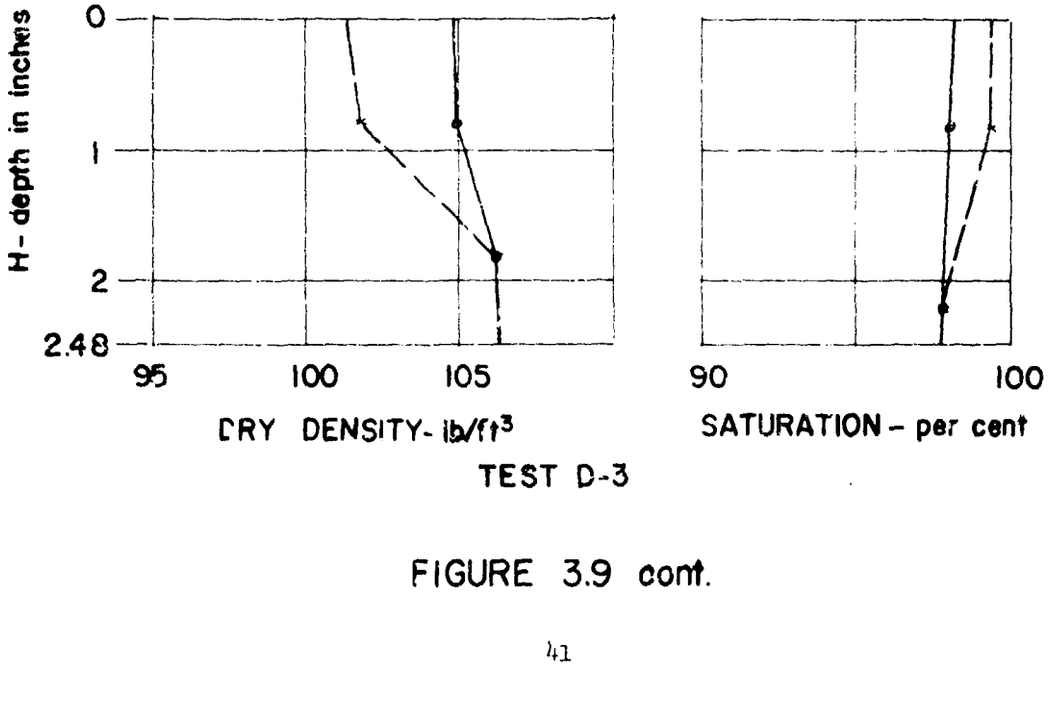

TEST D-3

FIGURE 3.9 cont.

Table 3.2

RANGE OF DRY DENSITY VARIATION

Test	Ratio height to diameter	Compaction pressure lb/in^2	Ave. water content percent	Range of dry density lb/ft^3
A-6	2.14	226	21.5	7.5
A-5	2.14	216	24.0	5.1
B-4	1.12	179	19.8	5.9
B-2	1.12	168	22.0	5.5
B-3	1.12	167	22.2	5.1
C-4	1.00	274	26.6	4.6
C-2	0.79	271	24.2	3.7
B-8	0.75	200	25.0	0.1
D-2	0.77	271	25.3	1.0
D-1	0.80	264	25.8	0.8
C-3	0.81	370	27.5	1.3
D-3	0.41	271	21.8	1.2
C-1	0.45	227	24.3	2.8

Table 3.3

EFFECTS OF REPEATED COMPACTION TO SAME PRESSURE

Test No.	Water content percent	Compaction pressure lb/in^2	Dry density lb/ft^3	
			Loading once	reloading four times
B-8	25.8	200	99.0	99.0
B-9	25.0	200	99.5	99.7
B-10	25.8	117	97.5	97.8

3.3 Discussion of test results

3.3.1 Compaction pressure

One of the objectives of this study was to determine a suitable compaction pressure for use in future work. The requirements for a suitable compaction pressure are: (1) that it provide a reasonably dense sample, although the density need not match that achieved by any other compaction process; (2) that it provide, for a given molding water content, substantially the same density regardless of small variations of the height to diameter ratio sample, or in dimensions of the compaction mold; and (3) that it be reasonable from the standpoint of available loading equipment.

The pressure required to meet these specifications can be judged from the curves plotted in Figure 3.4. Parts (a) and (b) of this figure show pressure versus dry density curves as a function of water content for molds A and B. When a curve of pressure versus dry density approaches a vertical line, it means that the sample has become substantially saturated, i.e. that application of the compaction pressure has caused all of the pore air to go into solution.* The compaction pressure required to achieve complete saturation is a function of the molding water content of the sample, being smaller for the samples with the higher water content. It may be seen that a compaction pressure of 200 lb/in^2 achieves very close to a state of complete saturation, except for the driest samples. In Figure 3.4(c), pressure versus dry density curves for samples compacted at the same water content but in different molds have been plotted. It may be seen that the mold size influenced the early portion of the curve, but for pressure in excess of 200 lb/in^2 the same density was achieved in both molds. Figure 3.4(d) shows the effect of the height to diameter ratio upon the pressure versus dry density curves. The early portions of these curves are different

*When the compaction pressure is removed, some of the air will come out of solution and thus the degree of saturation as measured after the sample is extruded from the mold will be somewhat less than 100%.

for the different height to diameter ratio, but once again the curves substantially coincide for pressures greater than 200 lb/in^2.

From these results, it is concluded that the requirements upon compaction pressure can be met through use of a pressure of 200 to 250 lbs/in^2. Curves of dry density as a function of molding water content obtained for compaction pressures in this range have been plotted in Figure 3.2(b). When the smaller height to diameter ratios are used, the static compaction at this pressure leads to a sample more dense than that obtained with the Harvard Miniature compaction procedure. The difference is small for water contents well wet of optimum water content, but is quite large for the drier samples. As mentioned earlier, there is at this stage no requirement that the densities obtained by static compaction coincide with those obtained by other procedures. Static compaction to 200 or 250 lbs/in^2 will provide samples well suited for research into time effects during one-dimensional pressure. Not only is there no benefit in using higher pressures, but there is a possible disadvantage in that soil may be squeezed out between the edge of the loading piston and the mold. Such a squeezing action was observed when the compaction pressure exceeded 300 lb/in^2, especially with the higher water contents and faster rates of compression.

3.3.2 Uniformity of density

The tests in which the thin layer of kaolinite was used to study the pattern of strains throughout the sample illustrated that great care must be given to the height to diameter ratio in any method wherein uniformity of density is being sought. The patterns of strains being observed in these tests provide a good visualization of the stress distribution, of the soil particle movement pattern, and of the role of wall friction during compaction process.

Examination of the data in Figures 3.5, 3.7, 3.8, 3.9, and in Table 3.2 points out the influence of the height to diameter ratio and of

the molding water content upon the variation in dry density and degree of saturation throughout the samples. Samples with a height to diameter ratio greater than 1 invariably showed large variations in dry density. Ratios on the order of 0.5 were small enough to reduce the density variations to very low values. The effect of height to diameter ratio also is shown in Figure 3.2(b), wherein it may be seen that, for the drier samples, high densities can be achieved only through use of relatively thin samples. Increasing the water content with a given height to diameter ratio will lead to more uniform density conditions. The wetter soils can more readily undergo plastic flow and thus achieve the necessary redistribution of stress in order to provide uniform density conditions. The mold which had a Teflon liner showed smaller variations in the dry density than the unlined mold of the same size. However, the lined mold did not give higher average dry densities than those obtained using the uncoated steel mold under similar conditions of water content, pressure, and height to diameter ratio. This circumstance is undoubtedly the result of the fact that the maximum dry density is limited to that value corresponding to a degree of saturation of 100%.

In all cases where the specimen was sub-divided longitudinally as well as transversely, the saturation was found to be higher at the edge than at the center of the compacted sample. There was, however, no consistent relationship between the densities at the center and edges of the samples.

The results given in Table 3.3 show that the density of a compacted clay will not increase appreciably if the clay is reloaded to its original compaction pressure. Thus a sample can be built up in layers, and the density of the lower layers will not change as each overlying layer is compacted.

The studies indicate that sufficient uniformity and density can be achieved through use of Teflon lined molds and height to diameter ratios smaller than 0.6.

3.4 Recommended static compaction procedure

Based upon the foregoing studies and upon general experience with the problem of laboratory compaction, the following procedures are recommended. Strictly speaking, these specifications apply only to work with the backswamp clay, and some further study will be needed when specimens of other soils are to be prepared.

(a). General requirements

(1). The loading frame which will apply the static compaction pressure should have a capacity of 250 lb/in^2, i.e., 20,000 pounds for a sample 10 inches in diameter. It should be possible to move the piston at a rate of 0.1 to 0.2 inches per minute, or preferably to control the rate of pressure increase to 20 lb/in^2 per minute.

(2). The interior wall of the compaction mold and the contact surface of the plunger head should be coated with a substance such as Teflon.

(b). Compaction procedure

(1). Mix a quantity of soil at the desired moisture content (usually within ± 2 percent of the optimum moisture content). Seal this soil-water mixture and allow it to equilibrate for at least 18 hours.

(2). Calculate the wet soil weight required for each layer. The calculation is based on the desired layer thickness and expected dry density of the soil. The maximum thickness of each layer after compaction should be no more than 6 inches in a 10 inch diameter mold.

(3). The wet soil is placed evenly in the mold and compacted statically to the volume desired, or alternatively, to a

pressure of from 200 to 250 lb/in^2.

(4). Scarify each compacted layer surface gently before placing subsequent layers.

(5). If the subsequent layer is not to be placed immediately, the compacted soil surface should be sealed using aluminum foil. In case of a long interruption, spray a very small amount of water on the scarified surface prior to placing the subsequent layer.

(6). A check should be made as to whether soil is being squeezed out between plunger head and mold during compaction. If so, the compression rate should be decreased accordingly.

Chapter 4

RAPID ONE-DIMENSIONAL COMPRESSION TESTS

4.1 Objective and scope of test program

MIT (1959b) reported upon a series of one-dimensional compression tests upon a fat backswamp clay, with a rise-time for the load approximately 100 milliseconds. The specimens used for these previous tests were prepared by a dynamic procedure which gave relatively low densities, and substantially all of the samples were compacted at water contents well wet of the optimum.

The same soil* was used for the series of tests reported in this chapter, but now static compaction was used at water contents both dry and wet of the optimum. Significantly greater dry densities were obtained in these new tests, and these great densities in turn meant a less compressible soil than in the previous tests. A simple modification was made to the loading apparatus and the rise-time of the load was reduced to about 30 milliseconds.

The test series involved six different samples, four of which were subjected to multiple loadings. The series is summarized in Table 4.1.

4.2 Apparatus and instrumentation

Certain changes were made in the apparatus used for the earlier program. The improved set-up is shown in Figure 4.1. The major improvements are described in the following sub-sections.

---

* The clay from the present tests came from Barrel 7.

Table 4.1

SUMMARY OF RAPID ONE-DIMENSIONAL COMPRESSION TESTS

(1) Test No.	(2) Dry Density lb/ft^3	(3) Water Content (w) percent	(4) Degree of Saturation (S) percent	(5) Initial Pressure (p_i) lb/in^2	(6) Time of p_i Applied (t_i) min.
E-1-a	97.0	26.3	96.4	15	30
E-1-b	"	"	"	"	"
E-2	97.0	17.7	64.8	15	30
E-3	103.5	21.6	94.1	15	30
E-4-a	99.5	24.9	97.2	10	30
E-4-b	"	"	"	"	"
E-5-a	99.5	12.5	44.4	10	30
E-5-b	"	"	"	"	"
E-6-a	90.5	30.0	94.0	10	30
E-6-b	"	"	"	"	"
E-6-c	"	"	"	"	"

Table 4.1 (cont.)

SUMMARY OF RAPID ONE-DIMENSIONAL COMPRESSION TESTS

(1) Test No.	(7) Pressure Increment (Δp) lb/in^2	(8) Pressure Rise-Time (t_r) milliseconds	(9) Immediate Deformation (ΔH_{30}) 1/1000 inch	(10) Deformation at end of one min. (ΔH_f) 1/1000 inch	(11) Amount of Creep ($\Delta H_f - \Delta H_{30}$) 1/1000 inch	(12) Creep-Ratio $\frac{\Delta H_f - \Delta H_{30}}{\Delta H_f}$ percent
E-1-a	35	30	3.0	9.3	6.3	68
E-1-b	"	30	~3.0	8.3	5.3	64
E-2	40	30	1.6	6.3	4.7	75
E-3	60	30	1.2	4.6	3.4	74
E-4-a	40	40	"	4.0	"	"
E-4-b	"	40	1.3	3.8	2.5	66
E-5-a	40	30	"	6.0	"	"
E-5-b	"	25	1.7	3.4	1.7	50
E-6-a	40	30	7.5	15.0	7.5	50
E-6-b	"	25	5.3	11.2	5.9	53
E-6-c	"	30	~5.3	10.8	5.5	51

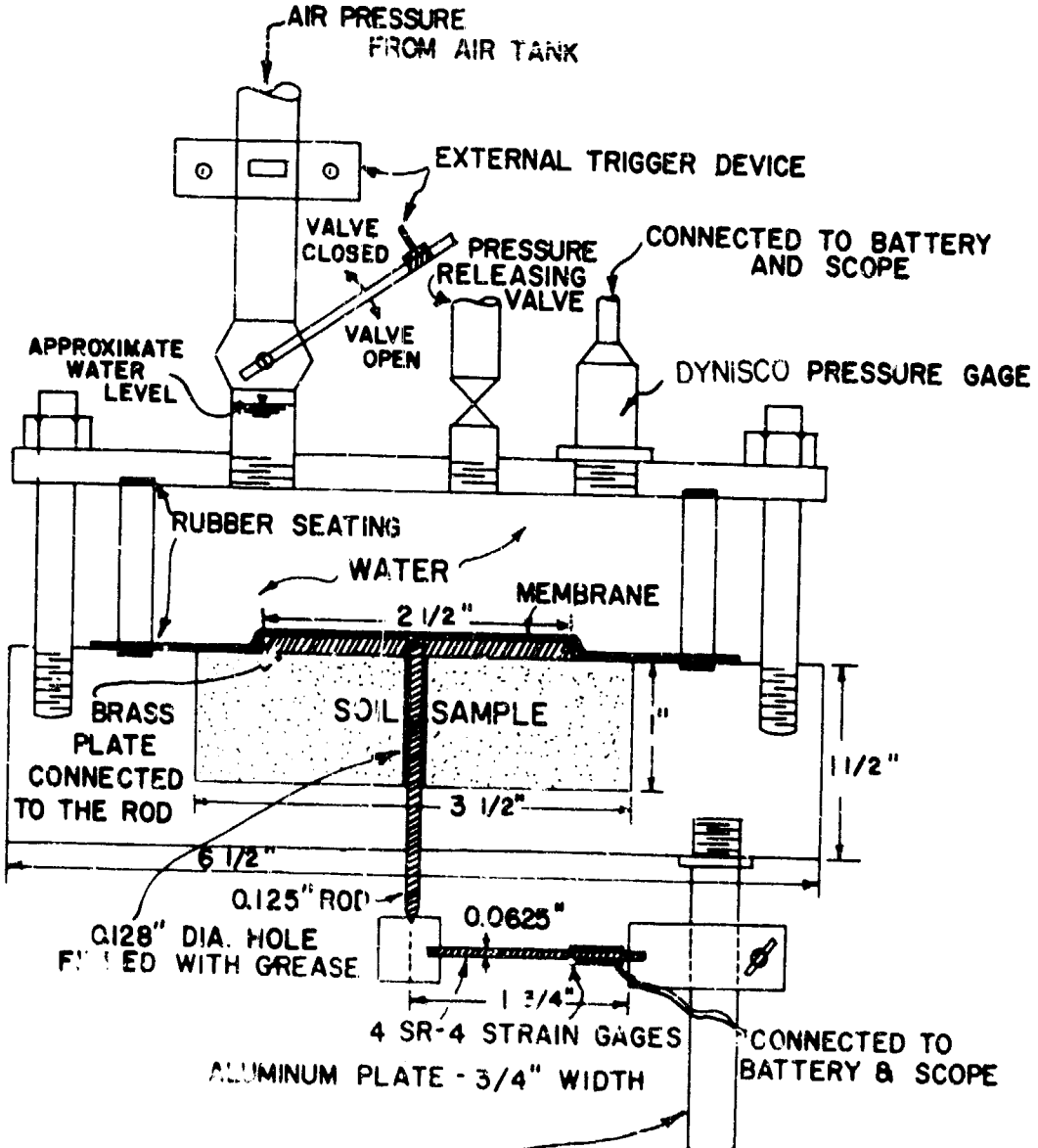

FIGURE 41 IMPROVED TESTING APPARATUS

4.2.1 Improved rise-time

As is indicated in Figure 4.1, the chamber immediately above the soil sample was filled with water up to the level of the actuating needle valve. Because relatively incompressible water has replaced compressible gas in this chamber, less flow of gas through the valve is required to bring the pressure up to any specified level.. Figure 4.7, appearing later in this chapter, contains a typical pressure vs. time record. It is seen that the pressure rises to approximately 85 percent on its final level in about 30 milliseconds, but requires another 75 milliseconds to reach the final pressure level.

4.2.2 Deflection gage

Improvement of the strain measuring system was required for several reasons. Now that water is used in the chamber immediately above the soil sample, leakage would become a serious problem if the sensing rod of the strain measuring system passed out through the chamber ceiling as before. The linear potentiometer used for the previous work had a sensitivity as was desired for such work. Moreover, the linear potentiometer had a "step-strain" response which made it somewhat difficult to interpret the strain vs. time records.

To overcome the first of these problems, it was decided that the sensing rod of the strain measuring system should pass through the sample and out through the base of the test cell. The system thus consists of a disc on top of the test specimen, with a rod attached to the disc and passing through the soil sample and cell base. It is felt that the rod located in this position has very little influence upon the response of the soil sample. For long duration tests, it is possible that pore fluid might leak through the bushing in the base of the cell, thus leading to partial drainage of the soil sample. For short duration tests, this is no problem.

Figure 4.2 shows the details of a new cantilever type strain gage

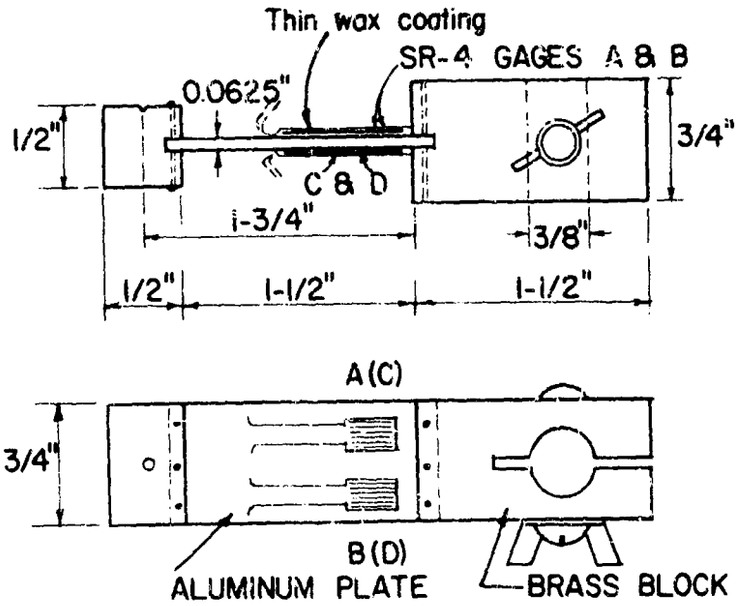

FIGURE 4.2 CANTILEVER DEFLECTION GAGE

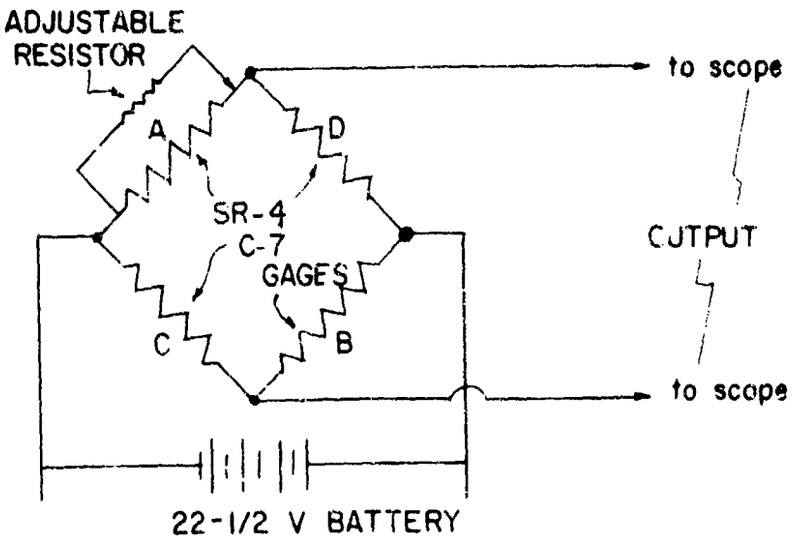

FIGURE 4.3 WIRING CIRCUIT FOR DEFLECTION GAGE

which was designed for the present work. The body of the gage is aluminum plate with a thickness of 0.0625 inches. A piece of metal bearing a center punch hole is rigidly attached to the outer end of the cantilever beam, and serves to assure that the sensing rod contacts the beam at the same location in each test. Four SR-4 type C-7 wire resistance gages were fastened tightly on both surfaces of the cantilever near the fixed end, and given a protective coating of wax. A standard Wheatstone bridge wiring arrangement was used, as it is indicated in Figure 4.3. The system was driven by a 22.5 volt dry cell and the calibration was obtained using a very sensitive X-Y recorder. It was found that the response of the deflection gage was stable and exhibited a straight line relationship between deflection and voltage output within certain ranges. A series of calibration curves are shown on Figure 4.4. Based upon these curves, an average calibration of 0.00075 in/millivolt has been used for total deflections up to 0.01 inches. Deflections as small as 0.0001 inches can be satisfactorily detected with this gage. Examination of the samples after the leading apparatus was disassembled showed that the disk did not punch into the surface of the sample, and hence all of the measured strains represented compression of the samples.

4.2.3 External triggering

In the present test program, the sweep of the oscilloscope was triggered externally as the needle valve opened to admit pressure to the test cell. This arrangement functioned very well and overcame the difficulties described in connection with the previous work. The same mechanism triggered two oscilloscopes: one used to record strain as a function of time, and the second used to record pressure as a function of time. The pressure applied to the sample was measured by a Dynisco pressure transducer, as described in connection with the previous work. A 6 volt dry cell was used to actuate the pressure gage, and the calibration curve is shown in Figure 4.5.

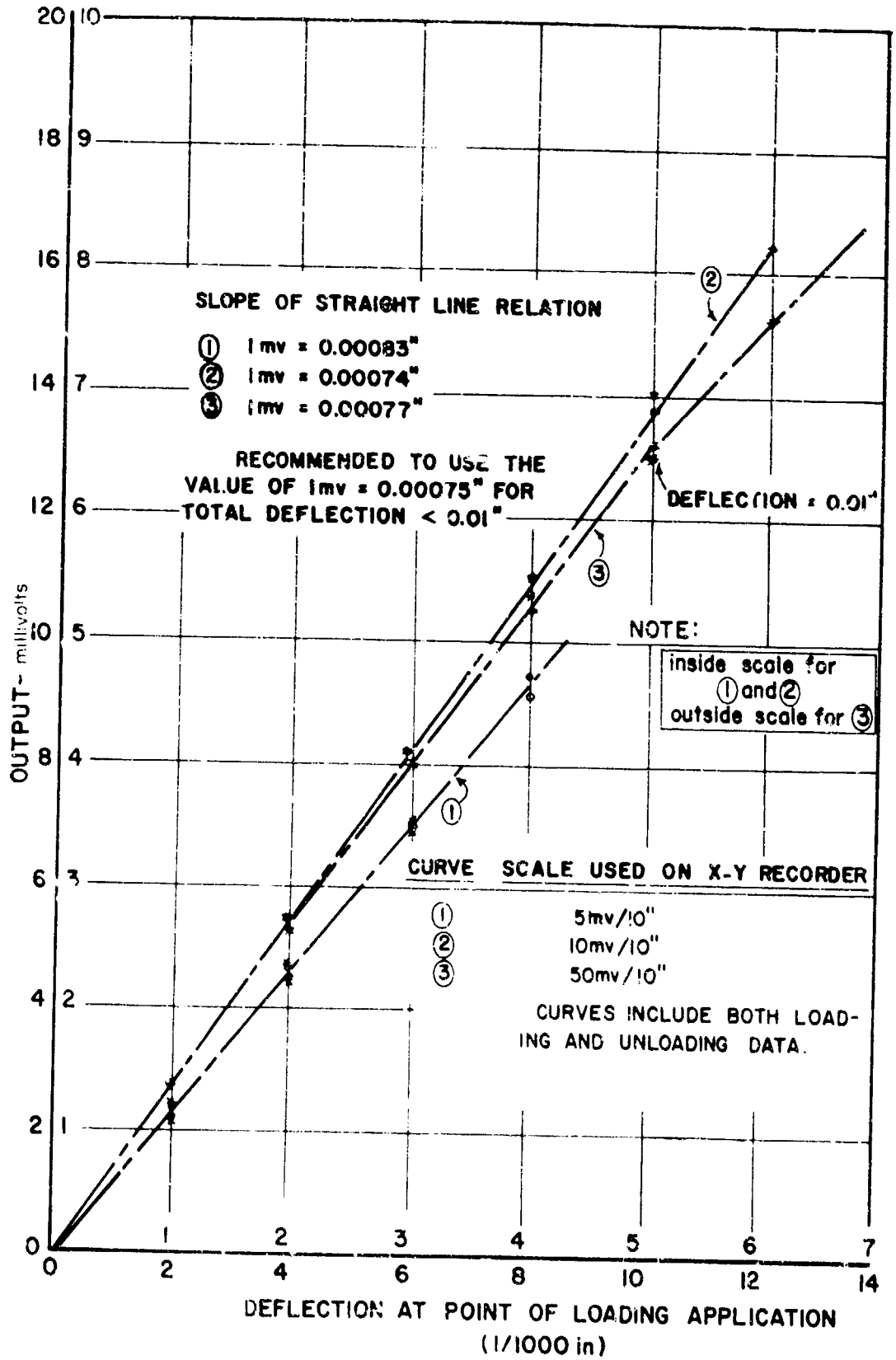

FIGURE 4.4 CALIBRATION CHART FOR DEFLECTION GAGE

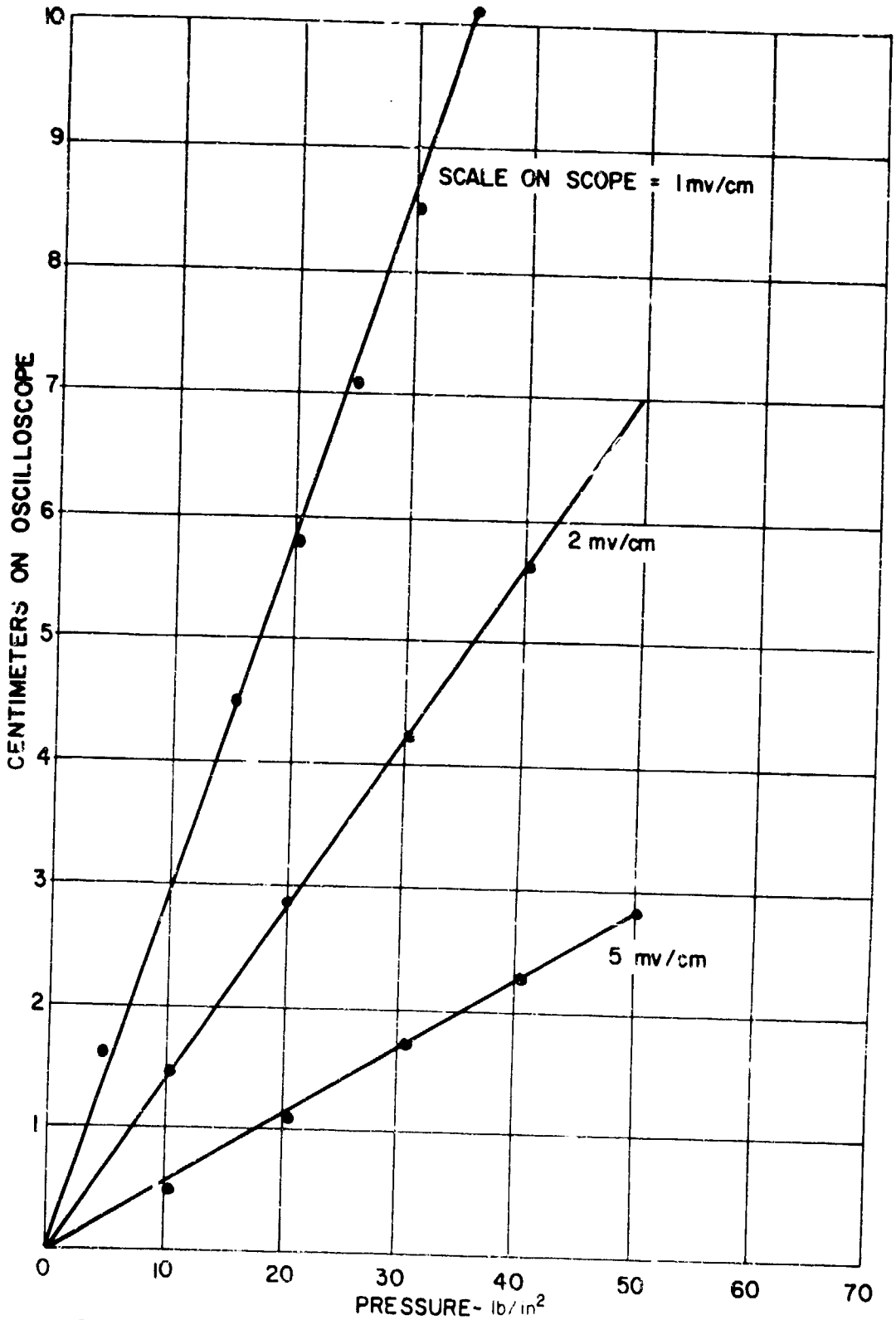

FIGURE 4.5 CALIBRATION CHART FOR PRESSURE GAGE

4.3 Test procedures

A quantity of the clay was brought to the desired water content and allowed to come to equilibrium in the humid room for at least 18 hours. Then the clay was compacted directly into the test chamber by the static compaction method described in Chapter 3. A compaction measure of 200 lb/in^2 was used for all samples, and Figure 4.6 shows the relationship of molding water content to the dry density. A few results obtained in Series G (see Chapter 5) using the same procedures have been included in this figure. Each sample was compacted in a single layer, using a compression rate of approximately 25 lbs/in^2 per minute.

The deflection rod was in place in the sample as compaction took place, with a small recess in the face of the compaction piston so that the rod could protrude above the top of the compacted specimen. After compaction, the top surface of each sample was trimmed flush with the top of the test chamber. The brass plate was screwed in place and the sample immediately sealed by the rubber membrane.

An initial pressure of from 10 to 15 lbs/in^2 was applied immediately after the test cell was properly mounted in the dynamic loading apparatus. This initial pressure was applied for approximately 30 minutes to insure that the strain measuring system was properly seated. Pressure increments of from 35 to 60 lbs/in^2 were then applied by rapidly opening the needle valve between the air tank and the water pressure chamber. In all tests, the oscilloscopes were set to record stress vs. time and strain vs. time. Typical results are shown in Figure 4.7. In four of the tests the pressure was reduced to the initial value and a subsequent dynamic loading applied.

4.4 Discussion of testing results

The results of all tests have been tabulated in Table 4.1. Typical curves of strain vs. the logarithm of time have been plotted in

Figure 4.8. In Figure 4.9, the final strain, immediate strain, and creep ratio have been plotted as a function of the molding water content. Included in Figure 4.8 are results from series 9 (see Chapter 5) and a typical curve from the previous report. Series G results have also been included in Figure 4.9.

A major principle was stated as the result of the previous work: the relative amount of creep strain increases as the total strain decreases; that is, the creep ratio increases as the total amount of strain decreases. In Figure 4.10, curves of creep ratio vs. molding water content obtained in the present work and the previous work are plotted for comparison. In confirmation of the principle, the present tests, which have greater densities and hence are much less compressible, exhibit a significantly higher creep ratio.

A closer look at the data from the present tests suggests that the principle restated above may apply strictly only for compaction on the wet side of the optimum water content. As may be seen in Figure 4.9, the total deformation sustained by a sample is related in a general way to the initial dry density. The minimum total deformation was obtained for a water content slightly on the wet side of the optimum water content. For points further on the wet side of the optimum water content, the soil proved to be quite compressible. As one moved from the optimum water content to water contents on the dry side of the optimum, the compressibility of the sample increased, but the increase was less than on the wet side. Thus, two samples having the same dry density exhibit different compressibilities depending upon whether the sample is compacted wet or dry of the optimum water content. The samples compacted on the dry side are less compressible even though they are less saturated. This result is in line with the theory postulated by LAMBE (1958) concerning the effect of molding water content upon the structure of compacted clays.

The curve of immediate deformation as a function of molding water content shows little if any tendency for the immediate compressi-

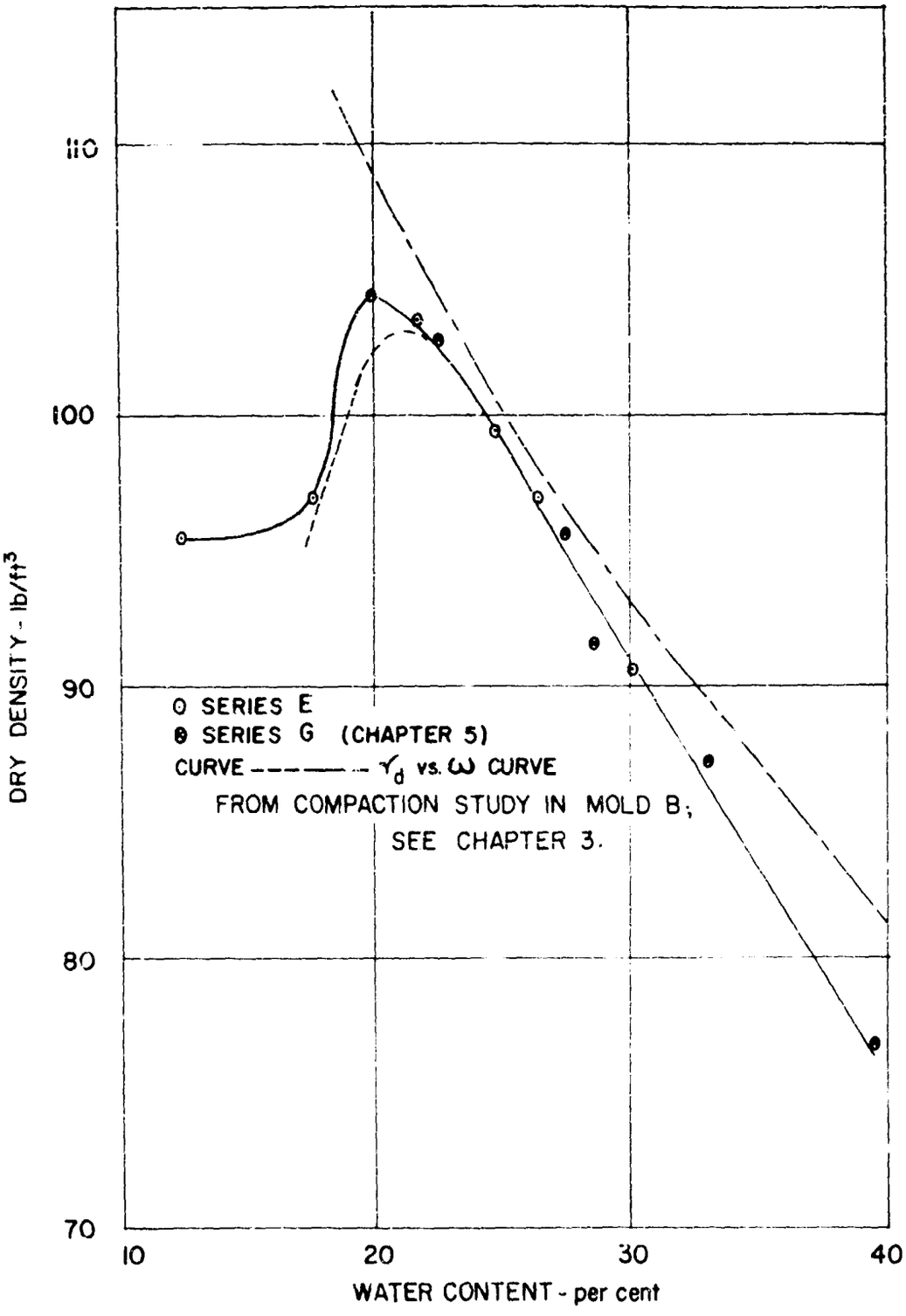

FIGURE 4.6 DRY DENSITY vs. WATER CONTENT

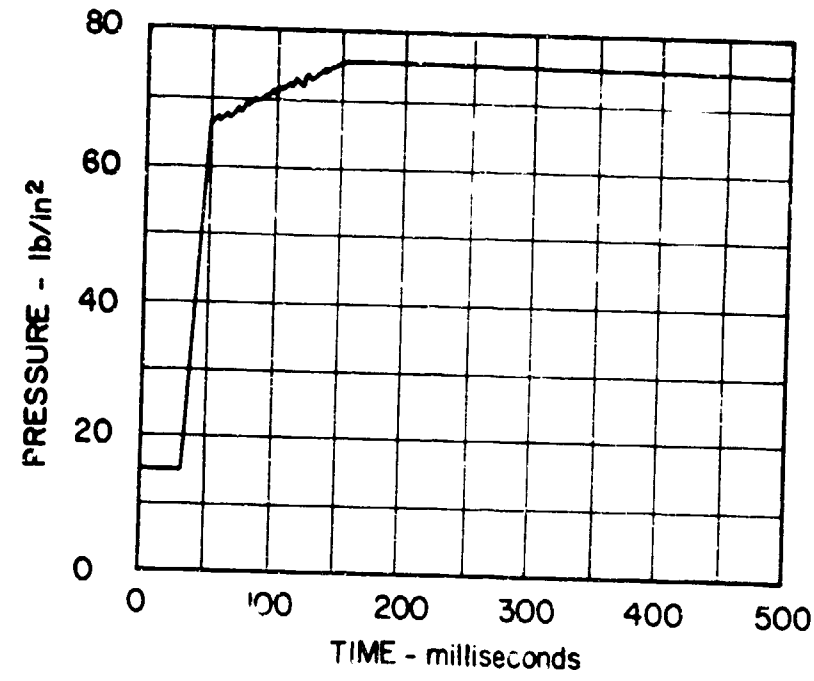

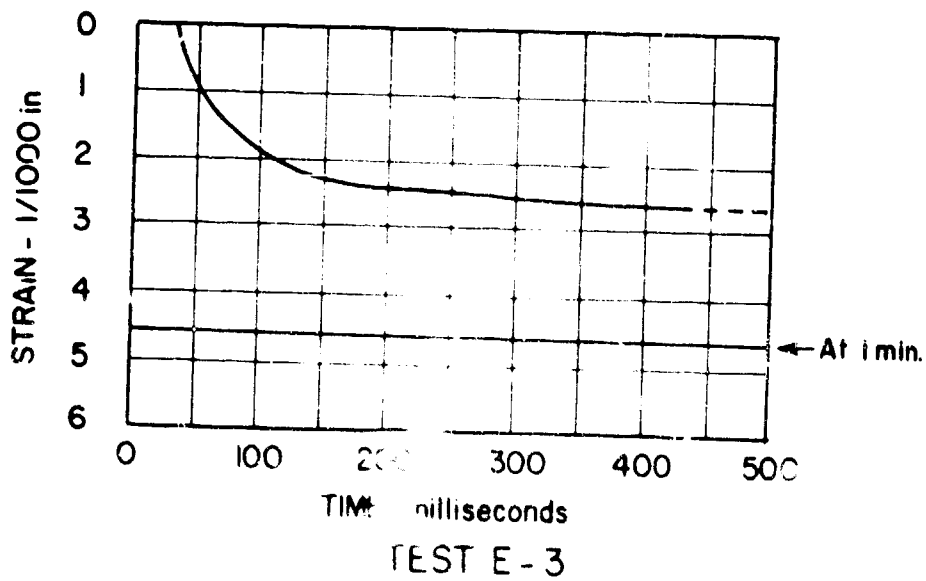

FIGURE 4.7 TYPICAL STRAIN AND PRESSURE VS TIME CURVES

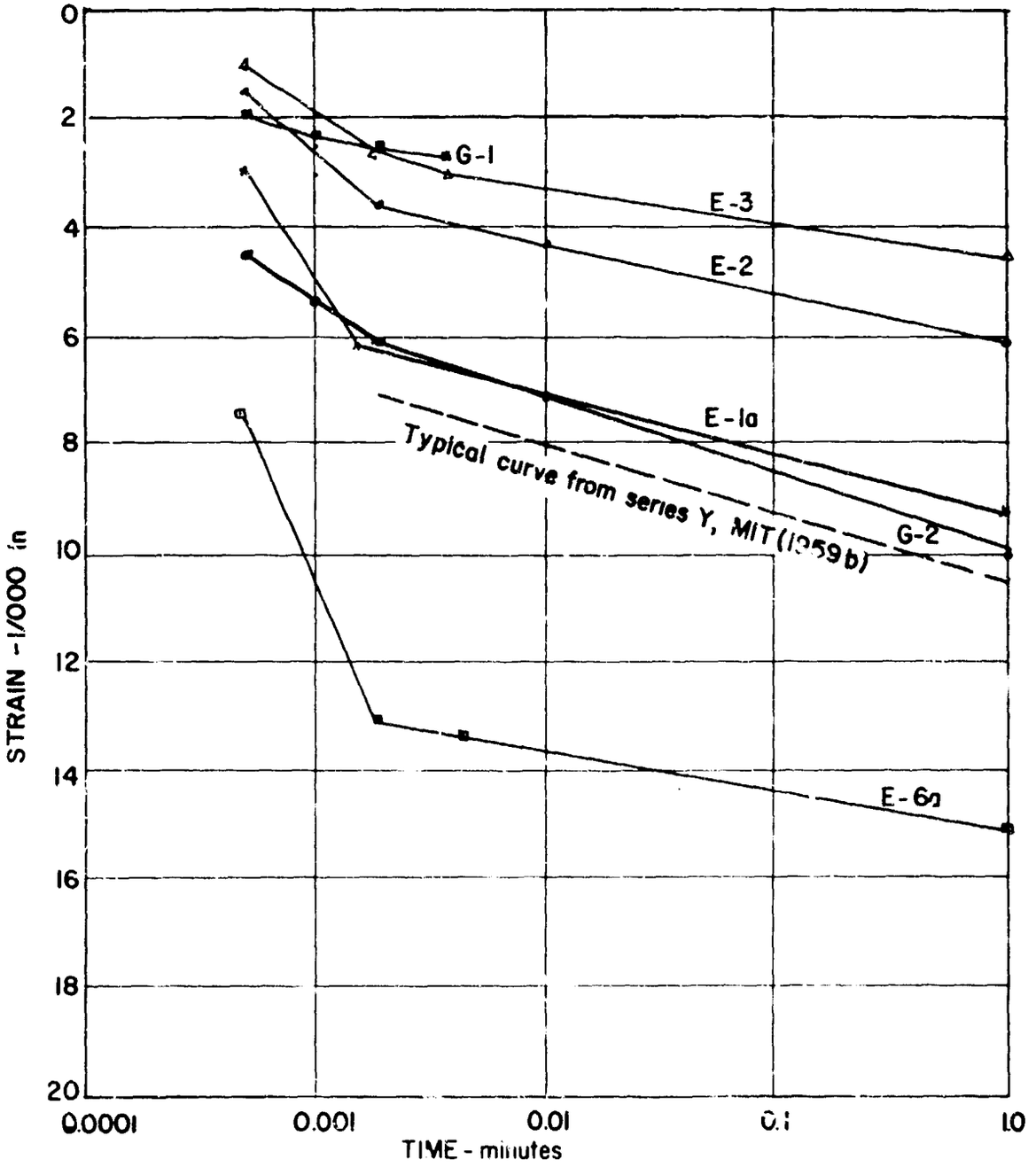

FIGURE 4.8 SUMMARY OF STRAIN VS. TIME CURVES

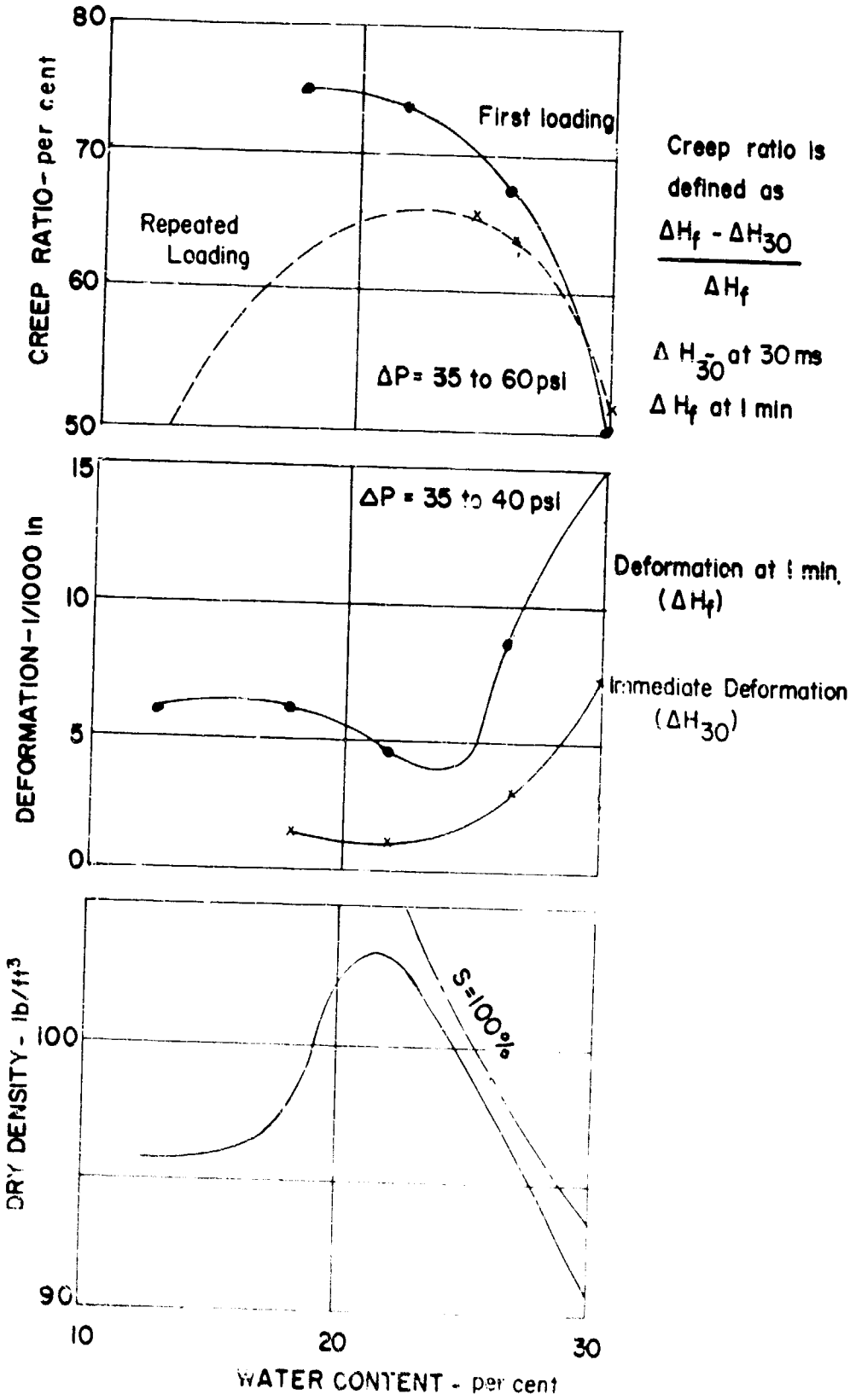

FIGURE 4.9 STRAIN AND CREEP RATIO VS. WATER CONTENT

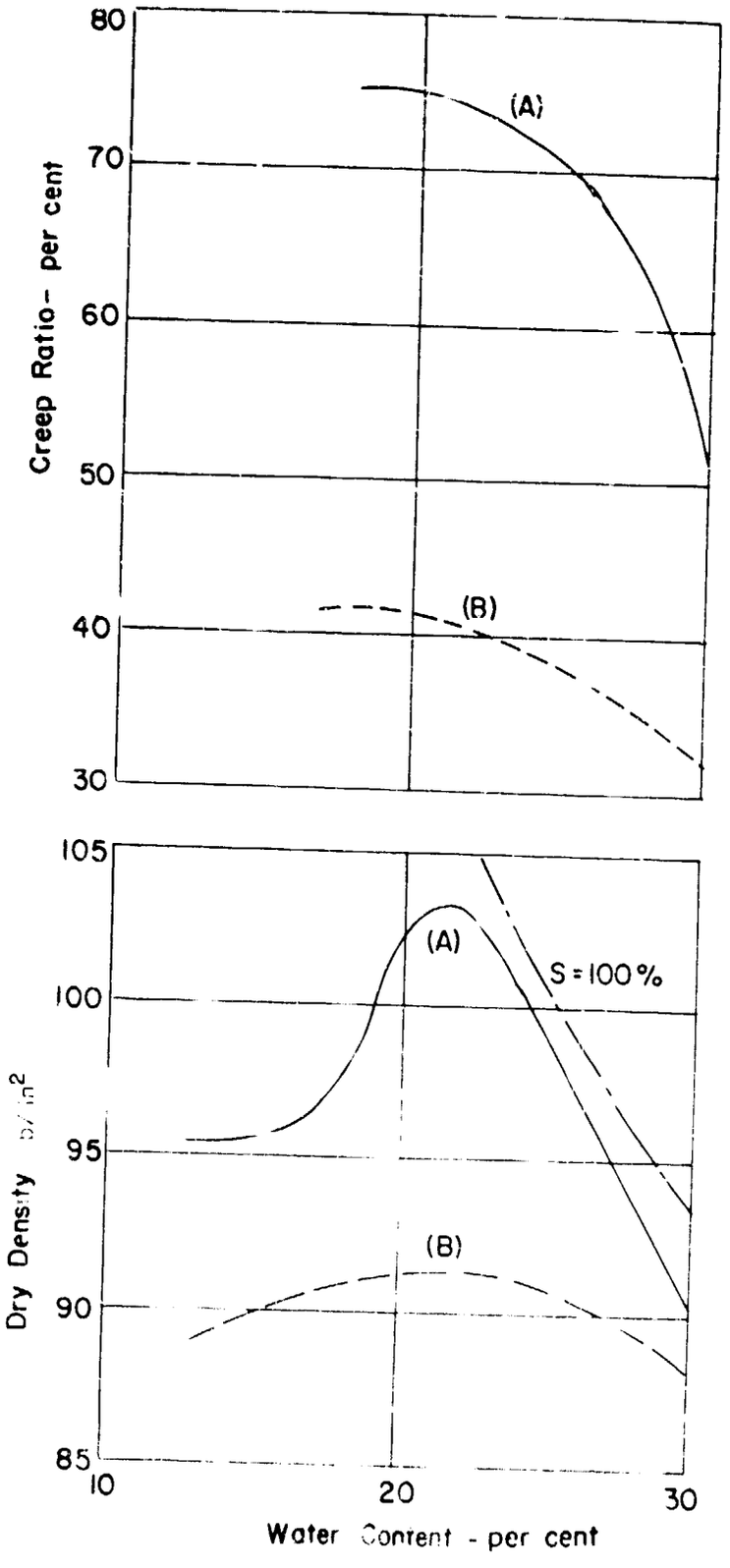

(A) - OBTAINED FROM THIS STUDY WHERE CREEP RATIO IS DEFINED AS

$$\frac{\Delta H_f - \Delta H_{30}}{\Delta H_f}$$

(B) - OBTAINED FROM DYNAMIC REPORT NO. 1959-9 WHERE CREEP RATIO IS DEFINED AS

$$\frac{\Delta H_f - \Delta H_{10}}{\Delta H_f}$$

(A) - BY 200 lb/in^2 STATIC COMPACTION METHOD

(B) - BY EQUIVALENT PROCTOR COMPACTION METHOD

FIGURE 4.10 COMPARISON WITH PREVIOUS WORK

bility to increase as one moves away from the optimum water content on the dry side. Thus the curve of creep ratio vs. molding water content appears to continue its upward trend on the dry side of the optimum water content, despite the fact that the total strain of the sample is increasing. The data in the dry region are incomplete, and hence it would be premature to conclude that the principle stated above is not generally valid. The results do suggest however, that the effect of structure of the clay must be carefully taken into account.

It appears that, in general, the immediate deformation of the samples was much the same for the first loading and for repeated loadings. However, the total deformation of the sample was less upon repeated loading, especially for samples compacted at the drier water contents. Thus, the creep ratio for reloading appears to be more directly related to the total strain undergone by the sample.

One result of the previous one-dimensional compression studies was that the curve of strain vs. the logarithm of the duration of the load was essentially a straight line from a time of approximately 150 milliseconds to a time of 1 minute. The current tests also produced a straight line relationship within the time range just stated, and the slopes obtained from the present data are very similar to the slopes from the previous work. However, as is seen in Figure 4.8, the curves bent upwards in a significant fashion for lower duration of load, i.e., a disproportionately large amount of creep strain occurred during the time interval from 30 milliseconds to 100 milliseconds. The fact that the load is actually increasing slightly during this time interval is partially responsible for the large apparent creep strain. However, even if a correction is made for the slight increase in load during this interval, it is still apparent that the strain vs. logarithm of time relationship is no longer a straight line when carried back as far as 30 milliseconds. Thus, the present tests have revealed a new and significant pattern of relaxation which occurs for the short loading times achieved in these tests.

4.5 Conclusions

Three main conclusions may be stated with the result of the tests performed to date upon the fat clay.

(a) The general validity of the following principle has been reaffirmed: as the total strain which is experienced by a material decreases, the fraction of this total strain which is creep under constant load increases.

(b) The structure of clay plays a significant role in determining both the total compression of the clay under load and also the fraction of the total compression which is creep strain.

(c) Important relaxation phenomena, not apparent for slower load rise-times, appear when a loading time on the order of 30 milliseconds is used.

Chapter 5
ONE-DIMENSIONAL COMPRESSION TESTS MEASURING PORE PRESSURES

5.1 Objectives and scope of the test program

The fact that a fat clay will undergo considerable compression creep at constant load intensity has been documented in a previous report, MIT(1959b), and in the previous chapter. The question naturally arises as to the cause of such behavior.

It must be re-emphasized that this creep is recorded during undrained compression, and hence is not the result of the hydrodynamic time-lag associated with the expulsion of water from a soil. The compression must result from a decrease in the volume of air within the soil, presumably from the combined effects of compression of the air and of the air going into solution in the pore water. For problems in which time is not a factor, there exists a straightforward theory for predicting the undrained compression of a partly saturated clay. The amounts of air volume lost through compression and through solution are both related in a definite way to the change in the pressure in the pore phase of the soil. Any increase in external pressure upon the soil is distributed between the mineral skeleton and pore phase in relation to the compressibilities of these two phases.

There are two obvious places at which time-dependence might enter into this simple theory. The compressibility of the mineral skeleton may be time-dependent, thus effecting the distribution of external pressure between the two phases. That is to say, there may be some form of structural viscosity. The process by which air is dissolved may also be time-dependent, even though pressure in the pore phase is constant. Researchers, in studying the behavior of soil, are always on the look-out for any evidence of structural viscosity, for such evidence would have considerable implications to problems such as shear strength behavior. Hence it is of great interest to attempt to pin down the cause of the observed compression creep.

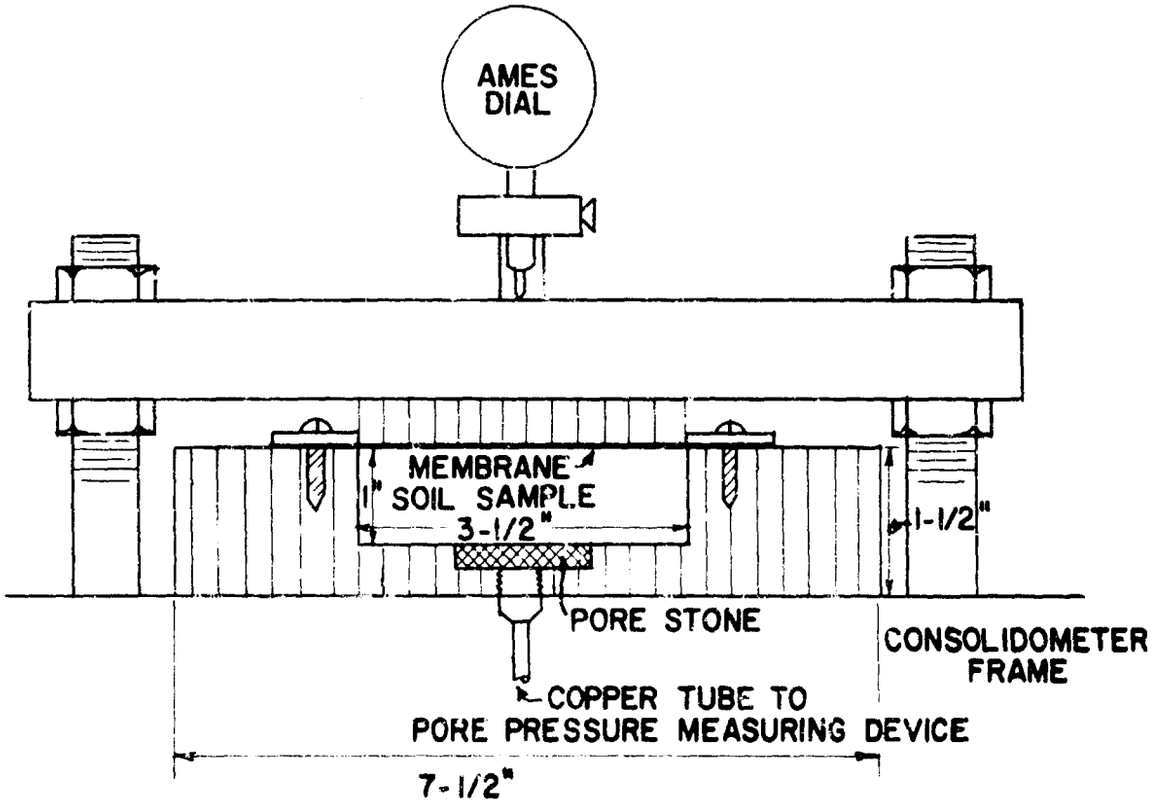

FIGURE 5.1 OEDOMETER FOR STATIC TESTS

The starting point for all research into soil behavior is the measurement of the pore water pressure so that the behavior of the mineral skeleton and pore phases may be separated. The work reported in this chapter is a preliminary effort to measure pore pressures during one-dimensional compression tests. Measurement of pore pressures in unsaturated soils with very slow rates of loading is difficult enough, and the problems encountered have been the subject for many papers appearing in the literature of Soil Mechanics during the last five years. The problems multiply rapidly when rapid load changes are introduced. Hence the efforts reported herein represent only a first start toward development of satisfactory techniques. One of the basic problems is the time-lag in the response of all pore pressure measuring systems. For ordinary systems used with a fat clay, this lag frequently amounts to several minutes. The theory of these time-lags, and the development of new equipment and techniques for reducing the time-lag, will be the subject of a companion report soon to be issued.

The experimental work reported herein has been divided into two phases. Series F involved 3 tests of a conventional nature: the external load was applied over an interval of several seconds, and strain and pore pressure variations were observed for the next hour. Series G involved 3 tests in which the external load was applied in about 30 milliseconds. All tests involved the fat, backswamp clay from Barrel 3*, and static compaction at 200 lb/in^2 was used to prepare all samples.

5.2 Static tests

5.2.1 Apparatus and testing procedures

These tests were carried out in the special oedometer shown in Figure 5.1. The top of the sample was sealed with a rubber membrane. A metal block rested atop the membrane, and served to transmit loads applied with a standard consolidation loading frame. The applied loads were measured by a platform scale which was part of the loading frame. Strains in the sample were recorded with an Ames dial.

*See MIT (1959b)

A Penman device obtainable from Testlab Corp., New York City, was used to measure the pore pressures. This device is based upon the conventional technique of observing any tendency for water to be expelled from or sucked into the soil, and compensating for this tendency by changing the backpressure; this operation is accomplished automatically in the Penman apparatus. The measuring apparatus was connected to the interior of the soil sample through a copper tube and an ordinary porous stone.

Samples were compacted directly into the oedometer by static compaction. Prior to placing the soil, the porous stone was boiled in de-aired water and the copper tube was carefully filled with de-aired water. During compaction of the soil, the end of the copper tube which eventually connects to the Penman device was left open and submerged in a pan of de-aired water. All samples were compacted well wet of optimum so as to minimize the tendency to pick up water at this stage. After a soil sample is compacted, it will have a tendency to suck water from the porous stone, and vapor bubbles may form in the porous stone unless the copper tube is open to a supply of water. If such bubbles form, they will cause serious time-lags in the pore pressure measuring system at a later stage of the test.

Following compaction, the top of the sample was sealed, the valve in the copper tube was closed, and an initial load was applied. Now the copper tube was connected to the Penman device. The initial load was applied for about two hours. Pressures of 50 to 104 lb/in^2 were then applied in a single increment. In one test, the additional load was later released to permit study of phenomena during unloading. A reading of the initial pore pressure was made just before applying the load increments.

5.2.2 Test results

The significant data regarding each test have been tabulated in Table 5.1, and curves of pore pressure and strain as a function of time appear in Figure 5.2. Note that the pore pressure prior to application of the pressure increment was positive in each case. This residual pore pressure was

Table 5.1

SUMMARY OF STATIC TESTS

Test No.	F-1	F-2	F-3
Water content w(percent)	39.4	28.6	33.0
Dry density (lb/ft3)	76.7	91.5	87.1
Degree of Saturation S(percent)	90.0	91.7	96.0
Initial Loading p_i(lb/in^2)	31.0	100.0	50.0
Loading Increment Δp(lb/in^2)	104.0	52.0	50.0
Change in pore pressure Δu(lb/in^2)	64.0	38.5	46.5
Pore pressure ratio $\Delta u/\Delta p$ (percent)	61.5	74.0	93.0
Total time during test - t (min.)	50.0	90.0	25 - (60)
Total settlement at end of test - δ (in.)	0.033	0.010	0.005
Time req'd to reach pore pressure equilibrium Δt (min.)	10	5	2
% of Δu at end of 1 min. after Δp is applied	48.4	86.0	98.0

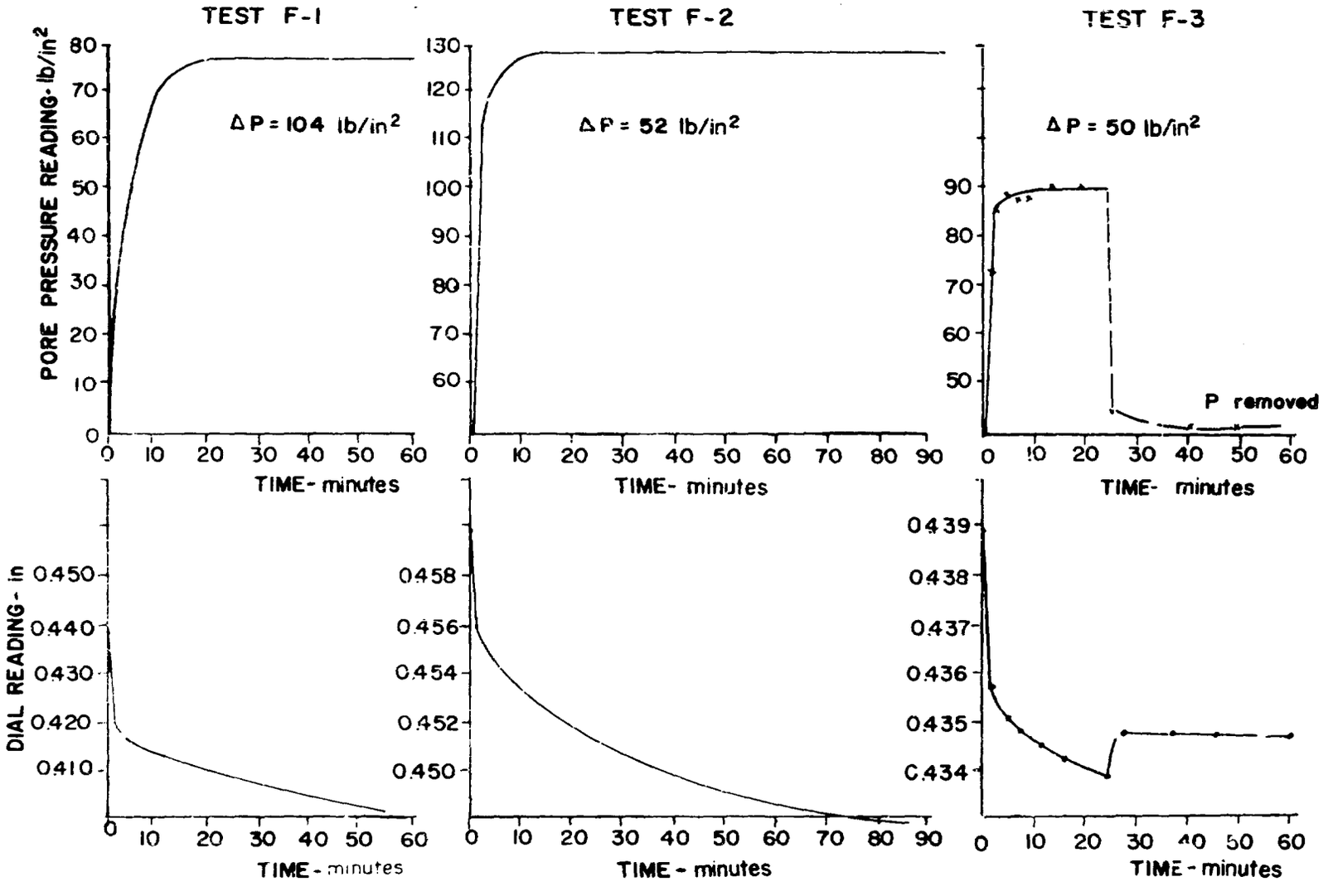

FIGURE 5.2 PORE PRESSURE AND STRAIN VS. TIME: STATIC TESTS

caused by the initial pressure. Note that the molding water content of sample F-1 was very great, and this fact accounts for the somewhat unusual behavior of this sample.

Figure [illegible] shows the one-dimensional creep in the present tests with results reported in MIT (1959b). During the time range from 1 to 10 minutes, the results appear to be very similar. However, the curves obtained from the present work curve downward earlier and to a greater extent, especially the curve from test F-1. It seems quite possible that some of the compression in these tests resulted from squeezing some clay up around the edges of the loading plate. Certainly the membrane which covers the sample will not entirely prevent such squeezing action. This criticism of the test procedure applied to the results in the previous report as well as to the present work. In the previous report, it was noted that the slopes of the long term compression time curves agreed well with the slopes obtained in tests where the uniform pressure was applied directly to the membrane rather than through a loading block. Hence, it appears that the squeezing-out action does not affect the portion of the strain vs. log time curve from 1 to 10 minutes, but that this action does influence the path of these curves for longer times. If this hypothesis is valid, then the creep behavior recorded in the present tests between 1 and 10 minutes is consistent with the patterns and principles which were discussed previously.

For a group of samples with similar structures in the mineral skeleton, the fraction of the external pressure increment appearing as pore pressure should increase with increasing degree of saturation. The present results behave in just this way, as may be seen from Table 5.1. From 2 to 10 minutes were required for the pore pressure to rise to its final level, the required time increasing as the degree of saturation increased. At the present stage of research, it is unwise to attribute this time rise behavior to any factor other than a time-lag in the pore pressure measuring system used for these particular tests.

Of particular interest is the fact that, once having reached a maximum value, the pore pressure in each test remained quite constant while the sample

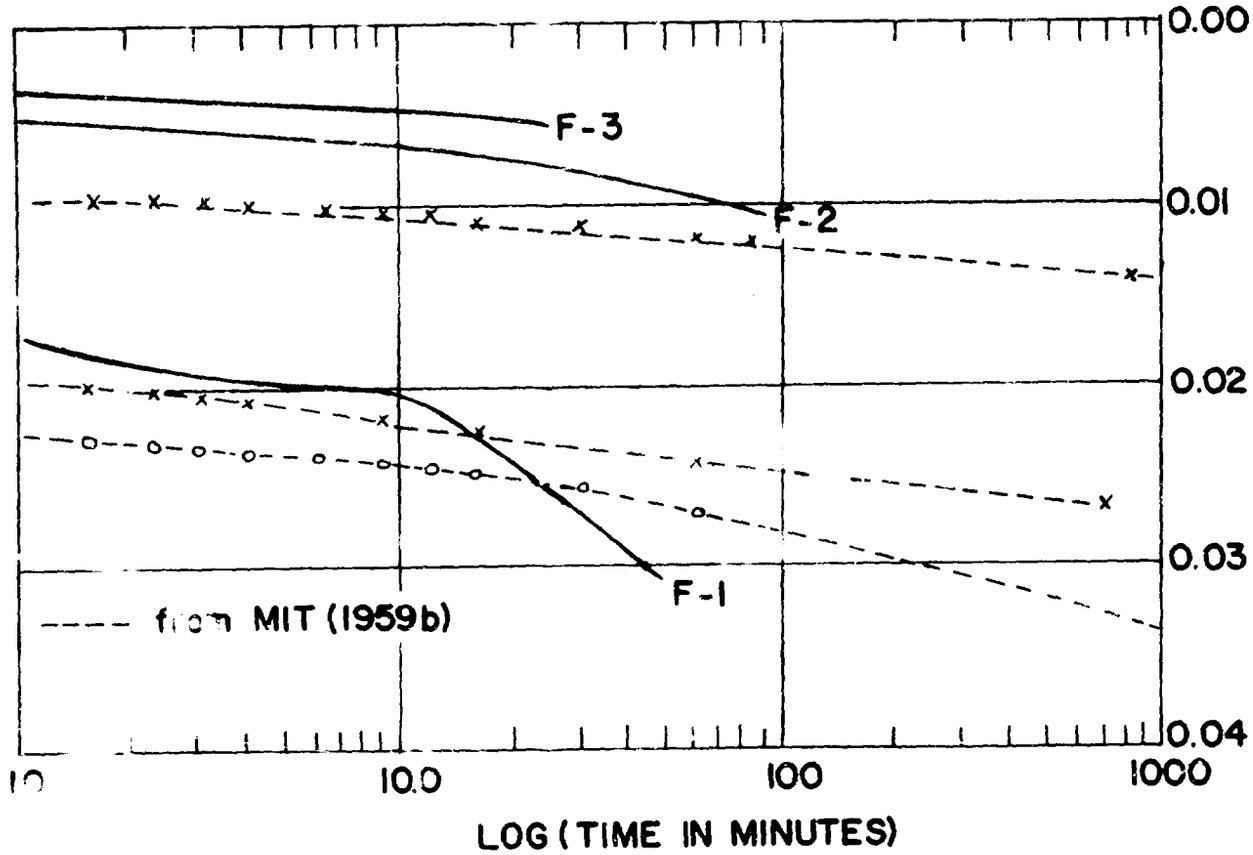

FIGURE 5.3 STRAIN VS. LOG TIME CURVES

continued to compress. Assuming that the compression represents decrease in air volume rather than a squeezing-out action, this result is a very important one from the standpoint of interpreting the cause of the air volume decrease. Discussion of this result will be delayed until the results of the second test series have been examined.

5.3 Dynamic tests

5.3.1 Apparatus and testing procedures

With the exception of provisions for the measurement of pore pressure, the apparatus and instrumentation were identical with that described in Chapter 4. The modification which permitted pore pressure measurements are shown in Figure 5.4. A depression 1 inch in diameter and 1/8 inch deep was cut in the bottom of the oedometer. Grooves were cut in the bottom of this depression, and served to channel water to a 1/8 inch diameter hole passing through the oedometer wall to an electrical pressure transducer.

A Dynisco pressure gage, manufactured by the Dynamic Instrument Company of Cambridge, Massachusetts, was used in these tests. The gage consists essentially of a diaphragm with unbonded strain gage wires. The gage was driven by a 6 volt dry cell, and the calibration curve has been given previously in Figure 4.5.

A porous stone was cemented into the depression using an Epoxy resin, the top surface of the stone being flush with the bottom of the oedometer. Two types of porous stones were used: a ceramic stone for tests G-1 and G-2, and a regular stone for test G-3. Use of a ceramic stone overcomes several problems inherent in the measurement of pore pressures with partially saturated soils. Such stones have very fine pore spaces, and hence resist any tendency for water to be sucked from the stone into the soil. Since such stones exclude air bubbles entering from the soil, they make it possible to measure pore water pressures less than atmospheric pressure in partially saturated soils. The main drawback

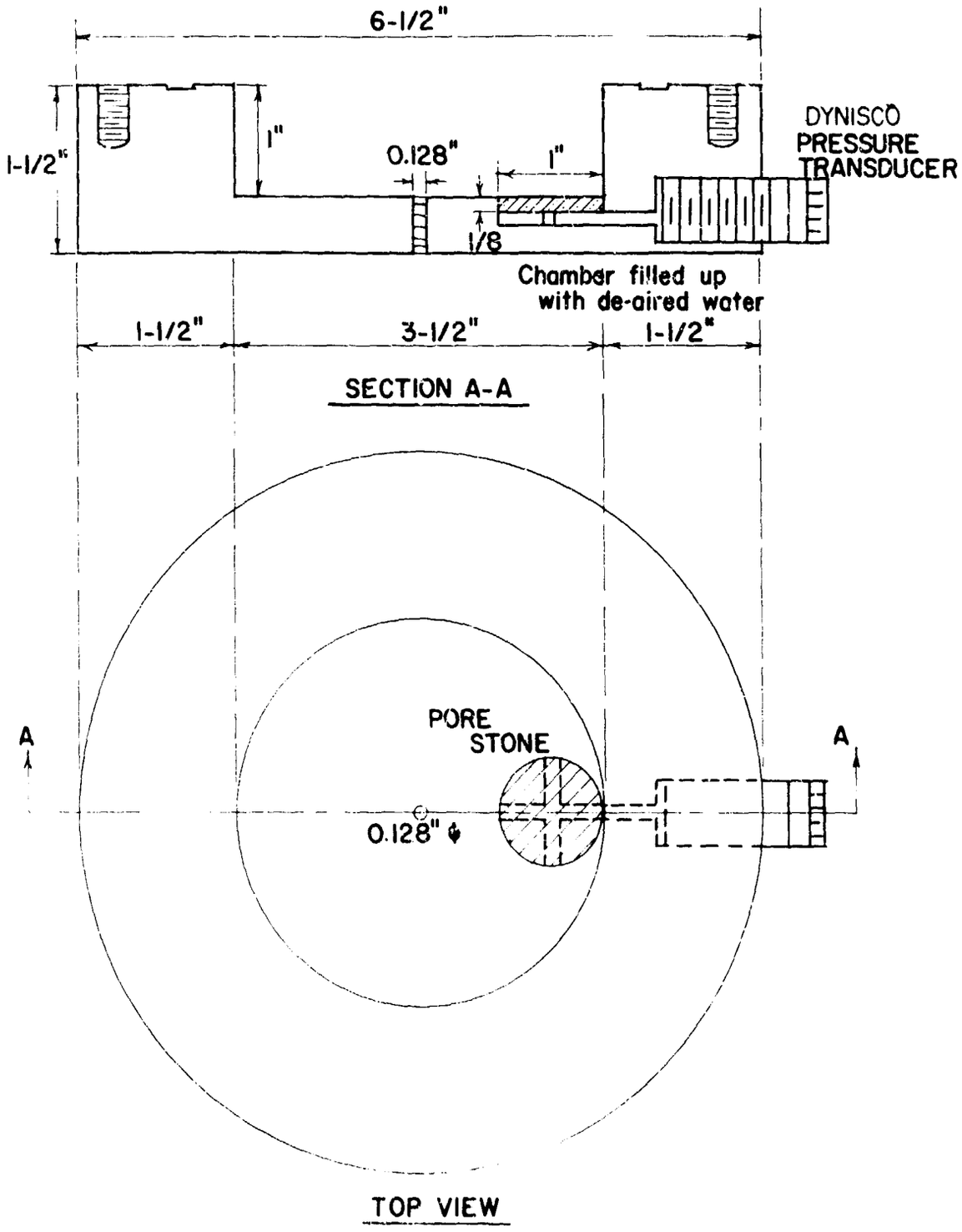

FIGURE 5.4 PORE PRESSURE MEASUREMENT SCHEME FOR DYNAMIC TESTS

of such stones is their very low permeability. The permeability of the stone used for this work was measured at 10^{-7} cm/sec.

Great care was taken to de-air the porous stone and the passages beneath the porous stone. This was done by drawing water through the system repeatedly, and then inserting the pressure gage with the whole assembly submerged in water. The output of the pressure gage was recorded upon an X-Y recorder whose response time was 1 second. The response time of the measuring system was checked by filling the oedometer with water and applying a pressure increment with a rise time of 30 milliseconds. In such calibration tests, any time-lag is the result of the resistance to flow of the porous stone, the compressibility of any air still trapped in the measuring system, and the flexibility of the pressure gage. The results of the calibration tests are given in Figures 5.5 and 5.6. The results obtained for the ceramic stone, particularly the fact that the time-lag varies with the pressure level, suggests that some air was still trapped within the stone. The response time with the regular stone was limited by that of the X-Y recorder, and would have been much faster had an oscilloscope been used to record the output of the gage.

Strain in the sample was sensed with the cantilever gage discussed in Chapter 4 and recorded on an oscilloscope. No measurement was made of the applied pressure. It is believed that loading times similar to those presented in Chapter 4 can be achieved consistently.

The samples were compacted directly into the oedometer, using the molding water contents indicated in Table 5.2. Pore pressure changes were recorded continuously throughout the process of putting the clay into the mold, applying and removing the compaction pressure. Curves of pore pressure vs. time during the compaction process are shown in Figure 5.7. Zero time for these curves is the moment at which compaction pressure was first applied. In test G-1, a slight negative pore pressure existed before the compaction pressure was applied, in test G-2 there was zero (gage) pore pressure at this time. With both of these samples, a negative pore pressure existed after removal of the compaction pressure

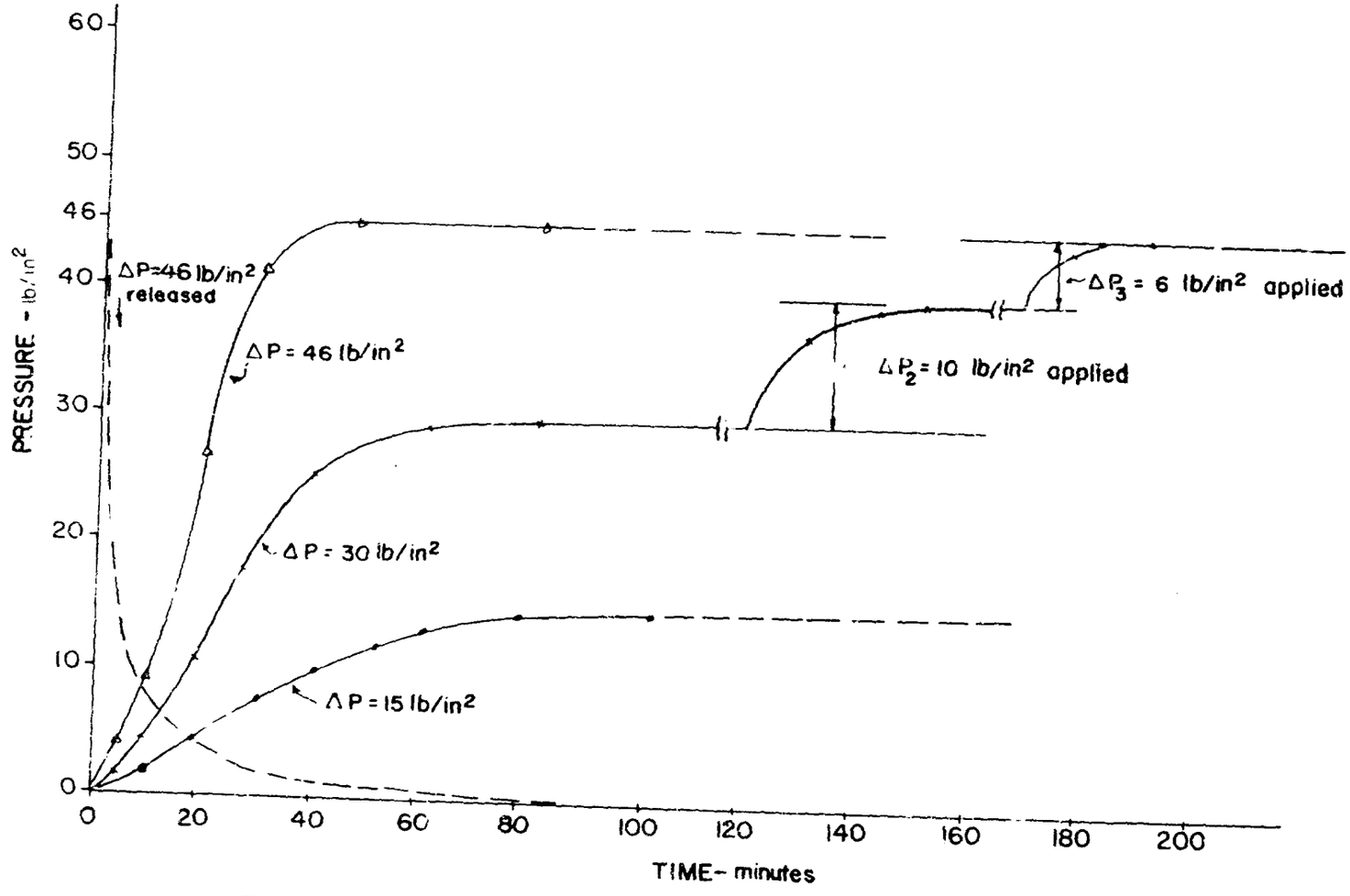

FIGURE 5.5 TIME-LAG THROUGH CERAMIC STONE

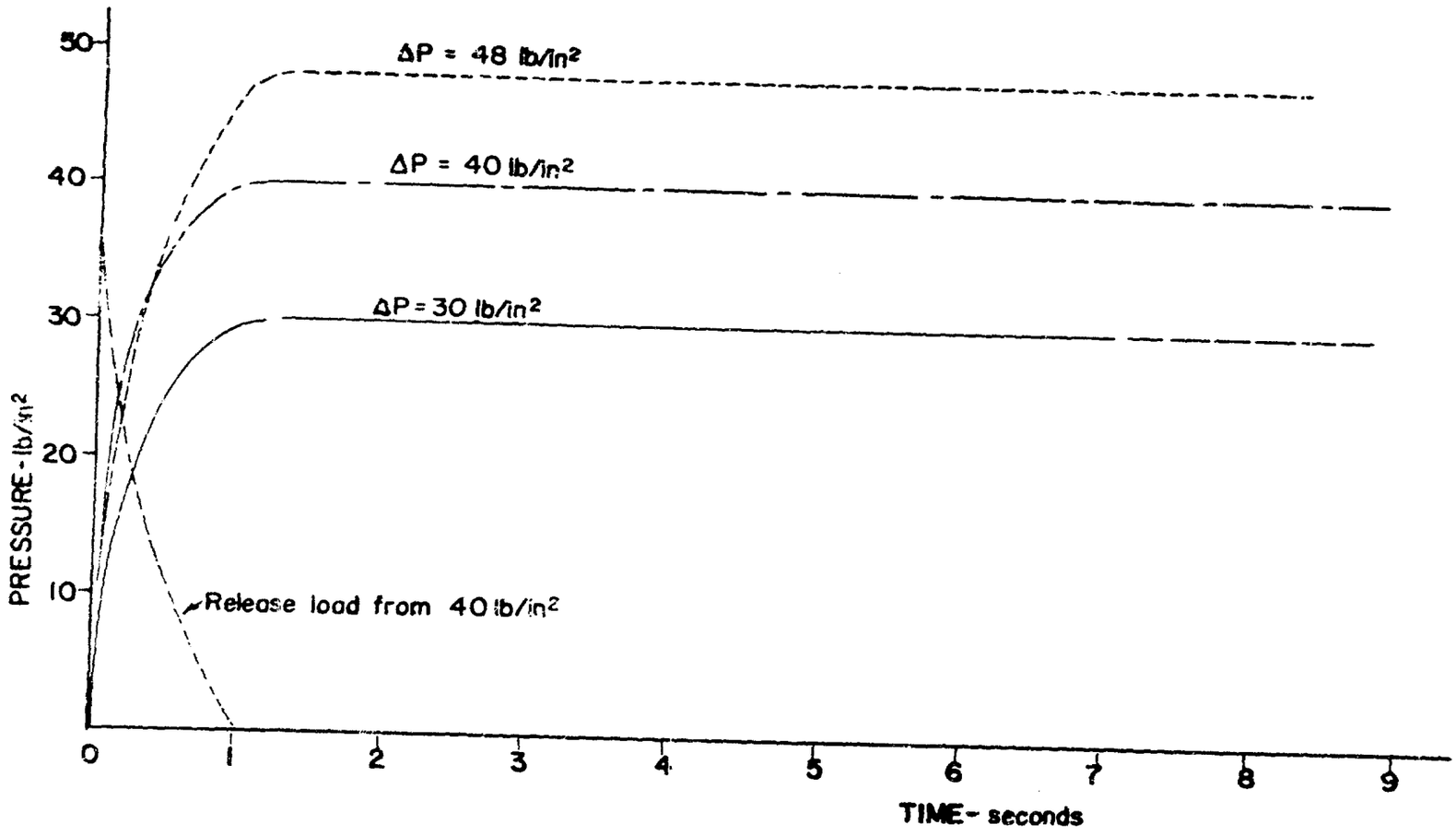

FIGURE 5.6 TIME-LAG THROUGH REGULAR POROUS STONE

Table 5.2

SUMMARY OF DYNAMIC TESTS

Test No.	G-1	G-2	G-3
Dry density - γ_d (lb/ft^3)	102.8	95.7	104.5
Water content - w (percent)	22.7	27.8	20.0
Degree of Saturation - S (percent)	96.1	99.1	98.5
Initial pressure - p_i (lb/in^2)	10	10	20
Time of p_i applied-t_i (min.)	25	30	40
Pressure increment - Δp (in/in^2)	35	35	40
Pressure rise time - t_r (milliseconds)	~30	~30	~30
Immediate deformation - ΔH_{30} (1/1000 inch)	2.0	4.5	--
Deformation at 1-min. - ΔH_f (1/1000 inch)	--	10.1	--
Amount of creep - $(\Delta H_f - \Delta H_{30})$ (1/1000 inch)	--	5.6	--
Creep ratio - $\frac{(\Delta H_f - \Delta H_{30})}{\Delta H_f}$ (percent)	--	55.5	--
Compaction intensity - p_c (lb/in^2)	200	200	200
Pore pressure equilibrated u_e (lb/in^2) after compaction	(+45)	(+97)	~0
Pore pressure equilibrated u_i (lb/in^2) under p_i	(-15)	(+ 4)	~ (-2)
Pore pressure equilibrized u_f (lb/in^2) under Δp	(+14)	~(+14)	--
Equilibrized time for u_e - t_e (min.)	15	10	--
Equilibrized time for u_f under Δp - t_f (min.)	3	[illegible]	--
Type of pore stone used	Ceramic	Ceramic	Regular

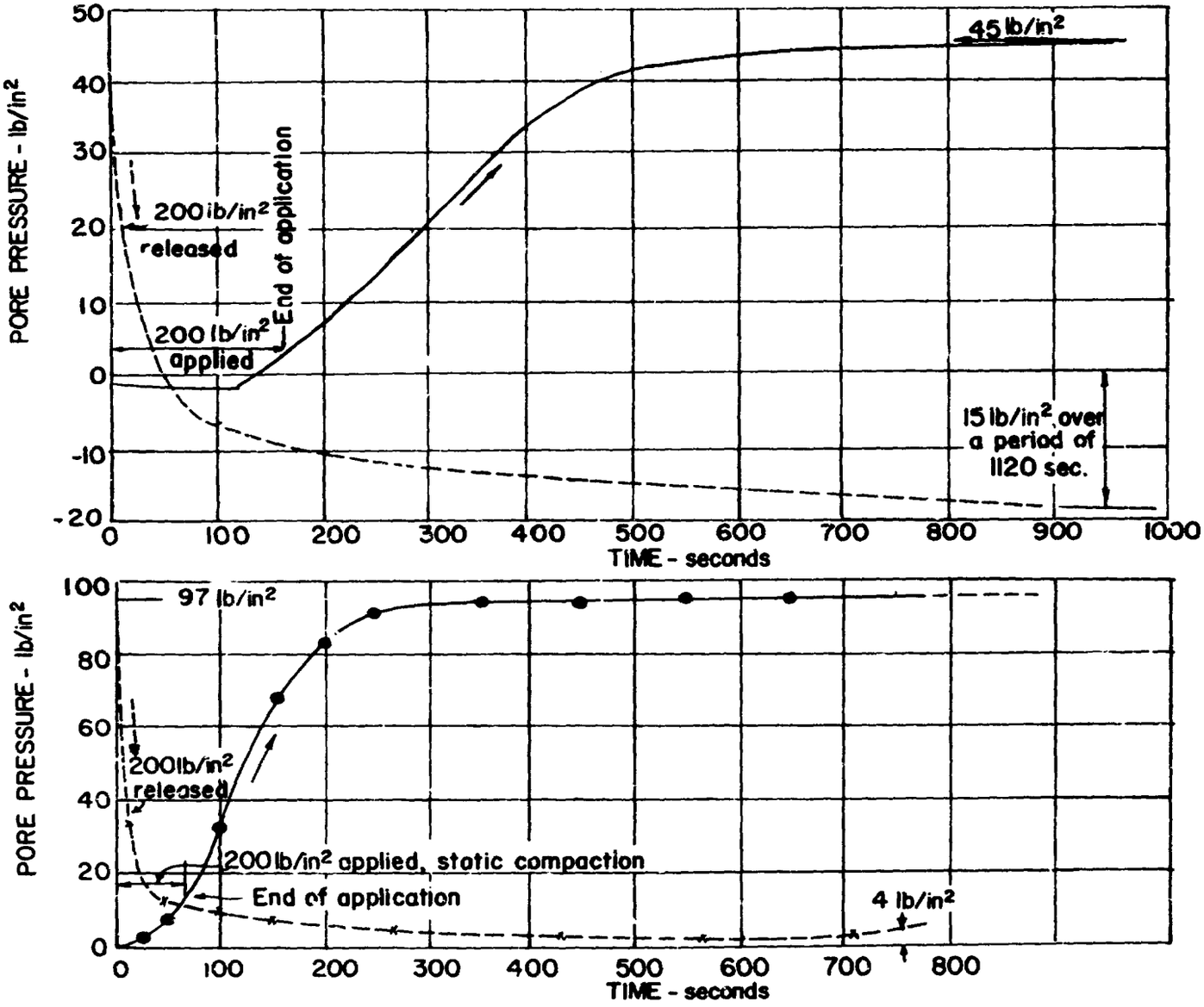

FIGURE 5-7 PORE PRESSURES DURING COMPACTION

Once the pore pressure reached an equilibrium value following removal of the compaction pressure, the sample was trimmed, sealed, and placed in the loading apparatus. The initial load was then applied and held for 30 to 40 minutes before the dynamic pressure increment was triggered.

5.3.2 Test results

The pore pressures measured during application of the dynamic load increment are given in Figure 5.8, and strain as a function of time has been plotted in Figure 5.9. No data were obtained from test G-3, owing to failure of the recording system. The data regarding creep have already been included in the discussion in Chapter 4, and no further comment will be made.

The rise-time for the pore pressure curves was extremely long. Some fraction of this delay was the result of the time-lag introduced by the permeability of the ceramic stone. The permeability of the soil contributed further to the time delay. The delays amounted to from 3 to greater than 30 minutes, and were of the same order as the lags encountered in the series F tests. Again, it would be unwarranted at this stage to assume that the lags arose from a source other than experimental error.

5.4 Discussion of pore pressure data

The results of the pore pressure measurements can be summarized by the following statements: (1) there is a long time delay before the pore pressure increases to its final level, but at this stage one cannot be sure that this delay is not the result of experimental error; and (2) there is evidence of compression creep at constant effective stress, although some of this creep may be shear flow rather than simply compression. In short, much research still remains to be done.

The first statement emphasizes the need for careful experimental and theoretical work to provide a basis for separating observed time delays into:

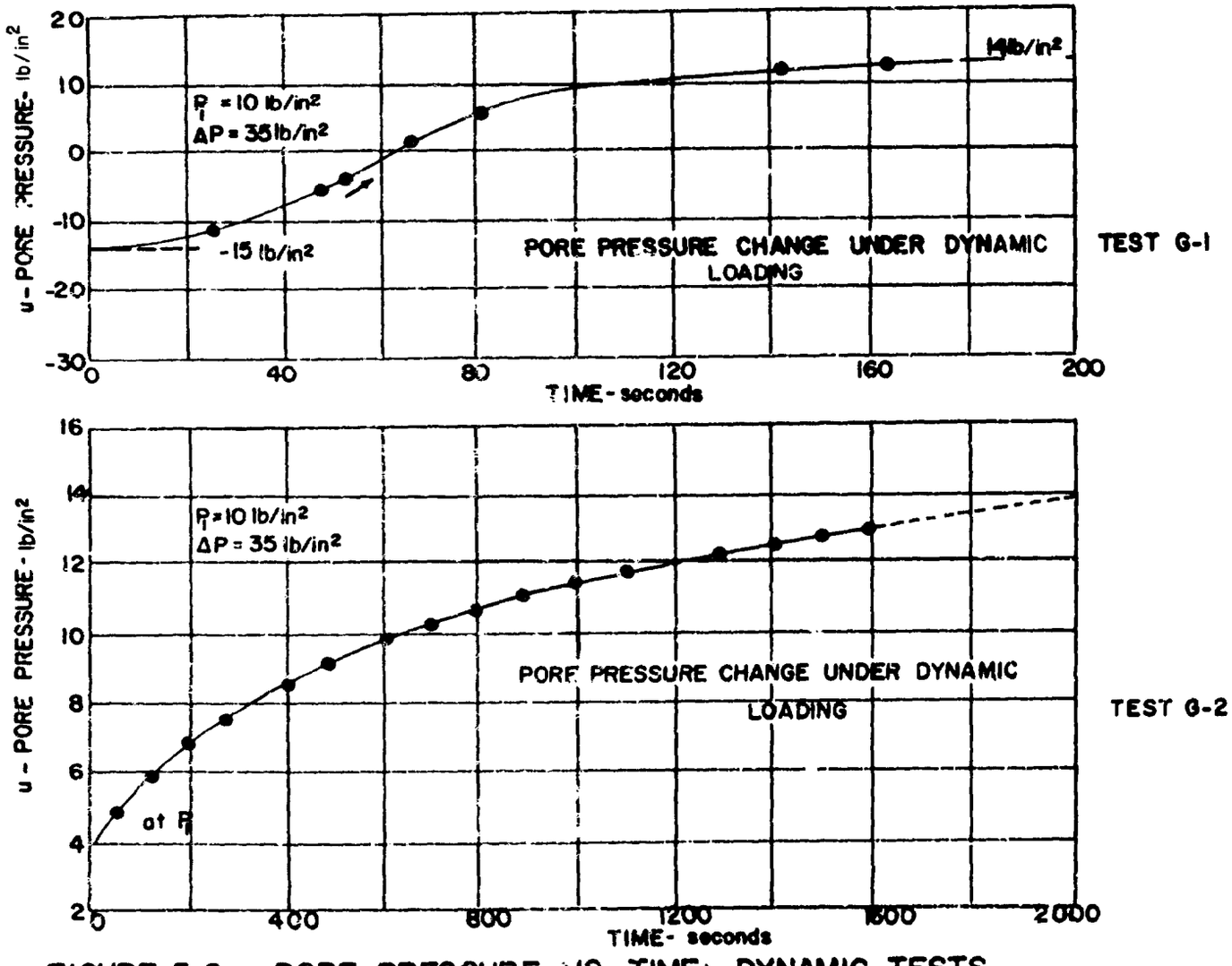

FIGURE 5.8 PORE PRESSURE VS. TIME: DYNAMIC TESTS

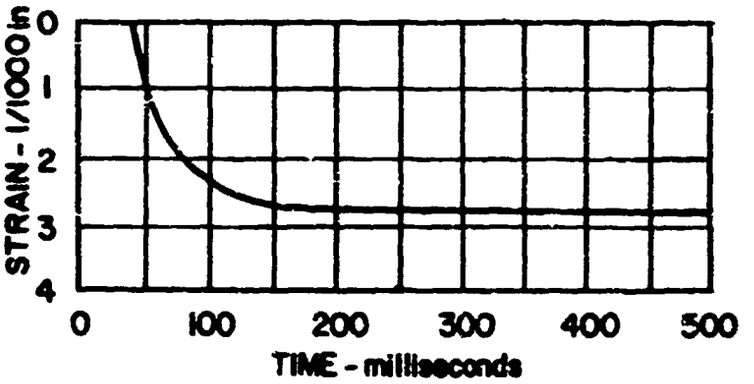

TEST G-1

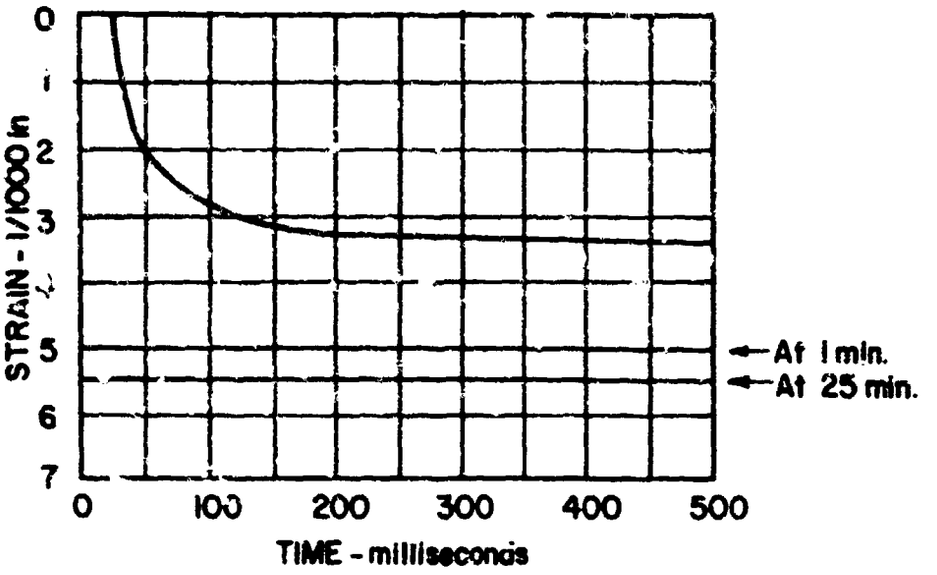

TEST G-2

FIGURE 5.9 STRAIN VS TIME: DYNAMIC TESTS

(1) that part which represents a property of the soil, and (2) that part which represents experimental error.

Possible implications of the second statement can be examined with the aid of a possible rheological model for the compression resistance of soil as shown in Figure 5.10. If both the effective stress and pore pressure are constant, so that the forces in springs A and D are constant, then continued strain can occur only if either: (1) dashpots C and F relax at exactly the same rate, or (2) spring D is very compressible as compared to spring A, or vice versa. The first condition implies that BOTH structural viscosity and time-dependence of air solution in water must be present. The second condition simply means that the pore phase is so compressible that the mineral structure can continue to compress without changing the pore pressure, or vice versa. An alternate version of the second condition would be: there actually are small pore pressure changes, but they are within experimental error.

It seems likely that the second condition can be excluded. The ratio of change in pore pressure to change in volume will, if anything, increase with continued compression. Using test F-2 as an example, a pore pressure change of 38.5 lb/in^2 developed during the first five minutes while the soil compressed 0.006 inches. During the next 10 minutes, the soil compressed another 0.001 inch without measurable pore pressure change. If the data for the first five minutes are correct, the pressure should have increased 6 lb/in^2 during the next 10 minutes, a change which definitely could have been measured.

Thus a very tentative conclusion might be stated: there exists both a structural viscosity and a time-dependence for the solution of air in water, and in the series F tests these two effects were balanced. In many ways this conclusion seems very unlikely and more study is certainly necessary. The possibility that the compression results from shear flow must be definitely excluded. Results reported by BISHOP ET AL (1960) suggest still another source of error: that air may be escaping through the membrane which covers the top of the sample.

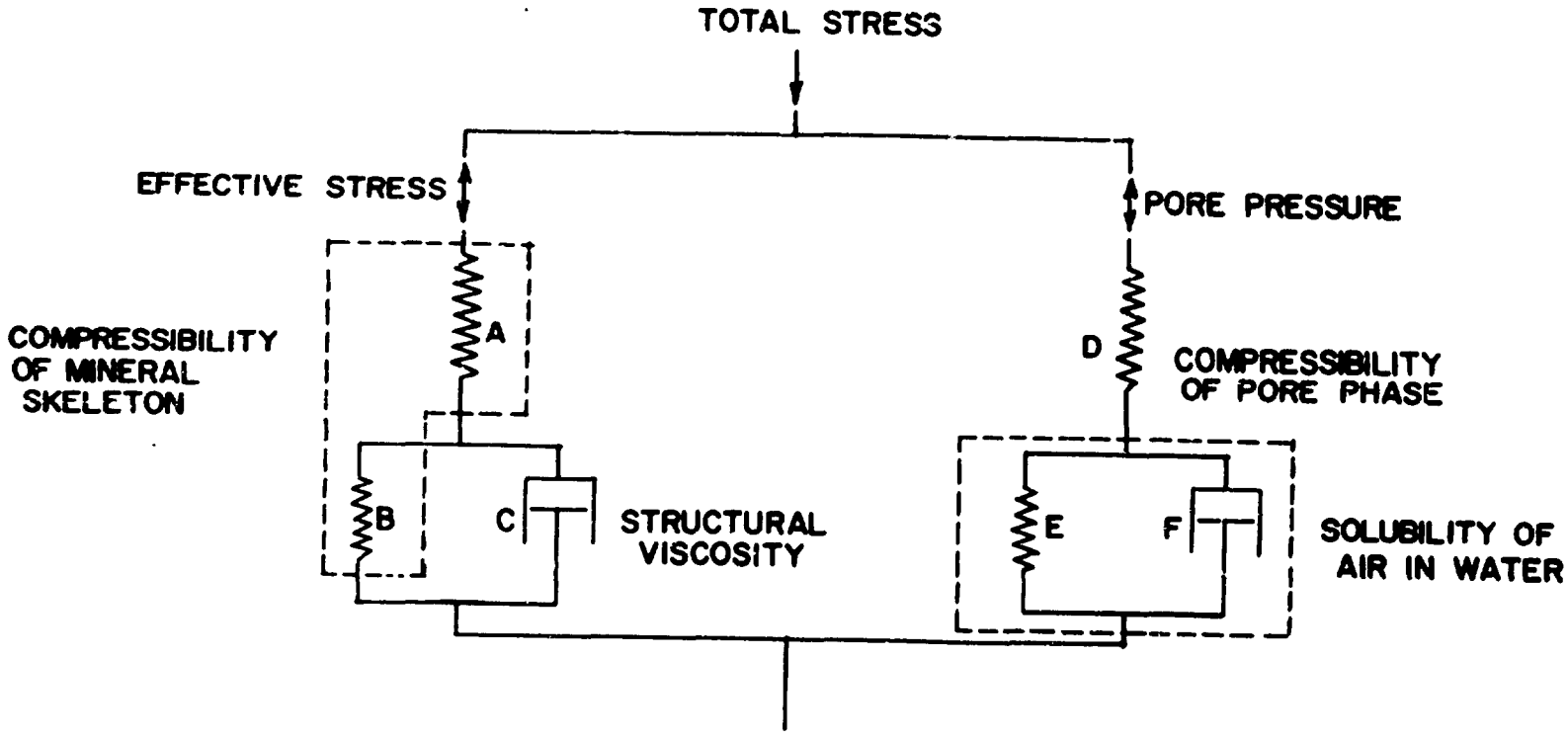

FIGURE 5.10 RHEOLOGICAL MODEL FOR COMPRESSION RESISTANCE

Chapter 6
SONIC WAVE PROPAGATION IN SOILS

6.1 Objectives of sonic wave propagation study

Interest in laboratory sonic wave propagation studies stems from two directions. In the first place, it is desirable to establish correlations between sonic velocity and such soil properties as compressibility and shear strength. Such correlations - if indeed they exist - would be of great practical value because the relative ease with which sonic velocity can be measured in the field compared to direct measurement of these soil properties in tests upon undisturbed samples. In the present effort to design hardened missile bases, great reliance has been placed upon seismic velocity as a measure of the compression resistance of soil deposits. In the second place, there is evidence which suggests that laboratory sonic velocity measurements are a valuable tool for studying the mechanism of stress transfer between soil particles. Some of this evidence will be discussed in the subsequent text.

The objective of efforts during the past year has been to establish the feasibility of making such measurements in the laboratory upon soft, slightly consolidated soils. This objective has been pursued through study of the literature and through preliminary development of suitable apparatus and techniques. Section 6.2 reviews, in very brief form, some theoretical work by other researchers concerning wave propagation in soil-like media. Section 6.3 contains a summary of the various experimental techniques which have been used successfully to measure sonic velocities in the laboratory. Section 6.4 discusses some of the experimental results which appear in the literature. Section 6.5 reports upon some velocity measurements in deep sea samples of a clay. Section 6.6 presents the progress to date in the development of a laboratory system for use in the current research effort.

6.2 Theories for wave propagation in porous media

When the problem of wave propagation in porous media is viewed as a whole, it is an extremely complex problem. To mention just a few aspects of the problem, one must consider: (1) propagation through the pore phase, including the dispersion of energy through a complex pattern of reflections from the many, many pore-mineral interfaces; (2) transmission of energy within any one mineral particle; (3) propagation of energy from one mineral particle to adjacent mineral particles, which requires consideration of the mechanism of stress transfer between particles; and (4) attenuation of energy due to relative motions between viscous pore fluid and mineral particles. In regard to the third item, it may be noted that the mechanism of stress transfer between particles has, for some time, been one of the most controversial subjects in the field of soil mechanics. Depending upon what expert is speaking and what sort of soil he has in mind, this stress transfer may take place by mineral-to mineral contact or the mineral may be separated by thin films of adsorbed water with unusual properties, and the stress transfer may give rise, at the points of contact, to elastic deformations, crushing, or slip between particles.

It is not surprising that past theoretical work has been characterized by grossly simplifying assumptions, thus permitting separate attacks upon the many aspects of the problem. The following sub-sections present extremely brief reviews of past work categorized by the nature of the simplifying assumptions. LAUGHTON (1957) contains a more thorough review, as does SYKES (1960).

6.2.1 Dilute suspensions of solids in water

The key assumption here is that there is no stress transfer between adjacent mineral particles. URICK (1947) assumed that dilute suspensions of sediment in water will possess the same sonic velocity as an ideal (monophase) material having the same gross density and compressibility as the actual two-phase material. Mineral particles are both more dense and less compressible than the water they replace. Since sonic velocity is inversely related

to both density and compressibility, the velocity may be expected to vary in a complex way as the percentage of solid material in suspension increases. Using typical values, Urick showed that, with increasing content of mineral particles, the sonic velocity should first decrease below that of water (overall density increases more rapidly than overall compressibility decreases) and then increase towards the velocity for the mineral matter (decrease in overall compressibility finally prevails). This prediction that sediments may have a sonic velocity slightly less than that for water (up to 5%) has been confirmed by experimental work.

This simple theory can apply only as long as the wave length is large compared to the size of the mineral particles. When this assumption is violated, then the reflections from the water-mineral interfaces become important. These reflections scatter (a form of dispersion) the energy, and thus effect the apparent wave velocity of the sediment. Attention must also be given to the energy loss (another form of dispersion) as the mineral particles are bounced back and forth through a fluid with some viscous resistance. AMENT (1953) describes theoretical work aimed at both of these problems. Both the reflection and relative motion effects depend upon the wave length (and hence frequency) of the wave, and there is much interest in determining the critical frequency below which dispersion will not be important. There is still much controversy as to the importance of dispersion in seismic field work.

6.2.2 Dry, granular systems

Workers such as MORSE (1952) have studied wave propagation through various packings of uniform spheres. The relationship between the force upon a ball and its deflection at points of loading can be calculated from elastic theory, with suitable attention to the fact that the stresses are very large at the contact points. From such studies, it has been predicted that the overall compressibility of a granular mass should vary as the 1/6 power of the confining pressure, and hence that the sonic velocity should vary as the 1/3 power of the confining pressure.

6.2.3 Porous solids

BIOT (1956) proposed a different model for taking into account the energy losses due to relative motion between water and mineral. This theory considers a porous, compressible solid saturated by a viscous, compressible liquid. Thus the mineral skeleton is treated as a coherent framework behaving in an elastic and linear fashion. As the framework and fluid are stressed, fluid will flow from pore space to pore space with attendant energy losses. The amount of dispersion is again dependent upon the frequency of the sonic wave.

6.2.4 General systems

LAUGHTON (1957) has attempted to generalize many of these ideas to treat the general case of mineral particles in contact in a fluid of finite compressibility. His work is mainly restricted to the problem of wave velocity, and is particularly concerned with the effect of ambient pressure upon the compressibility of the two phases and hence upon the overall compressibility.

6.3 Review of experimental procedures

Three general techniques for measuring the sonic velocity of porous media in the laboratory have been described in the literature and are summarized in the following sub-sections. The basis for all methods is some means of converting electrical energy into mechanical energy at one end of a sample of soil, and reconverting the mechanical energy which passes through the sample back into electrical energy. Piezo-electric crystals, made of materials as quartz, barium titanate, Rochelle salt, etc., are commonly used for this purpose.

6.3.1 Pulse technique

This technique involves a direct measurement of the time delay

between the instant at which the incoming electrical signal arrives at the input crystal, thus generating a mechanical disturbance, and the instant at which an electrical signal is generated in the output crystal as the result of the mechanical disturbance which has passed through the sample. Time-delay measurements are accomplished by displaying the output electrical signal upon an oscilloscope. A single, transient occurence would be difficult to observe and measure in this fashion, and hence the input pulse is repeated at intervals in such a way as to provide a steady picture on the oscilloscope, but also at a slow enough rate that the mechanical waves from any one electrical pulse have damped out before the next pulse is applied. Pulse rates up to several thousand per second can be used.

There are, of course, many experimental difficulties involved in applying this simple idea. The incoming electrical pulse, which generally has a square or spiked wave form, must have component frequencies which correspond to the resonant frequency of excitation of the crystal. A very precise means for determining the travel time must be provided, and it is necessary to make corrections to compensate for the fact that the mechanical disturbances originate and terminate at a poorly determined point somewhere within the input and output crystals rather than exactly at the faces of these crystals which contact the soil. The time of travel is usually measured either: (1) by having the incoming pulse trigger the sweep of the oscilloscope beam, and measuring the time of travel directly on the displayed wave form; or (2) by transmitting two identical pulses, one through the soil sample and the second through a material, such as mercury or water, for which the sonic velocity is known. In the latter method, the two generated electrical signals are displayed on a double-beam oscilloscope, and the length of the travel path in the reference material is adjusted until the arrival time is the same for the two waves. The sonic velocity of the soil is then simply equal to the ratio of the length of the soil sample to the length of the reference sample times the velocity of sound in the reference material. Figures 6.1 and 6.2 show apparatus and circuits which have been used in applying this latter approach.

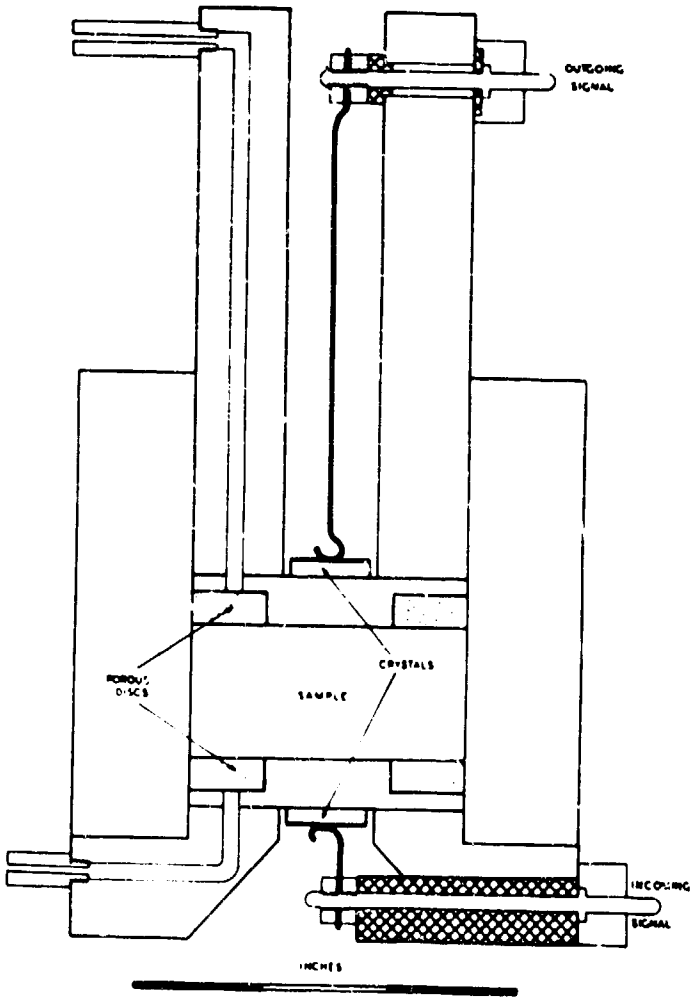

(Laughton, 1957)

FIGURE 6.1 CROSS-SECTION THROUGH LAUGHTON APPARATUS

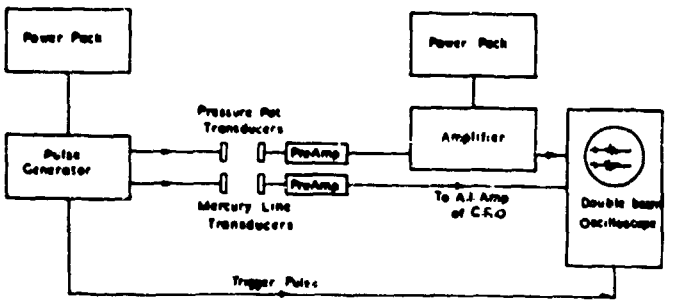

(Laughton, 1957)

FIGURE 6.2 ELECTRICAL CIRCUIT FOR LAUGHTON APPARATUS

Detailed descriptions of the pulse technique are given by LAUGHTON (1957), WYLLIE, GREGORY and GARDNER (1956), and HUGHES and JONES (1951). This technique provides the most accurate measurement of velocity, but because of the complex wave forms following the initial arrival is not satisfactory for measurements of the magnitude of attenuation. The technique requires complex electronic equipment.

6.3.2 Wave train technique

With this approach, which has been described by BUSBY and RICHARDSON (1957), a steady pattern of waves is established within the soil sample through continuous excitation of the input crystal. The attenuation in amplitude of the input signal is measured to evaluate adsorption and energy losses. Very little experimental data related to soil systems has been obtained to date.

6.3.3 Resonance technique

This technique is a special case of that described in the previous sub-section, in that the rate of repetition of the input signal is adjusted until the soil sample is made to resonate. The point of resonance can be determined with relative ease if the resonant frequency is sufficiently low, and the energy attenuation can also be evaluated. This approach has been used frequently to determine the Young's modulus of soil, employing specimens which are free to expand in a lateral direction. A recent application of this technique is described by WILSON and DIETRICH (1960). SHUMWAY (1956) describes a resonant chamber technique for velocity and attenuation measurements, with the soil held in a soft-walled container. However, the resonance technique does not appear to be applicable to the direct measurement of the dilatational wave velocity because of the very high frequencies involved with feasible dimensions for soil samples.

6.4 Review of past experimental work

The following sub-sections present reviews of previous experimental efforts which bear upon problems of particular interest to this research effort.

6.4.1 Density, water content, strength and velocity relationships in compacted clay

MARTIN (1957), working at M.I.T., used the soniscope, a commercial device for the field testing of concrete by a pulsing technique, to study the effects of molding water content, dry density, and strength on the sonic velocity of compacted Vicksburg loess.* The results of this work are summarized in Figures 6.3 through 6.6.

Figure 6.3 shows compaction data for three different compactive efforts. All soil samples were compacted in oiled cylindrical steel molds, fitted with removable sleeves. The molds had diameters of 2 and 2 1/2 inches and had lengths equal to the length of the sample. The figures show test data obtained on samples with a three inch length. The compacting hammer was two inches in diameter and weighed five lbs. Operation was manual with an 11 inch drop in the compaction of the first layer, ten inch and nine inch drops in the compaction of the middle and upper layers of the three inch sample.

Figure 6.4 shows the relation between sonic velocity and dry density as a function of water content. Figure 6.5 shows the shear strength from unconfined compression tests (one-half maximum deviator stress) and velocity as a function of the molding water content. Figure 6.6 shows the relationship between sonic velocity and shear strength. The data show a relatively well defined relationship between velocity and density for any given water content.

*This material is essentially the same as that described in M.I.T. (1959b). Such material generally classifies as a silty clay, with a liquid limit of about 35 and a plastic limit about 23.

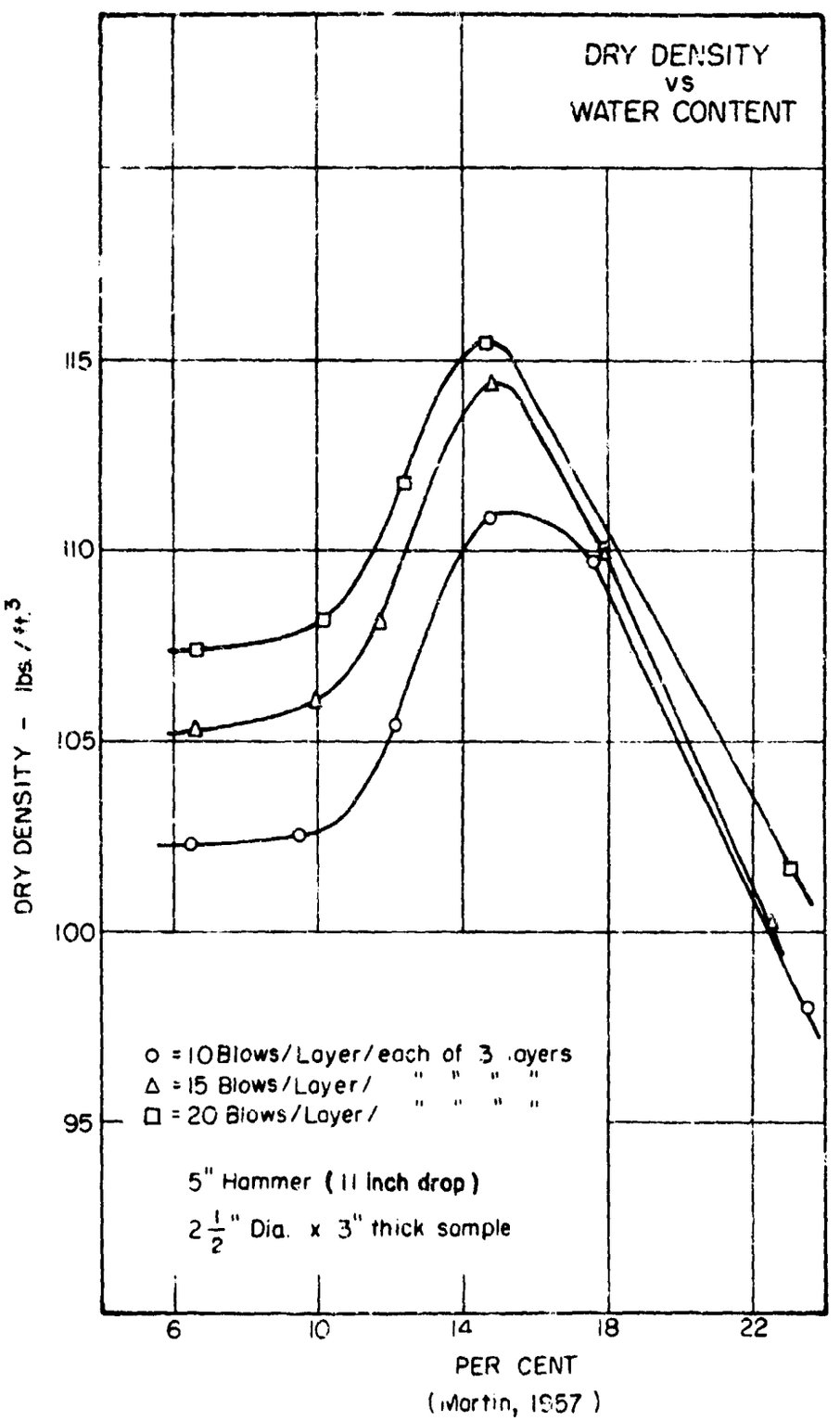

FIGURE 6.3 DRY DENSITY vs WATER CONTENT: CLAY FOR SONISCOPE TESTS

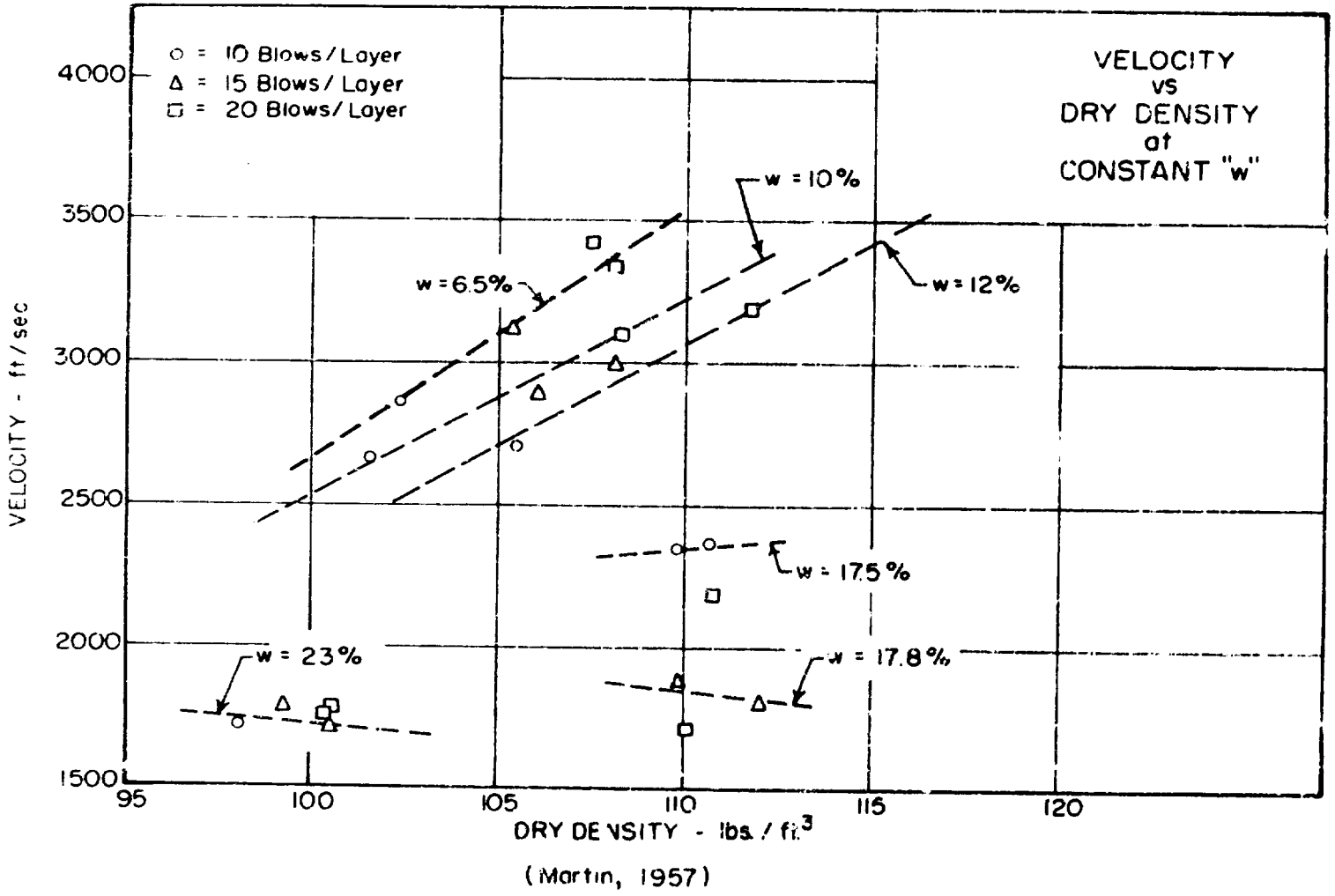

(Martin, 1957)

FIGURE 6.4 DILITATIONAL VELOCITY vs DRY DENSITY: SONISCOPE TESTS

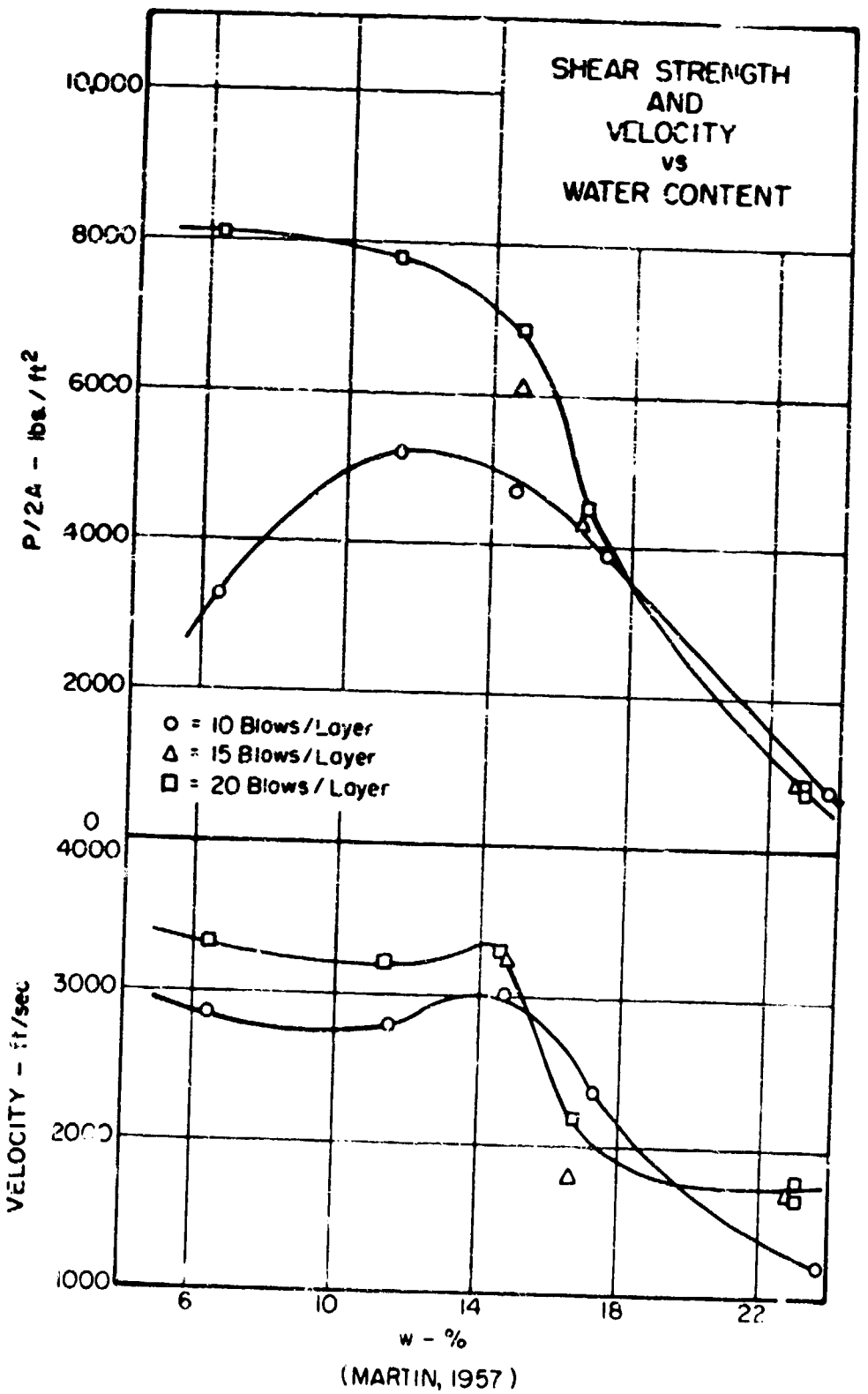

FIGURE 5.5 STRENGTH AND DILITATIONAL VELOCITY vs WATER CONTENT: SONISCOPE TESTS

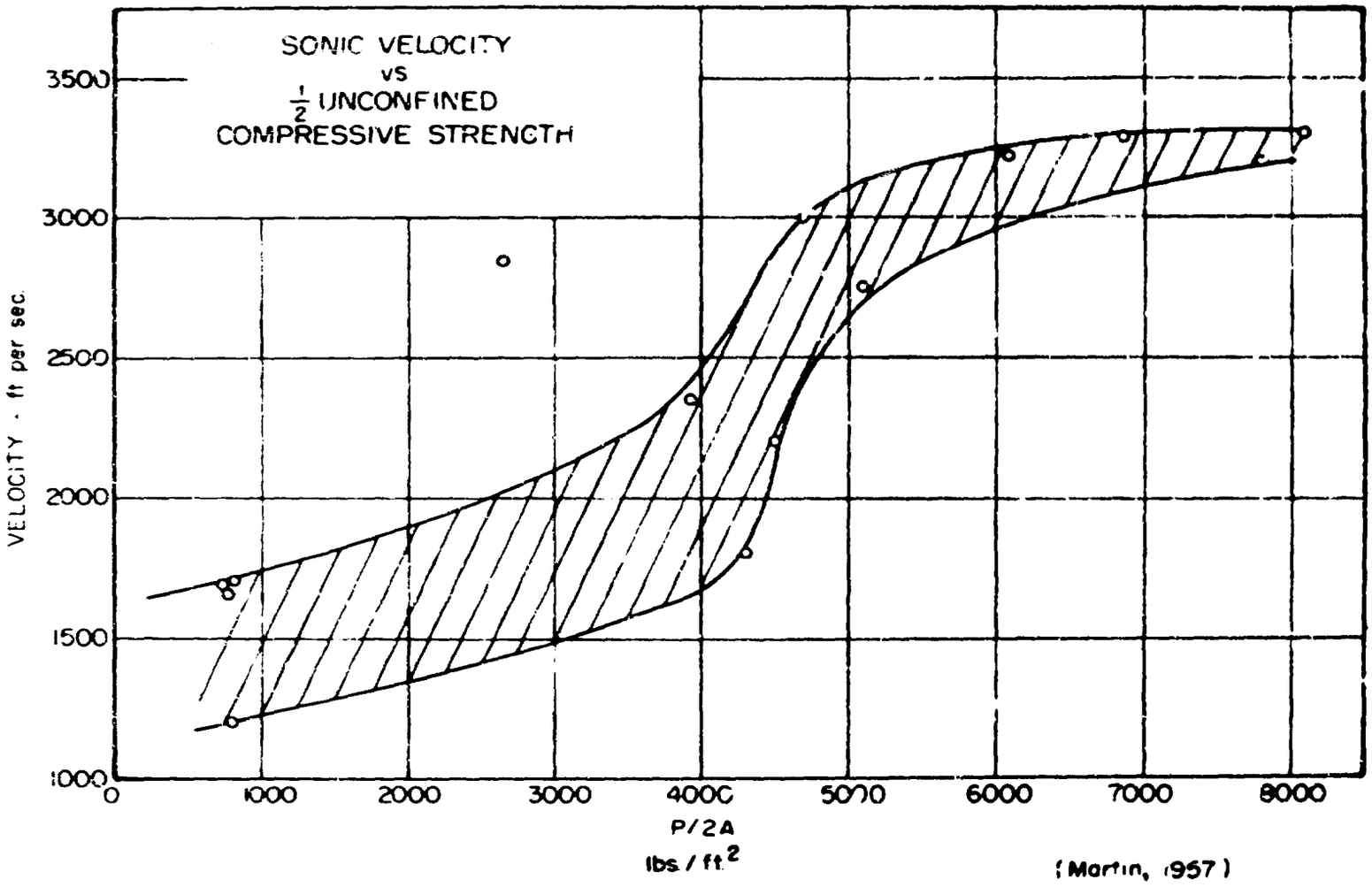

FIGURE 6.6 DILITATIONAL VELOCITY vs STRENGTH : SONISCOPE TESTS

The data in Figure 6.5 show a decided drop in velocity as the molding water content is increased above optimum, and since it is possible to have the same dry density for water contents wet and dry of the optimum water content, factors other than density must play an important role. The effect of saturation has been studied by WYLLIE, GREGORY and GARDNER (1956), and the results of tests on several materials are shown in Figure 6.7, in which velocity is plotted as a function of water and air saturation. The Britton sandstone, with a porosity of 29.9 percent, most nearly resembles the compacted loess (which has a porosity of 34 percent at a dry density of 111 lbs/ft^3). It can be seen that, as the degree of saturation increases above 80 percent, velocity increase occurs. If this effect of increasing saturation is valid, then for two samples of compacted soil at the same dry density, one sample compacted dry and the other compacted wet, one would expect the wet sample to have the higher velocity. However, the opposite was true for the compacted loess. It appears, then, that the reduction in velocity with increasing molding water content is a manifestation of a marked structural difference. Edge to face flocculation, which is thought to occur dry of optimum, undoubtedly results in better acoustic coupling between particles and thus a higher velocity. Wet of optimum, the structure is undoubtedly of a more oriented or dispersed nature, resulting in considerably less contact between individual particles.

6.4.2 Stress-strain-velocity relationships

WYLLIE, GREGORY and GARDNER (1958) measured axial and lateral strain as a function of stress on a cylindrical sample of Berea sandstone and computed Poisson's ratio: Figure 6.8. Using the expression for dilitational velocity in an infinite solid;

$$v_D = \left[\frac{gE(1-\mu)}{\gamma(1+\mu)(1-2\mu)}\right]^{\frac{1}{2}} \qquad (6.1)$$

Where: v_D = wave velocity
E = modulus of elasticity

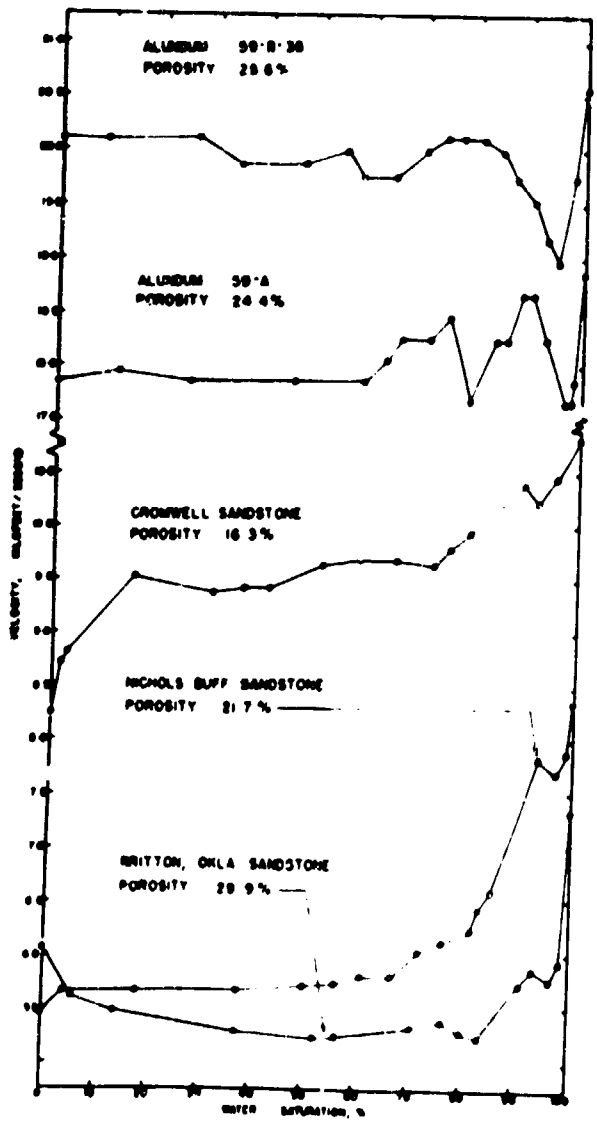

(Wyllie, Gregory & Gardener, 1956)

FIGURE 6.7 DILITATIONAL VELOCITY vs SATURATION: VARIOUS MATERIALS

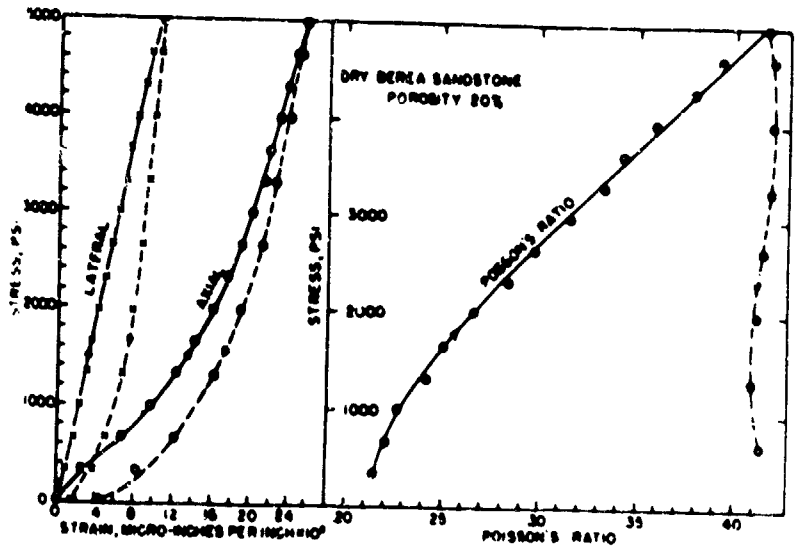

(Wyllie, Gregory & Gardner, 1958)

FIGURE 6.8 STRESS-STRAIN RELATIONSHIP FOR SANDSTONE

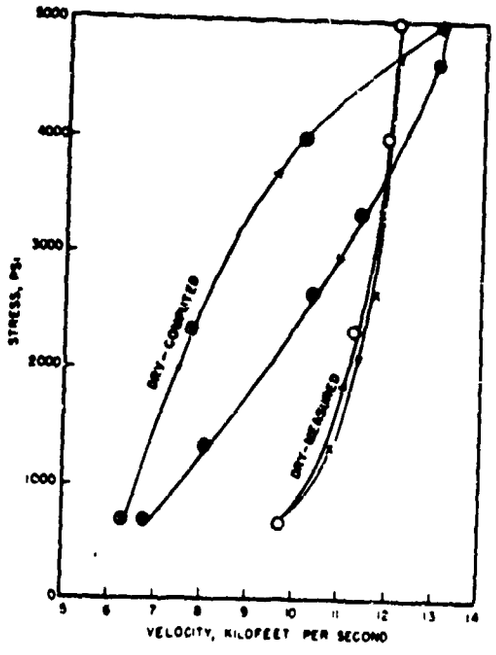

(Wyllie, Gregory & Gardener, 1958)

FIGURE 6.9 DILITATIONAL VELOCITY vs CONFINING STRESS: SANDSTONE

δ = density

g = acceleration of gravity

μ = Poisson's ratio

velocities were computed and are compared with measured velocities in Figure 6.9. In general, the computed velocity is less than the measured velocity. Since the sample had a length to diameter ratio of 2.5, one might argue that a more appropriate expression to use in computing velocities would be that valid for a long rod;

$$V^* = \left(\frac{gE}{\delta}\right)^{1/2} \qquad (6.2)$$

However, use of equation (6.2) would result in even smaller computed velocities. Unfortunately, there is no indication in the paper as to how the modulus was determined from the stress-strain curve, i.e., whether it is a secant or tangent modulus. The computations suggest that the secant modulus may have been used. In studies of wave propagation, it would seem to be more appropriate to use the slope of the tangent to the stress-strain curve at the appropriate stress level, since the wave front induces only a very small increment of stress above the existing axial stress. The use of the tangent modulus would tend to increase the computed value of velocity and bring the values in Figure 6.8 more in line with the measured values. In addition, there is little justification, at the present time, for assuming that the stress-strain relationship for a porous material under essentially static loading conditions is the same as the stress-strain relationship for a transient stress increase of the type developed as the wave propagates through the sample. For a transient case, the modulus should be higher because there likely is insufficient time for a change in the structural arrangement of the individual particles. Under static loading conditions, the soil has an opportunity to undergo any changes in structural arrangement, and creep and secondary compression may occur.

LAUGHTON (1957), by testing samples in the consolidation unit shown in Figure 6.1, was able to obtain data relating velocity, pressure and void ratio

at pressures as high as 1100 tons/ft^2. His results have been reproduced in Figures 6.10 and 6.11. The soil was an ocean bottom sediment, having a liquid limit of 61 and a plastic limit of 23. The velocity data were generally obtained at the end of a load increment after the sample had reached equilibrium under the given pressure. However, in each of the figures there is an insert showing the variation in velocity as a function of both applied pressure and average void ratio during a given increment of loading. The data in the insert for Figure 6.11, where the void ratio is the average value over the thickness of the sample, indicates that there was no appreciable change in velocity until the sample was approximately 40 to 50 percent consolidated; a very rapid change in velocity then occurred during the final stages of consolidation under the given increment pressure. This indicates that average conditions may not be sufficient to represent interrelationships between velocity and void ratio. It further indicates that values of velocities are likely to be strongly affected by slight differences throughout a given sample. The data in both Figures 6.10 and 6.11 show that velocity is not uniquely related to either void ratio or pressure. During the unloading period there is a very rapid change in velocity without any corresponding increase in void ratio. It is possible that the difference between the velocity and void ratio relationship during initial compression and the relationship during rebound represent, again, a basic difference in the structure of the material during initial compression and during rebound. That the variations cannot be attributed to a change in velocity in the water as a function of pressure in the water is shown in Figure 6.12, in which Laughton has presented data on the variation in velocity of water under hydrostatic pressure. The solid curves in Figure 6.12 show the variation of velocity for the samples that were initially consolidated to the pressure shown. Laughton was able to control the pore water pressure, and, after consolidation an increase in total pressure and pore pressure was applied to the sample without allowing drainage to take place, and the velocity was measured.

In order to obtain some indication of the validity of applying to soil systems the conventional equations which have been developed for solids, i.e.,

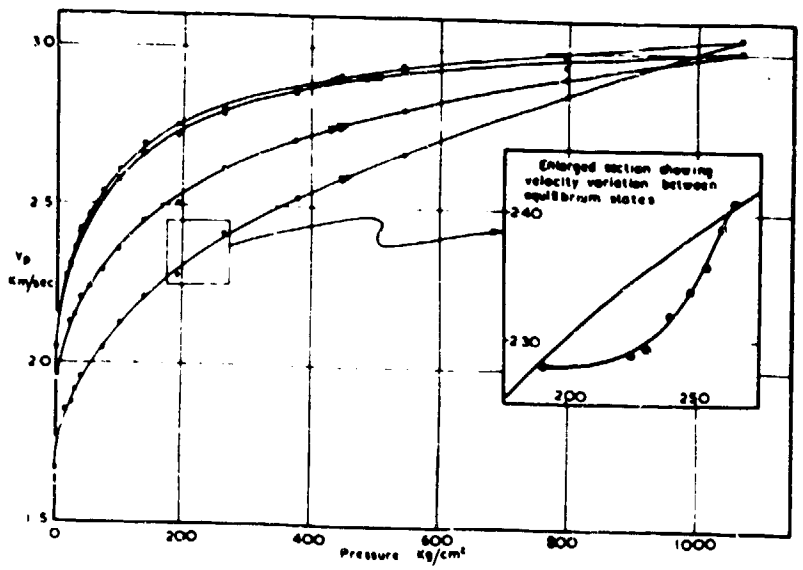

(Laughton, 1957)

FIGURE 6.10 DILITATIONAL VELOCITY vs CONFINING STRESS: OCEAN SEDIMENT

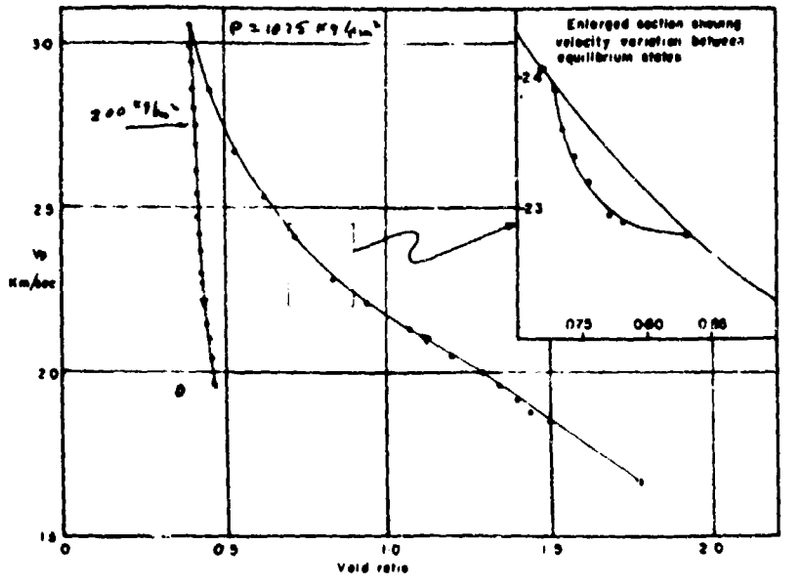

(Laughton, 1957)

FIGURE 6.11 DILITATIONAL VELOCITY vs VOID RATIO: OCEAN SEDIMENT

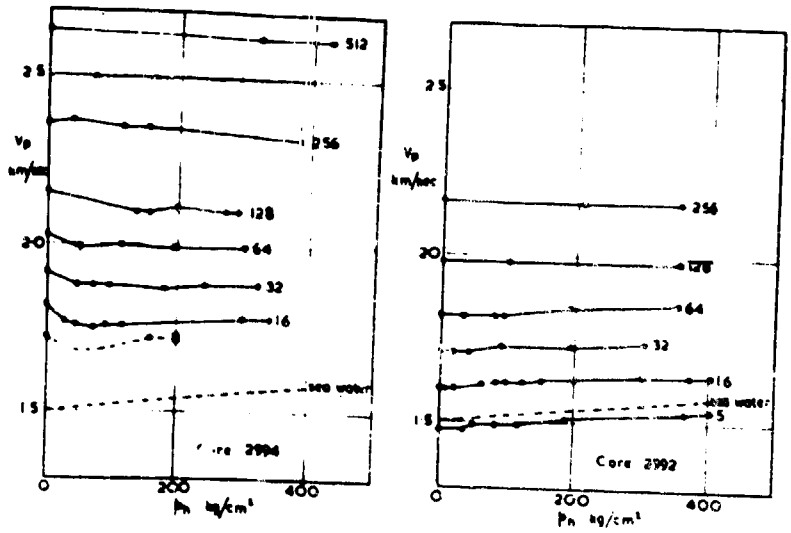

(Laughton, 1957)

FIGURE 6.12 DILITATIONAL VELOCITY vs PORE PRESSURE : OCEAN SEDIMENT

$$V^2 \propto \frac{gE}{\gamma} \qquad (6.3)$$

Laughton's data has been replotted in Figure 6.13 where various functions of coefficient volume compressibility m_v and velocity have been plotted. Although there are relationships between $1/m_v$ (comparable to E) and the square of velocity, the relationships are not linear. This tends to indicate that the use of the above expression will be somewhat limited in direct application to soils systems over a wide pressure range.

Laughton in his paper also mentions that shear velocity measurements were attempted and that no shear wave was detected until the pressure on the sample was equal to 500 kg/cm^2. If these results are indeed correct, they lead to extremely significant conclusions regarding the nature of stress transmission between soil particles. However, these results should be treated with some caution until there is further confirmation. With the crystals mounted on the back of the loading platens, it is possible that very poor acoustic coupling was developed between the loading platen and soil, resulting in insufficient shear wave energy being transmitted into and through the soil sample. In addition, it is possible that some of the shear deflection was taken out by the consolidation device itself; i.e., there is no guarantee that the platen is not isolated from the surrounding consolidation rings.

After the sample had been consolidated to high pressure, measurements of the velocities in the horizontal and vertical directions were made and in certain instances the velocity in the horizontal direction was 30 percent higher than the velocity in the vertical direction. This also suggest the possibility of structural alignment which tends to give orientation in a preferred direction.

WARD, SAMUELS, and BUTLER (1959) in connection with studies on London clay, measured wave velocities of these materials, presumably with a soniscope. Figure 6.14 shows the correlation between Young's modulus and strength. Figure 6.15 shows a similar correlation of $(1/m_v)$ with Young's modulus and shear strength. For this soil, a gross comparison indicates a reasonable relation between $1/m_v$ and square of velocity although there is considerable scatter.

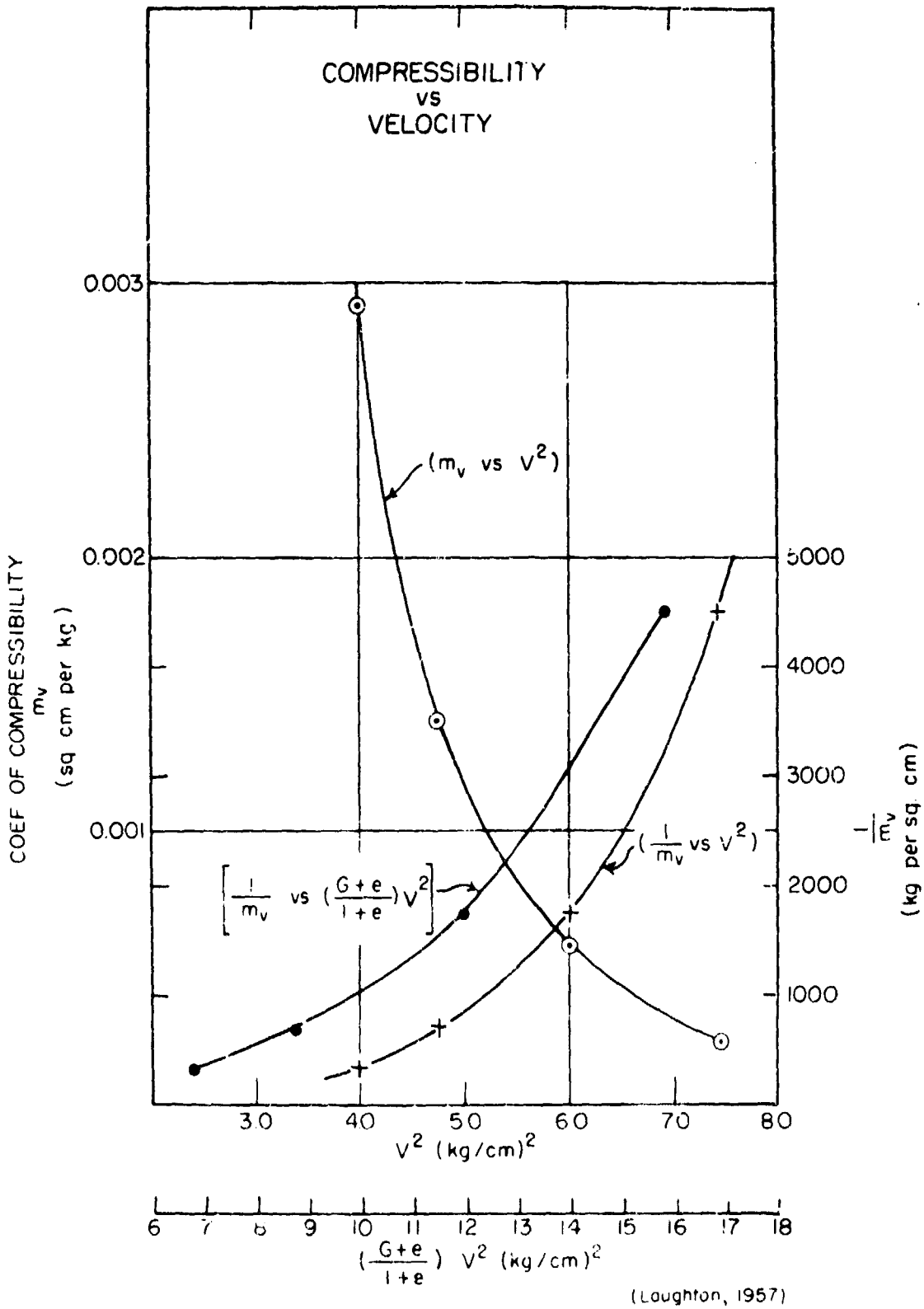

FIGURE 6.13 COMPRESSIBILITY vs DILITATIONAL VELOCITY : OCEAN SEDIMENT

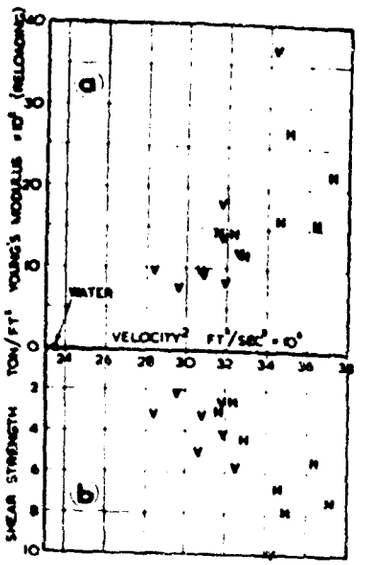

Correlation between the square of the wave velocity and (*a*) Young's modulus and (*b*) shear strength

(Ward, Samuels & Butler 1959)

FIGURE 6.14 DILITATIONAL VELOCITY vs YOUNG'S MODULUS AND STRENGTH: LONDON CLAY

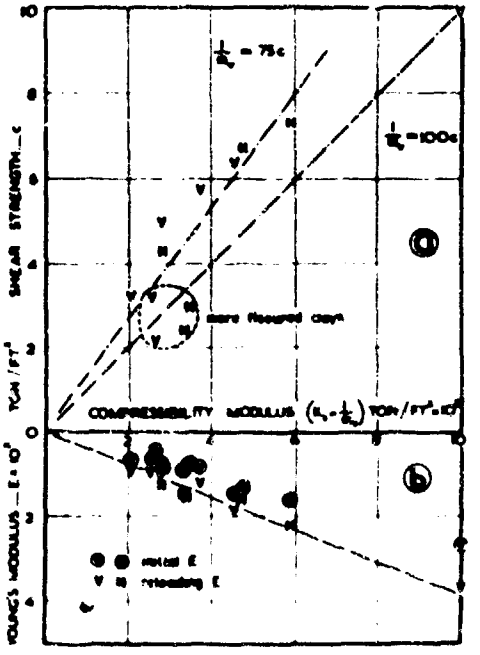

Correlation between modulus of compressibility and (a) shear strength and (b) Young's modulus

(Word, Samuels & Butler, 1959)

FIGURE 6.15 COMPRESSIBILITY vs STRENGTH AND YOUNG'S MODULUS: LONDON CLAY

The data which have been reviewed suggest the following concepts. The compression which takes place as a wave propagates is essentially elastic without slip between grains, whereas, under static loading, secondary effects due to the relative motion of the particles can occur with a resulting change in structure. It is probable that, where static compression is of the same nature as that occurring during wave propagation, it may be possible to get a reasonable correlation on the basis of the expression developed for solid materials, i.e., equation (6.3). The data presented in Figure 6.16 are of special interest in this connection. They show, that for the material tested, there is very rapid increase in the velocity of the material at pressures above 3,000 lb/in^2, and one would expect, on the basis of equation (6.3), a marked decrease in compressibility. However, the change in character of the material at high pressures previously has been shown by ROBERTS and DE SOUZA (1958) to be the result of an actual rupture and fracture of individual grains begins to take place, the compressibility of the material increases markedly.

6.5 Acoustic probe measurements in marine cores

Laboratory measurements of the sonic velocity in deep sea cores have been accomplished during the past year by a geology student working in the M.I.T. Soil Mechanics Laboratory: SYKES (1960). The work included a study of the relation between velocity and the standard identification properties of the clay. Sykes was supported by the research contract to the extent of providing him with space and with standard soil testing equipment and providing general guidance as to soil behavior and possible research applications of his techniques. Syke's thesis was submitted to the Department of Geology and Geophysics. The following is a summary of his thesis work.

Velocity measurements were made by the pulse technique, using the acoustic probes shown in Figure 6.17. Two such probes, with the radiating areas approximately 1.4 inches apart, were mounted on a probe holder, as shown

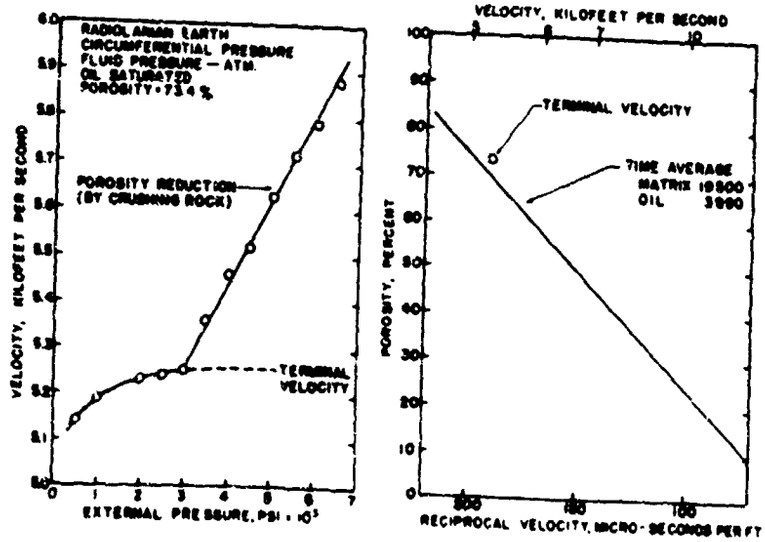

(Wyllie, Gregory & Gardner, 1958)

FIGURE 6.16 DILITATIONAL VELOCITY FOR RADIOLARIAN EARTH

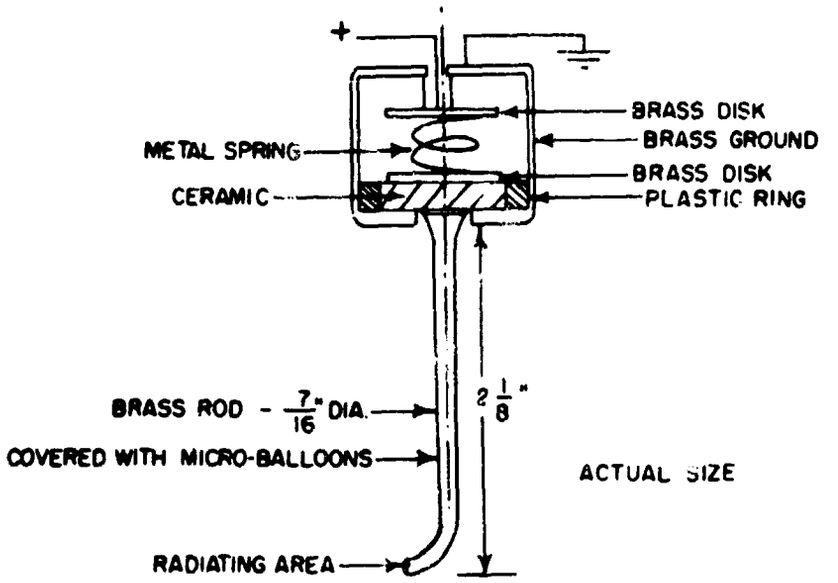

(a) SKETCH OF ACOUSTIC PROBE

(b) PHOTOGRAPH OF PROBE HOLDER

(Sykes, 1960)

FIGURE 6.17 ACOUSTIC PROBE

in the photograph. Samples tubes were cut longitudinally and one-half of the tube removed so as to expose the core. The two probes were then pushed into the core so as to measure the velocity along the axis of the core. In this way, several hundred velocity measurements were made along approximately 25 linear feet of cores.

The piezo-electric element (ceramic disk) of the acoustic probe resonated at 560 kilocycles. The ceramic disk was driven by an exponentially decaying sinusoid with this frequency. An L-R-C circuit driven by the Edgerton "Pinger" was used to generate this pulse. The pulse repetition rate was one per second. The initial portion of each pulse was used to trigger the oscilloscope sweep, using a delay line to delay the time of triggering so that the wave front arrival could be centered in the oscilloscope screen. The time of travel thus was the sum of the known triggering delay time and time interval measured on the screen. The correction for travel time through the acoustic probe was found from calibration tests where the probe was inserted in distilled water.

The cores were obtained in the Mediterranean Sea during the CHAIN 7 cruise in 1959. The soil was predominantly clay, with lens and seams of sand. All properties of the soil, including velocity, water content, limits, etc., varied in a very erratic pattern with depth. Typical properties are given in Table 6.1. In general, the water content was at or just above the liquid limit.

The measured velocities correlated extremely well with the water content of the clay, and all of the erratic variations in water content were reflected consistently by similar variations in the sonic velocities. On the average, the velocities were slightly greater than those of sea water, a result which is in agreement with those obtained by previous investigators. In many instances where the water content exceeded the liquid limit, the measured velocity vs. water content behavior thus confirmed the theory of URICK (1947),

Table 6.1

PROPERTIES OF MEDITERRANEAN SEA CORES

Clay fraction	~50 percent
Specific gravity	2.78 - 2.83
Water content	40 - 125 percent
Liquid limit	40 - 110 percent
Plastic limit	20 - 40 percent
Sonic velocity	1.47 - 1.63 kilometers/sec.

which points out that factors other than overall density must be considered in establishing the sonic velocity in a sediment.

Velocity-depth profiles as determined with these probes correlated reasonably well with sub-bottom reflections recorded with a high resolution echo-sounder during the cruise. No velocity versus depth correlation was observed in the core results. A consolidation test showed that the water content would vary by only a few percent at most as the effective stress on the sediment sample is increased from zero to an effective stress comparable to that existing at a depth of 30 feet of sediment. Therefore, it is not surprising that a velocity-depth correlation has not been noticed, for lithological changes caused water content variations which completely masked the effect of increasing effective stress.

The whole research effort confirmed that acoustic probes can be used to successfully measure velocities in sediments, provided the grain size of the sediment is not too large (the upper limit corresponds approximately with that of coarse silt). The measurements are thought to have an accuracy of 2%.

6.6 Development of laboratory sonic velocity device

Sykes in addition developed circuitry and procedures for measuring sonic velocity through samples in a consolidometer cell. The objective of this effort was to establish the feasibility of the experiment and to establish equipment requirements. The technique is patterned after that of LAUGHTON (1957), but envisions experiments at much lower pressures. A few preliminary tests were made with the apparatus to prove that sufficient energy could be pushed through the sample at these low pressures. Much of the electronic equipment mentioned in the following paragraphs was borrowed for this preliminary work and is not available to the research effort on a permanent basis.

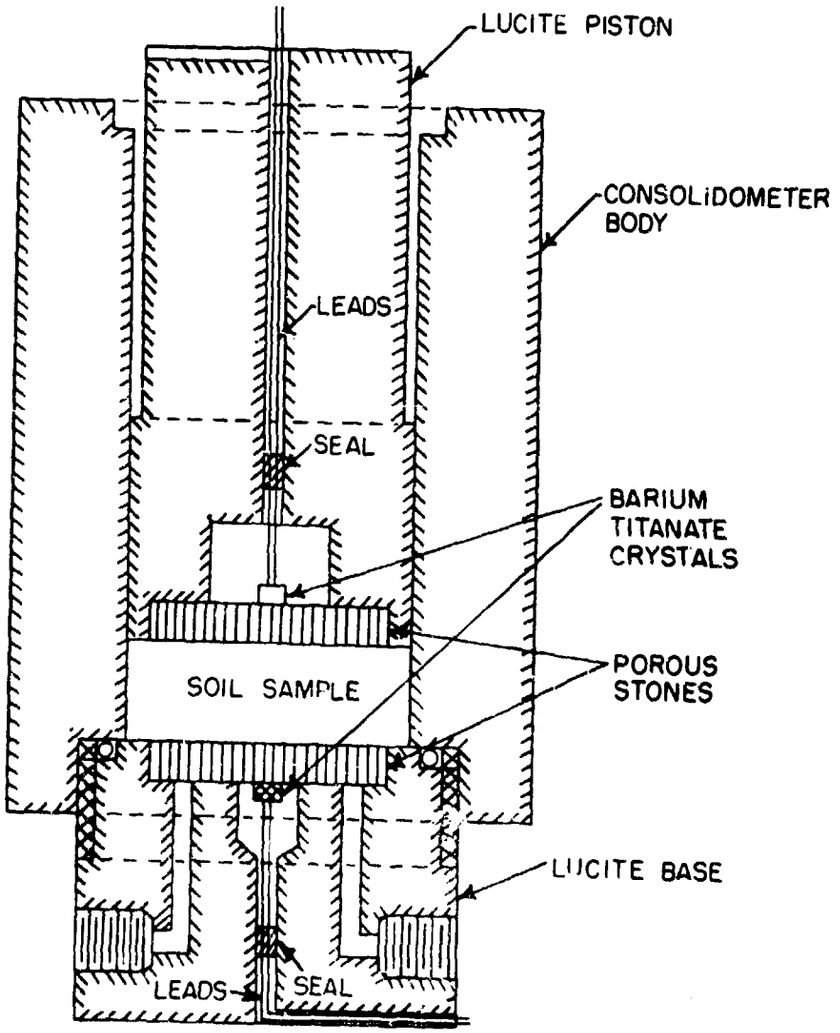

FIGURE 6.18 APPARATUS FOR PRELIMINARY WAVE PROPAGATION TESTS

A Lucite consolidometer was modified by mounting ceramic disks on the top and bottom porous stones. A section through the consolidometer unit showing the lucite container, the stones, transducers, leads and soil sample is shown in Figure 6.18. With this piece of equipment, it will be possible to consolidate samples one-dimensionally and to measure the corresponding wave velocity at any time during or after consolidation.

The ceramic disk transducers used in the preliminary investigations were obtained from Gulton Industries, Inc., Metuchen, New Jersey. The trade name of these barium titanite transducers is Glennite, and this particular type of transducer has a high so-called curie point, i.e., the transducer does not suffer from temperature effects at the low temperatures affecting ordinary barium titanite transducers. The transducers used in the consolidation unit have two wires silver-soldered to the two flat surfaces, and they have been covered with a special protective coating at the factory. These transducers vibrate both in the thickness direction and also in the radial direction. The particular crystals used (Model No. 2D3) had a thickness resonant frequency of about 800 kilocyles and a radial resonant frequency of about 400 to 500 kilocycles. Since the crystal is glued to the back of the stone, both of these frequencies will be transmitted and received, and in order to avoid confusion in interpreting results one must be filtered out. An L-C Filter was used to by-pass the higher frequency and exclude the lower frequency.

The upper transducer is used as a sending unit and is excited by a pulse generated by a Hewlett-Packard 212A Pulse Generator. This particular unit offers continuously variable pulses with widths varying from 0.07 to 10 microseconds and a repetition rate which can be varied from 50 to 5,000 repetitions per second. The optimum pulse width must be selected such that the fundamental sinusoidal frequency associated with the pulse is about the same as one of the natural frequencies of the crystals. The rate of pulse repetition must be such as to retrigger the scope so that a steady picture appears on the

oscilloscope. The pulse rate, however, must not be so high that the crystals are still vibrating before a second pulse triggers the transmitting crystal. For most of the present studies, the pulse generator has been operated at full voltage and with a repetition rate varying between 50 and 200 cycles per second. It has proven best to use a pulse width of the order of 0.5 microseconds.

The pulse received at the lower transducer is passed through a filter which removes the 400 kilocycle component; the signal is then amplified a hundred times and a second small filter is used to filter out the 60 cycle noise picked up in the room. The signal is then put on the "Y" input of a Hewlett-Packard oscilloscope.

The oscilloscope has been triggered by a pulse from the pulse generator. It is important as far as triggering is concerned to have a pulse which rises very quickly. If a sinusoidal type of pulse is used, then the time of triggering may vary somewhat if noise is present. If the pulse rises quickly as in the form of a spike or square wave, then the time of triggering will not vary much because of noise. If the travel time becomes too long, some type of delay should be used in order that the pulse can be blown up and examined critically as far as arrival time is concerned. Without a delay line, a sweep time of the order of 5 microseconds per centimeter has been used. However, with a proper delay line, the 1 microsecond scale could be used and time readings probably could be made to one-tenth of a microsecond.

A photograph illustrating the received wave form which is displayed on the oscilloscope is shown in Figure 6.19. The upper picture is for a sweep time of 5 microseconds per centimeter and the lower for a sweep time of 2 microseconds per centimeter. The experiment involved a 3/8 inch sample of soil from the marine cores, placed in the consolidation unit at a dry density of 47 lbs/ft^2 and a water content of 80 percent. The photograph shows some information coming at zero time which appears to be primarily noise, possibly pick-up

PHOTOGRAPHS OF RECEIVED WAVE FORM

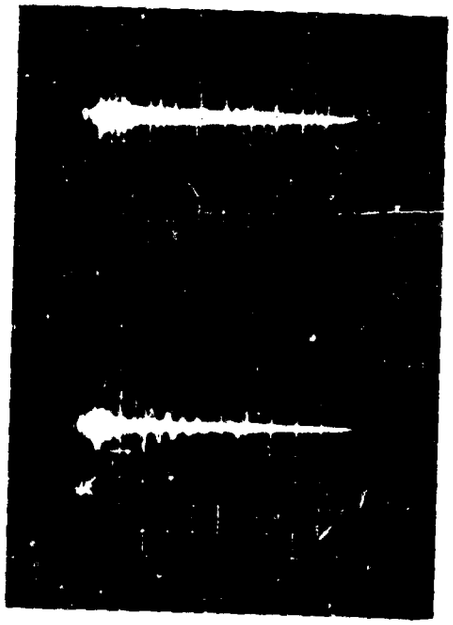

FIGURE 6.19 PHOTOGRAPHS OF RECEIVED WAVE FORM

from one transducer to the other which is not traveling by an acoustic path but merely by electrical radiation. This initial noise may cause some difficulty if the received pulse comes in so quickly that the initial arrival begins to overlap the noise. However, this initial information appears to decay from a maximum to approximately zero within about 10 microseconds. In the photograph, the direct pulse is seen to arrive at approximately 10 microseconds and roughly at 30 microseconds later a reflected pulse appears - this pulse probably being reflected off the sides of the consolidation unit.

Ideally, the received wave should consist of a single, well defined pulse. The actual received wave form is quite complex. Excluding the spurious signal which starts at zero time and the reflected portions of the wave, the wave consists of perhaps 10 cycles of a 800 kilocycle signal. The envelope to these 10 cycles first rises slowly and then decays gradually. The net result is that it is not easy to determine the time of arrival of the wave front in an exact way. Unfortunately, it does not seem possible to improve upon the nature of the wave form, for it is the result of the mechanical behavior of the transducer. When any system is excited at its resonant frequency, the amplitude of response builds up in proportion to the duration of excitation. When the excitation is removed, the response will continue for a number of cycles.

These problems, and those arising from the need to correct for travel times through the non-soil parts of the system, can be corrected by a technique using: (1) a parallel mechanical circuit through a reference material such as water or mercury, (2) simultaneous display of the two signals upon a dual-beam oscilloscope, and (3) comparison of the arrival times of some well defined portion of the 800 kilocycle wave form, such as the arrival time of the second peak, rather than an attempt to determine the exact start of the wave form.

6.7 Summary and conclusions

A study of past and present results has emphasized the great potential value of laboratory sonic wave measurements, especially as a method for studying the fundamentals of stress transmission between mineral particles. A very satisfactory start has been made toward development of equipment for use in the present research effort.

Chapter 7
SUMMARY OF CONCLUSIONS

7.1 Summary of conclusions

Since the research effort is still underway, any conclusions must of necessity be tentative. With this in mind, the main conclusions from the work reported herein may be summarized as follows:

(a). Nature of stress-strain relation for particulate mass: A complete description of the relationship between stress and strain in an assemblage of particles must take into consideration the following factors: (1) the particulate mass will behave in an extremely non-linear fashion even though it does not reach a maximum load-sustaining capacity; (2) the stress-strain ratio is extremely sensitive to the whole content of the stress system; (3) the mass dissipates energy as it strains; and (4) the stress-strain relation is time dependent. See Chapter 2.

(b). Two-phase nature of soils: The fact that soil consists of a mineral skeleton (solid phase) and a pore phase (water, gas, or water and gas) must be taken into consideration when analyzing the effect of time upon stress-strain properties. See Chapter 2.

(c). Need for data upon compression resistance: The dilitational modulus M is an important parameter in present protective construction design work, and there is great need for data regarding the probable magnitude of this modulus for in situ soils subject to waves of high amplitude and relatively long duration. See Chapter 2.

(d). Role of laboratory tests: The most promising role of laboratory

tests is: basic research into the effects of time, stress level and other factors upon the deformation of soil systems. See Chapter 2.

(e). Static compaction procedure: In order to obtain compacted samples of backswamp clay which have uniform density throughout each sample, static compaction to 250 lb/in^2 with maximum thickness to diameter ratio of 0.6 may be used. See Chapter 3.

(f). Magnitude of compression creep in compacted fat clay: When compacted fat clay in one-dimensional compression is loaded with a rise-time of 30 milliseconds, only 25 to 50 percent of the strain occurs during the loading interval. The amount of creep is especially large during the first 100 milliseconds after load application and then decreases and becomes linear with the logarithm of time. The general validity of the following principle has been reaffirmed: as the total strain experienced by a material decreases, the fraction of this total strain which is creep under constant load increases. However the effect of the structure of compacted clay must also be considered. See Chapter 4.

(g). Cause of compression creep in compacted fat clay: Pore pressures were measured during compression creep in one-dimensional compression, but the results were not entirely conclusive because of possible escape of air from the soil samples and because of time-lags in the pore pressures measuring systems. The tentative conclusion is that there exists both a structural viscosity and a time dependence for the solution of air in water. See Chapter 5.

(h). Measurement of sonic wave velocities in marine cores: Many measurements using an acoustic probe have shown the dependence of wave velocity upon the structure of the soil and have confirmed theories concerning the dilitational velocities of soft, saturated soils. See Chapter 6.

(i). Feasibility of laboratory sonic wave velocity measurements with soft soils: Based upon the tests with the acoustic probe and upon preliminary tests within an oedometer, such measurements appear to be feasible. See Chapter 6.

Appendix A

BIBLIOGRAPHY

AMENT, W.S. (1953) "Sound Propagation in Gross Mixtures", J. Acoust. Soc. Amer. Vol. 25, pp. 638-641.

BISHOP, A.W., ALPAN, I., BLIGHT, G.E., and DONALD, I.B., (1960) "Factors Controlling the Strength of Partially Saturated Soils", Proc. ASCE Research Conference on Shear Strength of Cohesive Soils.

BIOT, M.A. (1956) "Elastic Waves in Porous Solids, I and II", J. Acoust. Soc. Amer. Vol. 28, pp. 168-191.

BRANDT, H. (1955) "Study of the Speed of Sound in Porous Granular Media", Jour. Appl. Mech., Vol. 22, No. 4, p. 479.

BUSBY, J. and RICHARDSON, E.G. (1957) "The Absorption of Sound in Sediments", Geophysics Vol. 22, pp. 821-828.

HUGHES, D.S. and JONES, H.J. (1951) "Elastic Wave Velocities in Sedimentary Rocks", Trans. Amer. Geophysical Union, Vol. 32, pp. 173-178.

HUGHES, D.S. and KELLY, J.L. (1952) "Variation of Elastic Wave Velocities with Saturation in Sandstone", Geophysics, Vol. 17, No. 4, pp. 739-752.

LAMBE, T.W. (1958) "The Structure of Compacted Clay", Journal of Soil Mechanics and Foundations Div., ASCE, Vol. 84, No. SM2.

LAUGHTON, A.S. (1957) "Sound Propagation in Compacted Ocean Sediments", Geophysics, Vol. 22, p. 233.

MARTIN, J.W. (1957) "Correlation of Sonic Engineering Properties of Soils through Use of the Soniscope", SM Thesis, M.I.T.

MIT (1954) "The Response of Soils to Dynamic Loadings: No. 3 - Final Report On Laboratory Studies", Report to the Office of the Chief of Engineers, U.S. Army; AFSWP-118.

MIT (1957) "Dynamics No. 1 - Scope of Test Program and Equipment Specifications", Report to Waterways Experiment Station.

MIT (1959a) "Dynamics No. 2 - Test Equipment for High Speed Triaxial Tests", Report to the Waterways Experiment Station; Publication 100 of MIT Soil Engineering Division.

MIT (1959b) "Dynamics No. 3 - First Interim Report on Soil Tests", Report to the Waterways Experiment Station; DASA -1162; Publication 104 of MIT Soil Engineering Division.

MORSE, R.W. (1952) "Acoustic Propagation in Granular Media", Jour. Acoust. Soc. of Amer., Vol. 24, No. 6, pp. 696-700.

PATERSON, N.R. (1956) "Seismic Wave Propagation in Porous Granular Media", Geophysics Vol. 21, pp. 691-714.

PARKIN, B.R., (1959) "Impact Wave Propagation in Columns of Sand", Rand Corp., RM-2486.

PECK, R.B. and WHITMAN, R.V. (1959) "Geological and Soil Conditions Affecting Selection of Sites for Hardened Missile Installations", Space Technology Labs. Report TR-59-0000-00702 (Secret).

ROBERTS, J.E. and DE SOUZA, J.M. "The Compressibility of Sands", Proc. A.S.T.M., Vol. 58, p. 1269.

SEED, H.B., MITCHELL, J.K. and CHAN, C.K. (1960) "The Strength of Compacted Cohesive Soils", Proc. ASCE Research Conference on Shear Strength of Cohesive Soils.

SHUMWAY, G. (1956) "A Resonant Chamber Method for Sound Velocity and Attenuation Measurements in Sediments", Geophysics, Vol. 21, pp. 305-319.

SAUER, F.M., EVANS, G.W , ABLOW, C.M., and BRENNER, J., (1958) "Ground Motion Induced by Nuclear Explosions; A Study of Fundamental Problems"; Report of Stanford Research Institute to the Air Force Special Weapons Center, AFSWC-TN-58-23. (Confidental).

SYKES, L.R. (1960) "An Experimental Study of Compressional Velocities in Deep Sea Sediments", S.M. Thesis, M.I.T.

URICK, R.J. (1947) "A Sound Velocity Method for Determining the Compressibility of Finely Divided Substances", Jour. Appl. Physics, Vol. 18, p. 983.

WARD, W.H., SAMUELS, S.G. and BUTLER, M.E. (1959) "Further Studies of the Properties of London Clay", Geotechnique, Vol. 9, p. 33.

WILSON, S.D. and DIETRICH, R.J. (1960) "Effect of Consolidation Pressure on Elastic and Strength Properties of Clay", Proc. ASCE Research Conf. on Shear Strength of Cohesive Soils.

WYLLIE, M.R.J., GREGORY, A.R. and GARDNER, G.H.F. (1956) "Elastic Wave Velocities in Heterogenuous and Porous Media", Geophysics, Vol. 21, p. 41-70.

_____ _____ _____ (1958) "An Experimental Investigation of Factors Affecting Elastic Wave Velocities in Porous Media", Geophysics, Vol 23, p. 459.

Appendix B

LIST OF SYMBOLS

a	a distance
B	bulk modulus
b	a distance
D	flexural modulus of a plate, diameter of soil sample
d	a distance, diameter of soil sample
E	Young's modulus
e	void ratio
G	shear modulus, specific gravity of soil particles
g	acceleration of gravity
H	thickness of soil sample
L	length of soil sample
M	dilitational modulus
m_v	$1/M$
p_c	compaction pressure
p_i	initial pressure in one-dimensional compression tests
S	degree of saturation
v_o	initial impact velocity
T	duration of application of Δp
t_r	rise time for Δp
t_1	duration of application of p_i
u_e	pore pressure at equilibrium after compaction
u_f	pore pressure at equilibrium under Δp
u_i	pore pressure at equilibrium under p_i
v_p	dilitational wave velocity
v_s	shear wave velocity
v^*	compression wave velocity in long rod
w	water content
ΔH_f	final change in thickness of one-dimensional compression samples

ΔH_{30}	change in thickness of one-dimensional compression samples
Δp	increment of pressure in one-dimensional compression tests
ΔT	time required to reach pore pressure equilibrium
Δu	change in pore pressure
ε	strain in one-dimensional compression tests
γ	density
γ_d	dry density
λ	Lame constant
ρ	mass density
σ_{1f}	final axial stress
σ_{10}	initial axial stress
μ	Poisson's ratio